Investigation of the Lip Reed Using Computational Modelling and Experimental Studies with an Artificial Mouth

Orlando Richards

A thesis submitted in fulfilment of the requirements

for the degree of Doctor of Philosophy

to the

University of Edinburgh

2003

Abstract

The human lips form the valve used to control the flow of air into brass instruments. This "lip reed" is a complex system of muscle, skin and fluid. A basic analysis of the lip reed was performed by Helmholtz in the 19th century, but this analysis failed to explain some important characteristics of the valve operation of the reed. These characteristics are investigated in the present work, with a focus on the operation of "inward–striking" and "outward–striking" reed modes.

To investigate the lip reed, artificial mouths have recently been employed to facilitate scientific study of the behaviour of the reed. These devices model the human lips using natural latex rubber tubes filled with water. This study uses one such device to investigate, experimentally the relationships between the resonances of the reed and the resulting self-sustained oscillation when driving an acoustic resonator - a trombone in this case. The resonances of the reed are initially investigated by measuring the area of opening between the lips as they are driven by a known oscillating acoustic signal. Additionally, the resonances of the reed are investigated in two dimensions using a laser doppler vibrometer. Motion of the lips in two dimensions is analysed using a high speed digital video camera.

Using these results, computational investigations of lip models provide a great

deal of insight into the basic mechanics of the reed. Linear stability analysis shows that a model with at least two degrees of freedom is required to reproduce experimentally observed threshold playing frequencies. Time domain simulations are used to investigate the response of the models, and comparisons are made with the experimentally obtained response data. Strong similarities are found between the area of opening function of a two degree of freedom model and the area function recorded in experimental studies, when the opening area is described by an appropriate non-linear function of the reed position. These results greatly improve the understanding of the mechanics of the lip reed, and pave the way for the development of fully capable physical sound synthesis models.

Acknowledgements

I would like to thank my supervisors Murray Campbell and Clive Greated for their invaluable aid over my period of study. Joel Gilbert has also been hugely inspirational and helpful during this project. Thanks also to Mark Neal, Seona Bromage and Maarten van Walstijn for the many discussions that solved so many problems, and presented many others for investigation. I would also like to thank my colleagues in the Acoustics and Fluid Dynamics research group at the University of Edinburgh - Jim Buick, Sandra Carral, Scott Coltman, John Cosgrove, David Forehand, Calum Gray, Jonathan Kemp, Alan Marson, Tom McGillvary, Dawn Rockliff, Ted Schlicke, David Skulina, Steven Tonge and Alan Woolley. Thanks also to Vince Devine for his help in designing the artificial mouth, and for constructing it to such an incredibly high standard. Also, thanks to Frank Morris for his technical help and advice.

Financial support was provided by EPSRC.

I would also like to thank my fiancée Fiona Glasgow for her unfaltering support throughout my period of study, as well as for her excellent proof reading. Finally, utmost thanks go to my parents, Anne and Alan Richards, without whom none of this work would have been possible.

Contents

List of Figures

List of Tables

Chapter 1

Introduction

1.1 Introduction to brass instrument acoustics

Brass instruments are a subset of the wind instrument family, defined by the method of energy input into the system – the lips of the player form the reed, through which air is blown into the instrument. Wind instruments can generally be modelled by a simple feedback system, where the reed acts as a valve that allows an oscillating flow of air into the instrument, which in turn provides feedback that drives the motion of the reed. The resultant self–sustaining oscillation is therefore a result of aero–elastic coupling between the mechanical oscillator (the reed), the acoustic oscillator (the instrument) and the flow of air through the reed.

Helmholtz [34] laid much of the groundwork for the understanding of this feedback system, and in particular categorised the various types of reed as "striking outwards" or "striking inwards". These definitions referred to the response of a reed to a slow increase in supply pressure – a "striking outward" reed responds with an increase in opening aperture, and a "striking inward" reed responds with a decrease in opening aperture.

These categories of reeds can be modelled by using a one degree of freedom model, such as that used by Elliott and Bowsher [22] to model the lip reed. Such models have been extensively used to produce very realistic synthesised instrument sounds [2] [21] [38] [39] [55] [57] and also as scientific tools to further understand the feedback mechanisms of brass instruments. However, much work has shown that the limitations of these models make them unsuitable for reproducing certain experimentally observed phenomena [15] [16] [67] – particularly, the ability to play at frequencies both above and below the resonance frequency of the air column [17] [18] [19] [29] [48] [49] [50] [53]. This phenomenon, in particular, implies that the lip reed cannot be classified as either "striking inwards" or "striking outwards".

Experimental studies using an artificial mouth provide a robust, manageable solution to the problems presented by experimenting with human players. Gilbert and Petoit[32] designed an artificial mouth that was capable of producing measurements with a repeatability far beyond what was achievable with human

players. Subsequently, there have been several developments of artificial mouth studies, such as those by Cullen [17] [18], Neal[48], and Vergez and Rodet[61] [62].

1.2 Computational Simulation

The understanding of dynamic systems can be greatly enhanced by the use of computational modelling. Simulations of such systems can provide data that is unobtainable by experimental methods – such as the position and velocity of all parts of the system at a given time. However, such simulations rely on the development of a model that accurately represents the physical system. Simple one dimensional models can produce excellent results, especially in the generation of synthesised sounds. However, studies of the motion of the lip reed [16] [45] [67] have shown that it exhibits far more complex motion than can be represented by a single degree of freedom model. Additionally, studies of the threshold playing behaviour of artificial lip reeds has shown that the system can destabilise both below and above the air column resonators. Cullen [17] [18] used linear stability analysis to show that one degree of freedom models were incapable of reproducing this behaviour.

1.3 Aims and contents of thesis

The aims of this study are to:

1. develop a modified version of the artificial mouth.

2. measure the threshold behaviour of the artificial mouth while playing a trombone.

3. measure the frequency response of the artificial lips.

4. develop a transparent mouthpiece to allow visualisation of the lips.

5. investigate the motion of the lips during oscillation using high speed video recording and laser Doppler vibrometry.

6. develop a model of the lips that reproduces experimentally observed behaviour.

This study is composed of two main parts. Chapters 3 and 4 describe the experiments performed on the artificial mouth, using threshold playing analysis and lip response measurements in chapter 3, and visualisation of the lip motion using high speed video recording in chapter 4. Chapter 5 uses the results presented in the experimental chapters to investigate the viability of different types of models. Linear stability analysis techniques are used to show that a two degree of freedom model is required in order to reproduce the threshold playing behaviour presented in chapter 3. Time domain simulations then show that one

such two degree of freedom model can predict the experimentally observed mechanical response when a non–linear function defines the area of opening between the lips.

Chapter 2 reviews the basics of wind instrument acoustics relevant to this study. In particular, the requirements for self–sustained oscillation are investigated for inward striking and for outward striking reed types. A basic lip reed model is presented, giving the time–domain equations of motion for a one degree of freedom model. The requirements for self–sustained oscillation for inward or outward striking reed types are used to show that the lip reed can not be described as only one or the other type.

Chapter 3 presents details of a new version of the artificial mouth. This mouth is designed to be more flexible than previous models in the range of instruments it can play, as well as allowing greater potential for visualisation of the lips. Experiments are described that measure the frequency response of the lip reed, as well as the threshold playing behaviour. The ability of the lips to self–oscillate without an instrument attached is also investigated, with a focus on the role of the mouth cavity volume.

Chapter 4 describes experiments designed to measure the motion of the lips in many dimensions. Use is made of a high speed digital video camera, recording at frame rates up to 7100 frames per second, and a laser Doppler vibrometer is used to measure the displacements of individual points on the lip surface. The

data obtained with the high speed camera provides analysis of the lip opening area and lip opening height functions, as well as mapping the motion of one point on the lip surface in two dimensions. The laser Doppler vibrometer is used to measure the frequency response of a number of points on the lip surface, in different dimensions.

Chapter 5 has two main sections. In section 5.3 linear stability analysis of generic lip models with one and two degrees of freedom is used to show that a model with two degrees of freedom is capable of reproducing the type of threshold playing behaviour measured in chapter 3. In section 5.4, a two degree of freedom model is examined in the time domain. Comparisons are made between the frequency response of this model and those measured experimentally (from chapters 3 and 4). An initial study of a four degree of freedom model is described, and again comparisons are made between the frequency response of such a model and those observed experimentally.

Chapter 6 presents the conclusions of this thesis, together with some suggestions for future work, including possible modifications to the design of the artificial mouth used here.

Chapter 2

Physics of Musical Wind Instruments

2.1 Basic Wind Instrument Acoustics

Musical instrument research was greatly advanced by Helmholtz [34] in the latter half of the 19th century. His work in this field is presented in his book *On the Sensations of Tone* [34]. Helmholtz's work in this field covered a huge spectrum of acoustics, but of particular relevance to this study is his research on the physics of musical wind instruments. Particularly, Helmholtz proposed that the lips of a brass player could be represented by a simple model, where the area of opening between the lips would increase as the supply pressure was slowly increased. He called this type of reed a "striking outwards" reed. This chapter investigates the

behaviour of this type of model, as well as that of the "striking inwards" type.

Musical wind instruments can be described by a very simple feedback loop model [11] - shown in figure 2.1.

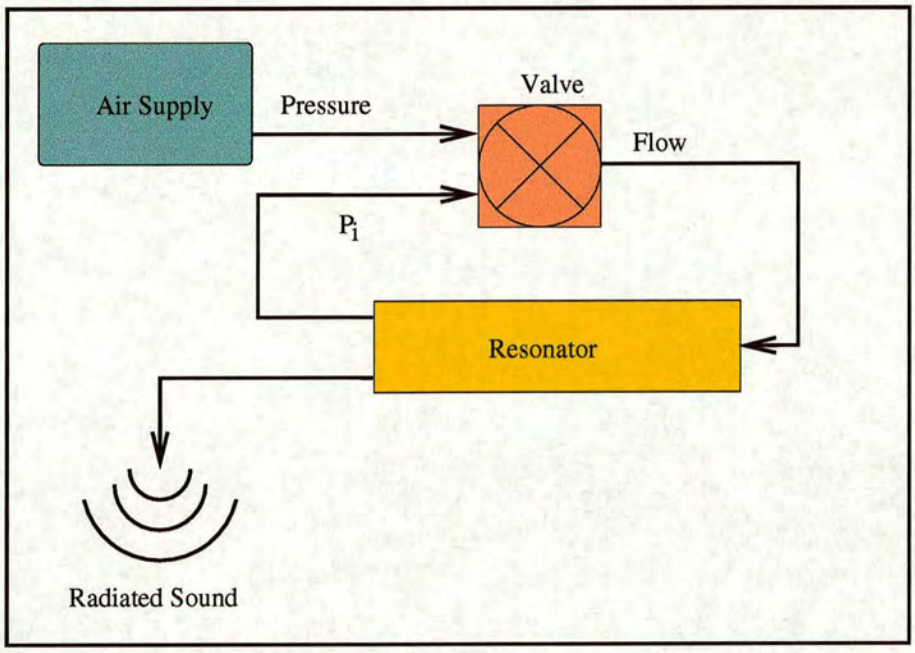

Figure 2.1: Basic feedback model of a wind instrument. The flow control valve is controlled by the supply pressure and the pressure in the instrument.

The flow of air into the instrument is moderated by a valve which is itself controlled by the supply pressure and the pressure in the instrument. In a clarinet, for example, the valve is the cane reed opening and closing against the mouthpiece lay. In a brass instrument it is the oscillating lips of the player. The pressure in the instrument oscillates as the pressure waves are reflected from the ends of the instrument. The frequency at which these oscillations occur is dependant on the shape and length of the air column. In the case of the cane reed and lip reed

instruments, the reed effectively acts as a closed end for pressure waves in the tube. Thus, a cylinder driven by such a reed has a harmonic resonance series with frequencies, ν_n, defined by:

$$\nu_n = \frac{2n-1}{4l}c, \tag{2.1}$$

where l is the length of the cylinder, c is the speed of sound in air, and n is the harmonic number $(1, 2, 3...)$. Brass instruments are designed to have an approximately harmonic series of resonances. The use of a flaring horn, for instance, has the effect of changing the effective length of the air column for varying frequencies [8]. Benade [9] [28] described a model of a brass instrument with a flaring horn that consisted of a cylindrical section which led into a flaring horn, the shape of which could be described by a Bessel function. He therefore calculated that the resonance frequencies of this model are approximately given by:

$$\nu_n \approx \frac{c}{4(l+x_0)}\left((2n-1)+\beta(\xi(\xi+1))^{0.5}\right), \tag{2.2}$$

where ξ is the *flare constant* of the horn, x_0 is the length of the horn section and l is the length of the cylindrical section.

The *input impedance*, Z, of the instrument is defined as the ratio of pressure,

p, and volume flow, u, at the input of the instrument [12] [28] [52]:

$$Z(\omega) = \frac{p(\omega)}{u(\omega)}. \tag{2.3}$$

It is possible to measure, experimentally, the input impedance of an instrument; this is described in sections 2.2 and 3.4.2.

Wind instruments are conventionally put into one of two categories: woodwind or brass instruments. The distinction between the two has little to do with the material from which they are constructed, but rather the mechanism used to play them. A more appropriate classification categorises the instruments by the type of reed they use, be it a "cane-style" reed, such as a clarinet or oboe reed, an "air" reed, as seen in the flute and recorder, or a "lip" reed, which drives all "brass" instruments, such as the trumpet or trombone. This study focuses on the lip reed instruments, and specifically on the behaviour of the lip reed itself.

Of these reed types, the "cane-style" reeds are the best understood. The basic physics involved in their behaviour has been well established since Helmholtz's [34] time, with subsequent research into their behaviour focusing on the non–linear characteristics (see, for example, van Walstijn [60] and Dalmont et al [20]). Helmholtz's description of the lip reed, on the other hand, failed to explain significant physical phenomena experienced by musicians - specifically the ability to pitch a note at any frequency around an instrument's natural resonance. This "lipping" phenomenon is often used by jazz musicians, amongst others.

2.2 Resonator Physics

As seen in figure 2.1, a wind instrument can be represented as a flow control valve coupled to a resonator. The resonator represents the column of air inside the bore of the instrument. In the case of certain brass instruments, such as the trombone, this bore is cylindrical for most of its length and open at one end (the bell end). The lips of the player close off the mouthpiece end. Air is injected into the mouthpiece, providing the energy input into the system, and creates a pressure wave (a plane–wave in the first approximation) down the length of the resonator. When this wave reaches the end, some of its energy is reflected back up the resonator, and some escapes out of the end of the tube. If the frequency of the injected air flow is close to a resonance frequency of the air column, a standing wave is created in the bore. The resonances of the instrument can be found experimentally by measuring the input impedance, Z, of the instrument, defined in equation 2.3. Figure 2.2 shows an example input impedance measurement for a King brand tenor trombone with a mouthpiece attached (see section 3.4.2).

To simplify the process of modelling the reed and instrument system, it is often useful to consider only low amplitude oscillations around a fixed equilibrium state. This examination of *threshold* playing can yield clear and informative data on the behaviour of the system. When the oscillating flow injected into the instrument has a low amplitude and has a frequency close to one of the resonant modes of the instrument, the series of harmonic peaks shown in figure 2.2 can be reduced

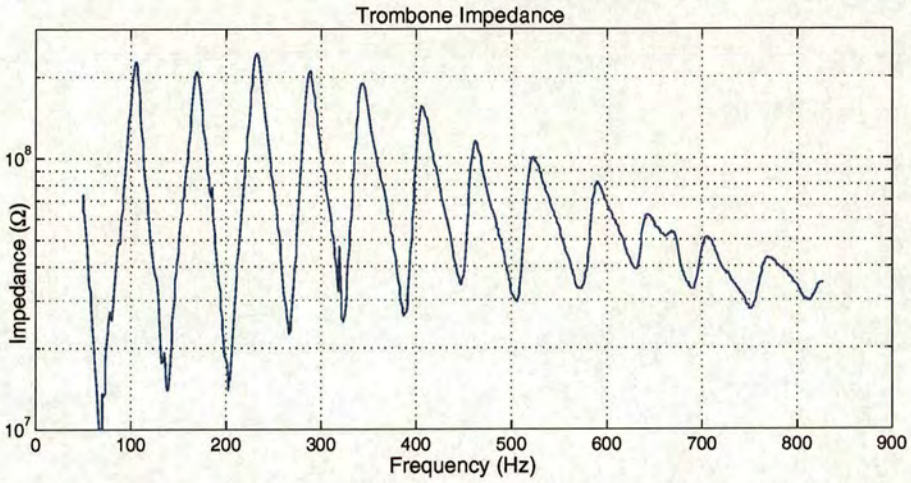

Figure 2.2: Magnitude of the input impedance of a tenor trombone with mouthpiece attached, with the slide unextended.

to just the one peak of interest [31]. This allows the system to be modelled as a one degree of freedom resonator, with input impedance [14]:

$$Z(\omega) = Z_i \left(1 + \frac{jQ_i(\omega_u^2 - \omega_i^2)}{\omega_u \omega_i}\right)^{-1}, \tag{2.4}$$

where j is the square root of -1, ω_i is the instrument resonance frequency of interest, Z_i is the amplitude of the impedance at this frequency, Q_i is the quality factor of this resonance and ω_u is the frequency of the flow admitted through the reed [18]. The subscript i is used here, and throughout this study, as an abbreviation for "instrument". Modelling the resonator in this simplified manner makes the modelling of the reed–resonator system much simpler (see chapter 5). Equation 2.4 can be rewritten as a time domain equation:

$$\frac{\partial^2 \psi}{\partial t^2} + \frac{\omega_i}{Q_i}\frac{\partial \psi}{\partial t} + \omega_i^2 \psi = \frac{Z_i \omega_i}{Q_i} u, \tag{2.5}$$

where $\frac{\partial \psi}{\partial t}$ is the pressure in the instrument mouthpiece and u is the oscillating component of the volume flow injected into the instrument through the reed. Non–linear propagation effects, such as shock wave formation [30] [35] [46] [47], can be ignored by restricting this system to a low amplitude regime, and by investigating only relatively low frequencies (where the wavelength is much greater than the diameter of the bore of the instrument) the plane wave approximation is sufficient.

2.3 Reed Physics

The function of a reed in a wind instrument is to act as an oscillating flow control valve, admitting a flow of air into the instrument resonator which co-operates with the natural air column resonances of the instrument. This co-operation results in *self-sustained oscillation*, where the reed and resonator each reinforce the other's oscillation. Helmholtz [34] originally described two classes of reeds:

- "Striking Outwards" - where the reed responds to a slow increase in the supply pressure by increasing its area of opening. Helmholtz discovered that these reeds, when coupled to a resonator, play above their natural resonance frequency.

- "Striking Inwards" - where the opposite is true - the reed area decreases as a result of an increased supply pressure. When coupled to a resonator,

reeds of this type play below their natural resonance frequency.

More recently, Fletcher [26] rigorously defined these reed classifications.

The fact that these reeds will play above or below their natural resonance frequencies can be understood by considering the requirement that the oscillations in the air column and the reed must reinforce each other. In order for the oscillations in the air column to be regenerated by the flow of air through the reed, the mean value of the oscillating component of the flow should be positive while the pressure at the reed end of the instrument is positive. If the flow was negative while the instrument pressure was positive, the standing wave would be diminished rather than reinforced. This reinforcement will occur if the phase difference between the oscillating component of the flow, u, and the oscillating component of the pressure in the instrument mouthpiece, p_i, is less than $\pi/2$.

This was explained by Campbell [11] in terms of the energy transfer into the system. The instantaneous rate of energy transfer, W, into the air column by the flow through the lips, U, is given by:

$$W = P_i U. \tag{2.6}$$

P_i is the pressure in the instrument mouthpiece, which is the sum of a static pressure $\overline{P_i}$ and an oscillating component p_i. U is the sum of a static flow component

$\overline{U}$ and an oscillating component u. Thus equation 2.6 becomes:

$$\begin{aligned} W &= \left(\overline{P_i} + p_i\right)\left(\overline{U} + u\right) \\ &= \overline{P_i U} + p_i \overline{U} + \overline{P_i} u + p_i u. \end{aligned} \tag{2.7}$$

The $\overline{P_i U}$ term describes the dissipation of energy in the mean flow. This does not affect the energy balance of the oscillating system. The $p_i \overline{U}$ and $\overline{P_i} u$ terms average to zero over a complete cycle. This means that the net rate of energy transfer into the air column is given by the $p_i u$ term. Thus, the energy input into the system will be positive if $p_i u$ is positive over a cycle, which will be the case when the phase difference between p_i and u is less than $\pi/2$.

We define ΔP as the pressure difference across the reed:

$$\Delta P = P_0 - P_i, \tag{2.8}$$

where P_0 is the supply pressure (the pressure in the player's mouth, for example) and P_i is the pressure inside the instrument mouthpiece. Defining Δp as the oscillating component of the pressure difference across the reed and making the assumption that the supply pressure is approximately constant, we get:

$$\Delta p = -p_i. \tag{2.9}$$

By assuming that the flow through the lip channel is quasi–stationary, frictionless and incompressible it can be assumed that the oscillating component of the flow through the reed, u, is approximately in phase with the oscillating component of the area of opening controlled by the reed, s_{reed}. We define the phase difference Φ between the opening area of the reed and the pressure difference across the reed as:

$$\begin{aligned} \Phi &= \angle u - \angle \Delta p \\ &= \angle s_{reed} - \angle \Delta p. \end{aligned} \tag{2.10}$$

Applying the regeneration requirements described above, and remembering that Δp is π radians out of phase with the mouthpiece pressure p_i, the condition for self-sustained oscillation becomes:

$$\Phi > \frac{\pi}{2} \quad \text{or} \quad \Phi < -\frac{\pi}{2}. \tag{2.11}$$

The driving force F_d, which can also be described as the sum of a static ($\overline{F_d}$) and oscillating (f_d) component, is provided by the pressure difference ΔP. We define a positive force to be one which increases the opening area of the reed, so for an *outward striking* reed f_d is in phase with Δp, and for an *inward striking* reed f_d is exactly out of phase with Δp.

For a driven, damped, simple harmonic oscillator, the complex displacement $\tilde{x}$ can be written as [25] [28]:

$$\tilde{x} = \frac{\tilde{F}/m}{(\omega_0^2 - \omega_d^2) + j2\alpha\omega_d}, \tag{2.12}$$

where ω_d is the frequency of the driving force, ω_0 is the resonance frequency of the oscillator, $\tilde{F}$ is the complex driving force, m is the mass of the oscillator and α is a damping coefficient.

The frequency dependent phase difference between the driving force and the displacement is given by the argument of $\tilde{x}/\tilde{F}$:

$$\begin{aligned}
\phi_x - \phi_d &= arg\left[\frac{\frac{1}{m}}{(\omega_0^2-\omega_d^2)+j2\alpha\omega_d}\right] \\
&= arg\left[\left(\frac{\frac{1}{m}}{(\omega_0^2-\omega_d^2)+j2\alpha\omega_d}\right)\left(\frac{(\omega_0^2-\omega_d^2)-j2\alpha\omega_d}{(\omega_0^2-\omega_d^2)-j2\alpha\omega_d}\right)\right] \\
&= arg\left[\frac{(\omega_0^2-\omega_d^2)-j2\alpha\omega_d}{m((\omega_0^2-\omega_d^2)^2+4\alpha^2\omega_d^2)}\right] \\
&= arg\left[(\omega_0^2 - \omega_d^2) - j2\alpha\omega_d\right],
\end{aligned} \tag{2.13}$$

where ϕ_x is the phase of the displacement and ϕ_d is the phase of the driving force. From this it can be seen that when $\omega_d \cong 0$, $\phi_x - \phi_d = 0$. When $\omega_d = \omega_0$, $\phi_x - \phi_d = -\pi/2$. When $\omega_d >> \omega_0$, $\phi_x - \phi_d \Rightarrow -\pi$. It is now possible to calculate the phase relationships between Δp and s_{reed} for both inward and outward striking reeds. Given that for an inward striking reed the force is π radians out of phase with the pressure difference, but for an outward striking reed the force is *in* phase

with the pressure difference, Φ for an outward striking reed is given by:

$$\begin{aligned} \Phi^{outward} &= \phi_{reed} - \phi_d \\ &= \phi_{reed} - \phi_{\Delta p}, \end{aligned} \tag{2.14}$$

and for an inward striking reed by:

$$\begin{aligned} \Phi^{inward} &= \phi_{reed} - \phi_d \\ &= \phi_{reed} - (\phi_{\Delta p} - \pi). \end{aligned} \tag{2.15}$$

Reed Type	$\Phi(\omega_d \cong 0)$	$\Phi(\omega_d = \omega_0)$	$\Phi(\omega_d >> \omega_0)$
Inward Striking	π	$\pi/2$	0
Outward Striking	0	$-\pi/2$	$-\pi$

Table 2.1: Phase relationships between driving pressure and lip opening area for inward and outward striking reed types

From table 2.1 it can be seen that if a reed is driven at its resonance frequency, its type can be determined by examining the phase relationship between the driving pressure and the opening area.

Furthermore, it is now possible to explain why an outward striking reed must play *above* the reed and instrument resonances, and why an inward striking reed must play *below* the reed and instrument resonances. It was established above that in order for self-sustained oscillation to take place, the phase difference between the volume flow and the pressure in the mouthpiece must be between $\pm\pi/2$, and consequently the phase difference between the reed opening area and

the pressure difference across the reed must be less than $-\pi/2$ or greater than $\pi/2$ (see equation 2.11). Figure 2.3 shows that in order to satisfy this condition, the playing frequency must be *above* the reed resonance frequency of an outward striking reed, or *below* the reed resonance frequency of the inward striking reed - which matches what Helmholtz discovered when he initially defined "striking inward" and "striking outward" reed types.

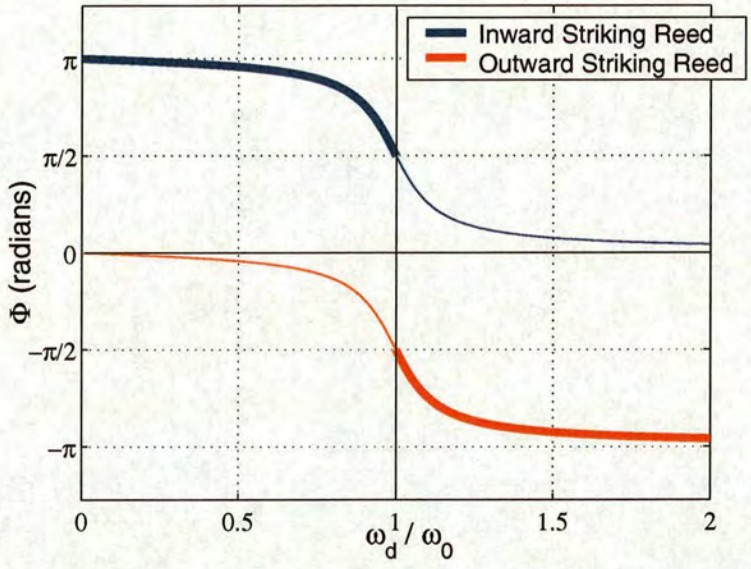

Figure 2.3: Phase difference between driving pressure and area of opening between the lips as a function of driving frequency. The bold lines represent the areas where self-sustaining oscillation is possible.

The same analysis can be applied when the instrument is considered as the driven harmonic oscillator instead of the reed. The feedback circuit presented in figure 2.1 shows that the resonator is driven by the reed, and at the same time the reed is driven by the resonator. As described in section 2.2, a single mode of the resonator can be represented as a simple harmonic oscillator (defined by

equation 2.5).

The equivalent of equation 2.12 for the acoustic resonator is given by:

$$\tilde{p_i} = \frac{\partial \tilde{\psi}}{\partial t} = \frac{\frac{Z_i \omega_i}{Q_i} \frac{\partial \tilde{U}}{\partial t}}{(\omega_i^2 - \omega_u^2) + j\frac{\omega_i}{Q_i}\omega_u}. \tag{2.16}$$

Given that the flow is a sum of static ($\overline{U}$) and oscillating (u) components, and the complex form of u, $\tilde{u}$, can be written as:

$$\tilde{u} = |u| e^{j(\omega_u t + \phi_u)}, \tag{2.17}$$

where ω_u is the frequency of the oscillating component of the flow and ϕ_u is its phase, equation 2.16 becomes:

$$\tilde{p_i} = \frac{\frac{Z_i \omega_i}{Q_i} j\omega_u \tilde{u}}{(\omega_i^2 - \omega_u^2) + j\frac{\omega_i}{Q_i}\omega_u}. \tag{2.18}$$

Consequently, the phase difference between the instrument pressure and the flow through the reed is given by:

$$\begin{aligned} \phi_{p_i} - \phi_u &= arg\left[\frac{\frac{Z_i \omega_i}{Q_i}\omega_u}{\frac{\omega_i}{Q_i}\omega_u - j(\omega_i^2 - \omega_u^2)}\right] \\ &= arg\left[\left(\frac{\frac{Z_i \omega_i}{Q}\omega_u}{\frac{\omega_i}{Q_i}\omega_u - j(\omega_i^2 - \omega_u^2)}\right)\left(\frac{\frac{\omega_i}{Q_i}\omega_u + j(\omega_i^2 - \omega_u^2)}{\frac{\omega_i}{Q_i}\omega_u + j(\omega_i^2 - \omega_u^2)}\right)\right] \\ &= arg\left[\frac{\omega_i}{Q_i}\omega_u + j(\omega_i^2 - \omega_u^2)\right]. \end{aligned} \tag{2.19}$$

Moving from the instrument pressure p_i to the pressure difference across the reed Δp, equation 2.19 becomes:

$$\phi_{\Delta p} - \phi_u = arg\left[-2\frac{\omega_i}{Q_i}\omega_u - j(\omega_i^2 - \omega_u^2)\right]. \tag{2.20}$$

Given that Φ was defined for the reed as the phase shift of u from the reference Δp, we can establish $\Phi^{resonator}$ using the same definition:

$$\Phi^{resonator} = \phi_u - \phi_{\Delta p} = -arg\left[-2\frac{\omega_i}{Q_i}\omega_u - j(\omega_i^2 - \omega_u^2)\right]. \tag{2.21}$$

This function is plotted in figure 2.4. It can be seen from this graph that in order for the instrument to play below its resonance frequency ω_i, the phase between volume flow and the pressure difference must be between $+\pi/2$ and $+\pi$, corresponding to the phase relationship produced by an *inward striking* reed. To play above, the phase must lie between $-\pi/2$ and $-\pi$, corresponding to an *outward striking* reed.

Thus, each reed type has these defining characteristics:

- An **outward striking reed** must play *above* both the resonance frequency of the reed and the resonance frequency of the air column. When the reed is driven at resonance, the phase difference Φ is $-\pi/2$.

- An **inward striking reed** must play *below* both the resonance frequency

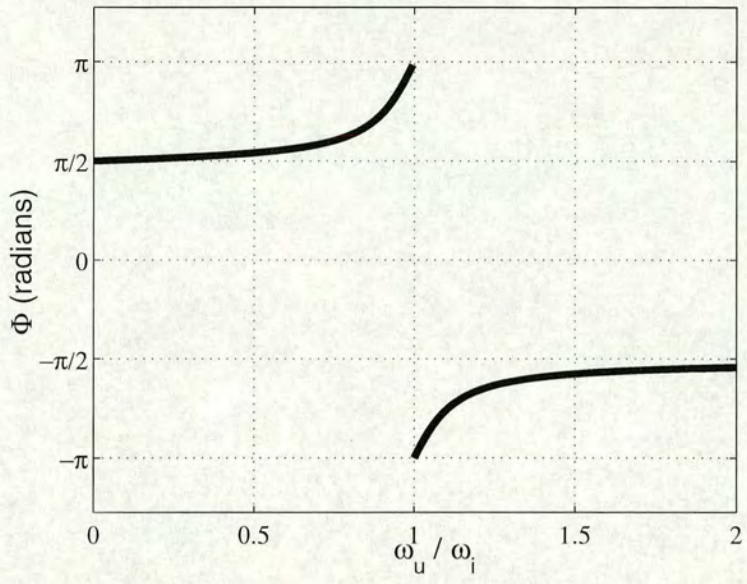

Figure 2.4: Phase difference between volume flow and pressure difference as a function of volume flow frequency.

of the reed and the resonance frequency of the air column. When the reed is driven at resonance, the phase difference Φ is $+\pi/2$.

2.4 Basic Model

The reed is coupled to the resonator in a feedback loop (see figure 2.1), controlled by the flow U and the pressure difference across the reed ΔP (and consequently, by assuming a static supply pressure, by the pressure in the mouthpiece, P_i). Section 2.3 gave phase relationships for a driven oscillator. The lip reed can be modelled by a set of equations describing the driven motion of the oscillators in

the system:

$$\frac{\partial^2 \mathbf{X}}{\partial^2 t} + \mathbf{B_x}\frac{\partial \mathbf{X}}{\partial t} + \mathbf{K_x}\mathbf{X} = \mathbf{F}(\mathbf{X}, P_i, P_0), \tag{2.22}$$

where $\mathbf{X}$ is the vector representing the displacement of the lip, $\mathbf{B_X}$ is the matrix of effective damping coefficients, $\mathbf{K_X}$ is the matrix of effective spring coefficients, and $\mathbf{F(X, P_i, P_0)}$ is the vector giving the effective driving force divided by the effective mass of each dimension of the lip displacement.

For small amplitudes, this mechanical oscillator can be assumed to be coupled to only one air column resonance, close to the resonance frequency of the lip reed. Thus the equation of motion of the acoustic oscillator can be written as:

$$\frac{\partial^2 \psi}{\partial^2 t} + \frac{\omega_i}{Q_i}\frac{\partial \psi}{\partial t} + \omega_i^2 \psi = \frac{Z_i \omega_i}{Q_i} U(\mathbf{X}, \frac{\partial \psi}{\partial t}, P_0), \tag{2.23}$$

where $\frac{\partial \psi}{\partial t}$ is the oscillating mouthpiece pressure, p_i, ω_i is the relevant resonance frequency of the air column, Q_i is its quality factor and Z_i is the amplitude of its impedance. The flow into the instrument, U, is controlled by the opening area between the lips and the pressure difference across the lips.

A simple one degree–of–freedom lip model is shown in figure 2.5. The lips are represented by a mass m on a spring and dashpot with spring constant k and damping coefficient γ. The lip is constrained to move only in the y-direction. For simplicity it is assumed that the top and bottom lip motions are symmetric, and that the lip opening area is rectangular with a fixed width d. The lips are

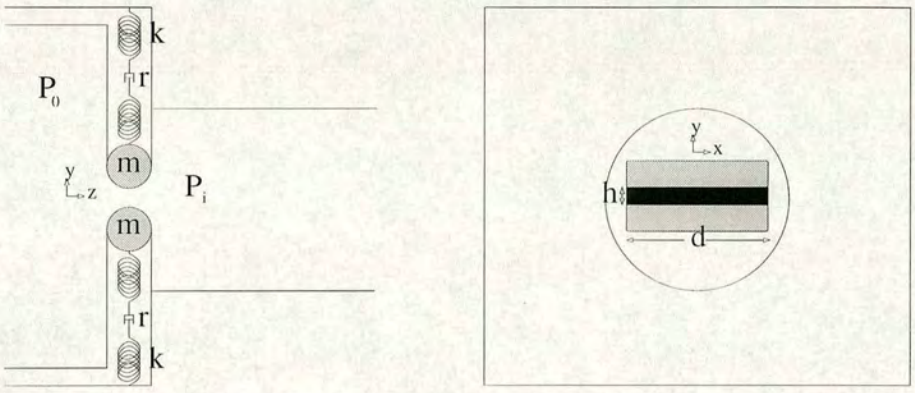

Figure 2.5: The lips can be represented by a simple damped mass on a spring model. To further simplify matters, the top and bottom lip are assumed to behave symmetrically ($h = 2y$), and the opening between them to be rectangular.

driven by the pressure difference, ΔP, between the mouth pressure P_0 and the mouthpiece pressure P_i. This driving force has two main components - the direct pressure differential and the "Bernoulli pressure" caused by the resulting flow of air, U.

The equation of motion for this model is therefore given by:

$$\frac{\partial^2 y}{\partial^2 t} + \frac{\omega_l}{Q_l}\frac{\partial y}{\partial t} + \omega_l^2 y = \frac{F(y, \frac{\partial \psi}{\partial t}, P_0)}{m_l}, \tag{2.24}$$

where ω_l is the resonance frequency of the lip, Q_l is the quality factor of that resonance and m_l is the mass of the lip.

The force term $F(y, \frac{\partial \psi}{\partial t}, P_0)$ describes the fluid forces on the lip. This is a combination of the force due to the pressure difference across the lips, and the force due to the flow through the lip channel.

The behaviour of the model presented here, and further models, is discussed further in chapter 5.

2.5 Striking behaviour of the lip reed

The phase and frequency relationships described in section 2.3 show that Helmholtz' [34] classification of the lip reed as a "striking–outwards" reed would require that it played only above the natural resonance of the resonator being played. However, this is at odds with the experience of musicians who find that they are able to force a note over a wide range of pitches - including above, below and at an acoustic resonance of the instrument being played [13].

Elliott and Bowsher [22] studied this phenomena, but their results were inconclusive. Chen and Weinreich [15] performed experiments using a custom built apparatus in place of an instrument that was designed to act as a single mode acoustical resonator. The resonant frequency of the device could be altered, and the acoustic impedance could be measured without the musician removing his lips from the device. The results of these experiments showed that the musician could play both above and below the resonance frequency of the device.

Yoshikawa [67] performed a series of experiments comparing the playing frequency with the resonance frequency of the instrument. His results also showed that the lip reed could play above or below the resonance frequency of the instru-

ment.

Experiments performed by Cullen [17] [18] and Neal [48] using an artificial mouth (with artificial lips) showed that the device they used to represent human lips could also play above and below the acoustic resonance.

Clearly, the evidence shows that Helmholtz' model of the lip reed fails to fully explain the behaviour of the lip reed. This study performs further analysis of the lip reed, using experimental studies using an artificial mouth and computational modelling.

Chapter 3

Threshold Experiments with an Artificial Mouth

3.1 Introduction

Historically, quantitative and thorough experiments on brass players have been difficult to carry out. Several problems present themselves to the inquisitive scientist, including:

- Limited lung capacity – the instrument can only be blown for a short time, and with variable pressure over that time.
- Embouchure adjustment – both conscious and sub-conscious movements by the player present a varying embouchure. A high level of consistency

between experiments is therefore impossible.

- Measurement – it is very difficult to attach measurement instruments to a human player. Introducing foreign objects into the player's mouth may also affect their playing ability and embouchure [66] [67].

- Repeatability – control parameters will vary not only from day to day, but from measurement to measurement [10].

The use of an artificial mouth overcomes these problems:

- Limited lung capacity – the mouth can play indefinitely, and with a constant pressure and flow rate.

- Embouchure adjustment – there are no sub-conscious adjustments to its embouchure.

- Measurement – it can be invaded with a a great rangee of measuring devices.

- Repeatability – a given configuration will remain approximately constant over long periods.

- Accessibility – artificial mouths are available at any time, for any length of time.

This study uses an artificial mouth which was inspired by the design used by Cullen [18] (as shown in figure 3.1). Figure 3.2 shows a photograph of this new artificial mouth. The artificial mouth uses latex tubes filled with water to represent

the human lips, and these are mounted on a hermetically sealed box (representing the mouth) into which air is blown by a pump.

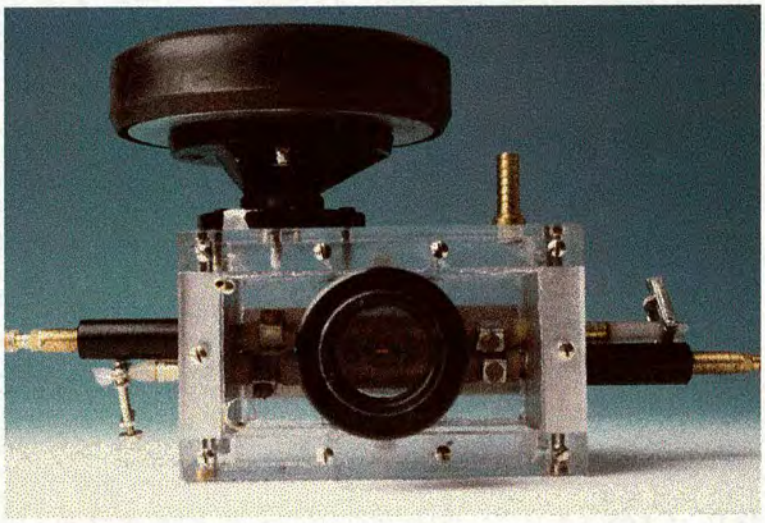

Figure 3.1: Cullen's version of the artificial mouth.

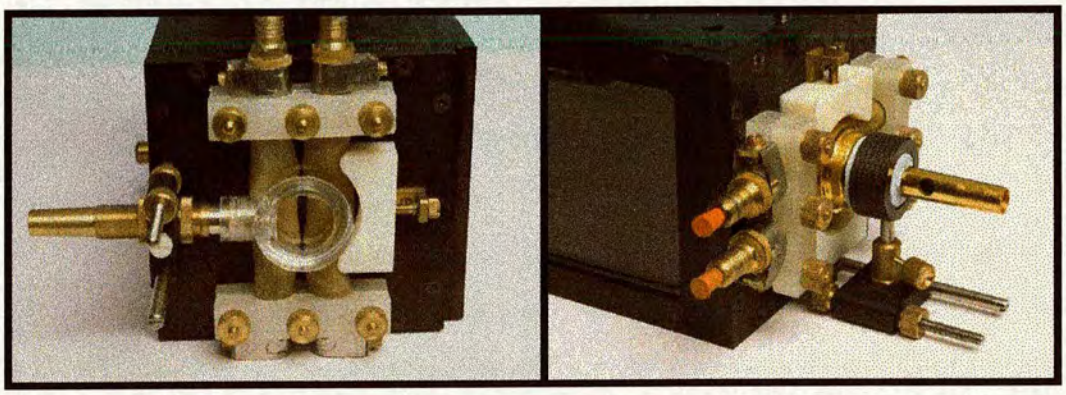

Figure 3.2: New version of the artificial mouth. This device is described fully in section 3.2. The image on the left shows the front of the artificial mouth with the transparent mouthpiece attached (see section 3.3). The image on the right shows the mouth with a Denis Wick 6BS mouthpiece attached.

The main difference between the mouth used in this study and that used by Cullen is that this version has the lips mounted *outside* the mouth cavity. This allows many different types of mouthpieces and instruments to be played by the

artificial mouth. This comes at the cost of having a reduction in the stability of the mouthpiece rim against the lips – in the system shown in figure 3.1 the mouthpiece rim was firmly bolted onto the front plate of the mouth, providing a far more rigid mounting than that provided by the new version of the mouth. It was therefore necessary to take great care not to disturb the mouthpiece when adjusting the apparatus.

In order to achieve a greater level of control over the parameters of the embouchure, several components were added:

- The equilibrium position of the lips is controlled by the "lip guide" blocks.
- The water pressure in the lips is controlled and measured by attaching a head of water, with variable height, to the lips.
- The position of the mouthpiece relative to the "teeth" is controlled and measured using a trolley and rail mechanism.
- The vertical postion of the mouthpiece can be accurately set using the trolley and mouthpiece holder.

Cullen showed that the lateral tension of the latex lips had little effect on the embouchure [18]. Consequently, control of this tension was omitted from the design of this artificial mouth.

3.2 Technical Details of the Artificial Mouth

Figures 3.3, 3.4 and 3.5 show the schematic diagrams for the new artificial mouth.

The artificial mouth was principally made of aluminium, and constructed from

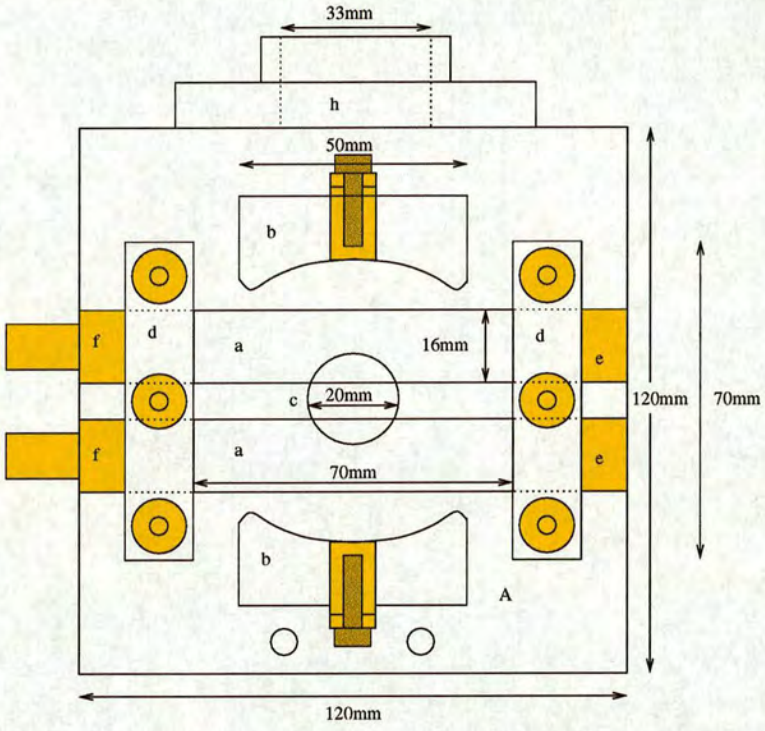

Figure 3.3: Schematic diagram of the artificial mouth (front view). The latex lips (a) were mounted on the front plate of the mouth (A) by the holding blocks (d), which held the brass mounts (e) and (f) which were slid inside the latex tubes of the lips. The lip guides (b) set the equilibrium position of the lips. The speaker mount (h) allowed a standard horn type speaker to be mounted. The hole (c) allows the air to flow from the mouth cavity through the lips.

a series of plates (A), (B), (C), (D), (E) and (F). The edges of these plates were liberally coated with vacuum grease and bolted together to form air–tight seals. The plates were 9.5mm in thickness. Plates (D) and (E) provided viewing windows allowing the mouth cavity to be observed. Plate (B) had two 8mm

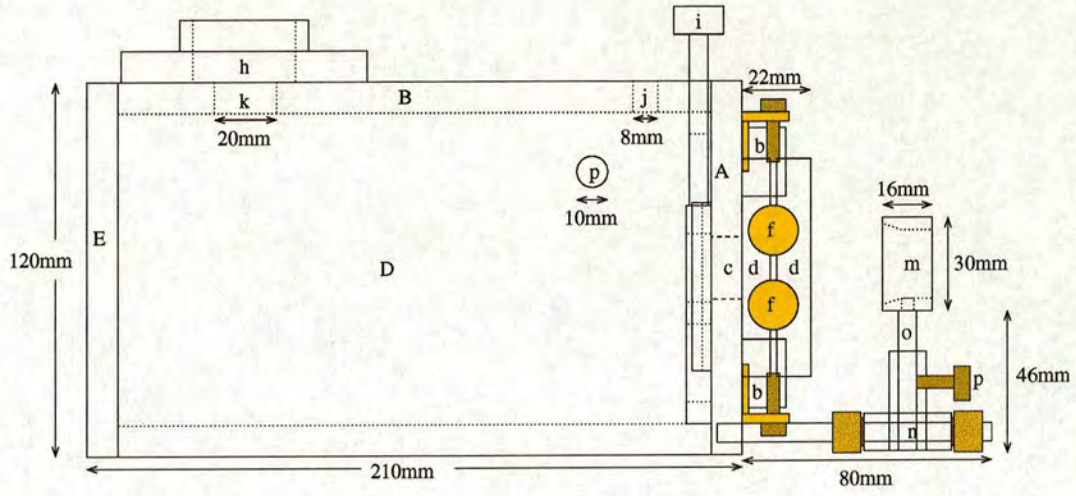

Figure 3.4: Schematic diagram of the artificial mouth (side view). The main plates of the mouth A, B, C (not visible), D, E and F were bolted together and sealed with vacuum grease. The speaker mount (h) was positioned over the hole (k) in the top plate to allow a loudspeaker to force air in and out of the mouth cavity. The hole (j) allowed measuring devices to measure the conditions inside the mouth cavity. The brass mounts (f) were placed inside the lips, and then held in place by the holding blocks (d). The lip guides (b) set the equilibrium opening position. The mouthpiece was held in the holder (m) which was mounted on a pole (o) secured in the transport mechanism (n). The height and angle of the holder was fixed with the PVC bolt (p). The "teeth" hole (c) allowed the air to flow from the mouth cavity through the lips. The "tongue" valve (i) provided a simple on/off control of the flow.

diameter holes (j) and one 20mm hole (k) cut in as shown. The (j) holes allowed microphones and manometers to be inserted into the mouth cavity.

A speaker mount (h) was used to mount a speaker over the hole (k). This mount was designed to accommodate a standard horn driver thread to allow a wide selection of speakers to be used. An adapter was also constructed to allow a standard cone loudspeaker to be attached to this speaker mount. This adapter is shown in figure 3.6. Plate (A) had a 20mm diameter hole cut in its centre (c) - the "teeth" hole, so called because it provided the support behind the lips

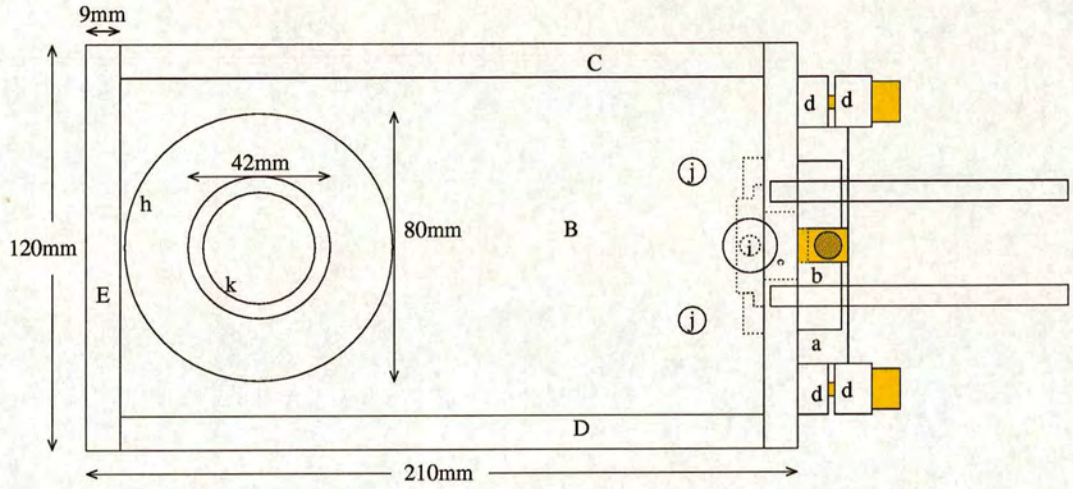

Figure 3.5: Schematic diagram of the artificial mouth (top view). The main plates of the mouth A, B, C, D, E and F (not visible) were bolted together and sealed with vacuum grease. The speaker mount (k) allowed a speaker to force air through the hole (k). The hole (c) allowed air to flow from the mouth cavity between the lips (a). The lips were held in place with the holding blocks (d), and their equilibrium position was set by the lip guides (b). The "tongue" valve (i) provided a simple on/off control of the flow.

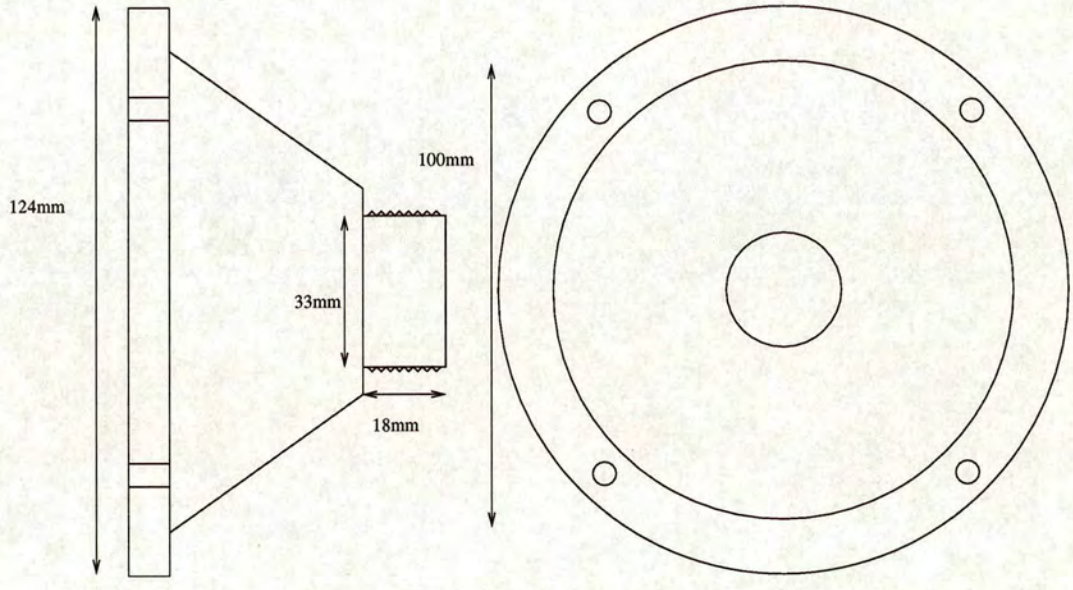

Figure 3.6: Loudspeaker adapter for mounting a cone speaker on the horn thread mount piece.

in a similar fashion to the teeth of a human player. The base plate (F) has a standard camera mount threaded hole partially drilled into it to assist with secure mounting.

The lips themselves (a) were latex tubes filled with water. Two different types of latex were used, with material thickness of 0.2mm and 0.3mm. These were provided by John Ward and Sons – an English manufacturer of latex rubber gloves. All lips were 16mm internal diameter. The latex tubes were coated in talcum powder and slipped over the brass mounts (e) and (f). These pieces were 16mm external diameter brass tubes. The right hand mounts (e) were closed at the external end, and open on the internal end. The left hand mounts (f) were open at both ends, but with a hose fitting on the external end. This allowed a hose to be attached to each lip to control and measure water pressure inside the lip. The hoses were raised up above the mouth to provide a water column of measurable height, which allowed calculation of the water pressure in the lips.

The lips were secured in place using the holding blocks (d). These blocks were made from from PVC, and were clamped together using the brass bolts and nuts (g). Once the lips were in place, they had an effective length of 70mm.

The lip equilibrium positions were controlled using the lip guides (b), again made from PVC. These allowed the equilibrium position of the lips to be easily controlled.

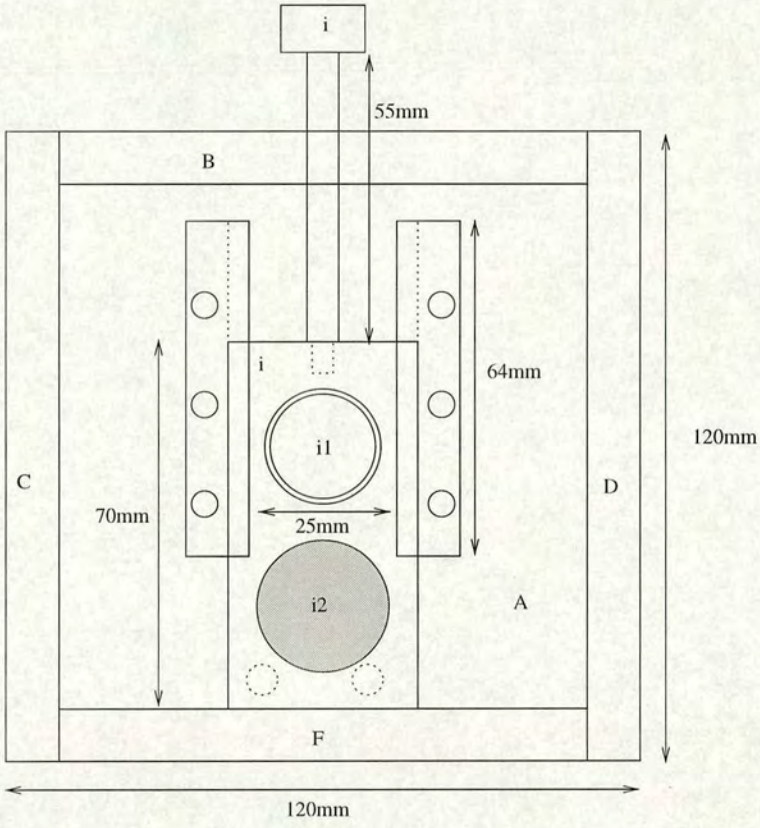

Figure 3.7: Schematic diagram of the artificial mouth (inside view). The "tongue" mechanism (i) provided a simple on/off control of the flow. The flow was stopped by sliding the perspex window (i2) into place over the "teeth" hole, and started by sliding the hole (i1) in front of the "teeth" hole.The front plate (A) was bolted to the plates B, C, D and F and sealed with vacuum grease.

A "tongue" mechanism (i) was also incorporated, and is shown in figure 3.7. This was a sliding panel on the inside of the front plate with two windows. One window was open (i1), while the other was closed off with a perspex window (i2).

The instrument mouthpiece was mounted in the holder (m), which was made from PVC, and was tapered at one side to accommodate the mouthpiece cup. The mouthpiece was held firmly in this mount by sealing it in with blu-tak. The holder (m) was then secured in the transport mechanism (n). This transport

mechanism consisted of a brass holder with a locking bolt and an aluminium base plate mounted on two rails. One of these rails was threaded, and had one nut on either side of the base plate to allow accurate and secure positioning of the mouthpiece. The threaded rail had a 1mm/rotation thread, and so any travel could be easily measured.

The mouth was designed to be modular, so that certain parts could be added or removed as necessary. For instance, in order to mount the transparent mouthpiece (discussed in section 3.3) one of the lip guides (b) had to be removed, and the mouthpiece holder (m) and transport mechanism (n) were removed and replaced with a special adapter designed to accommodate the transparent mouthpiece (see figure 3.8).

3.3 Transparent Mouthpiece

In order to view the motion of the lips a special transparent mouthpiece, shown in figures 3.8 and 3.9, was constructed. The design was inspired by similar mouthpieces used in similar studies [5] [16] [45] [68].

The mouthpiece cup was constructed from perspex, and the high-quality glass viewing window was fixed to the cup using silicon glue. A 2.2mm diameter hole was drilled into the side of the cup to allow a probe microphone to be inserted. The mouthpiece shank was cut from a Denis Wick 6BS trombone mouthpiece

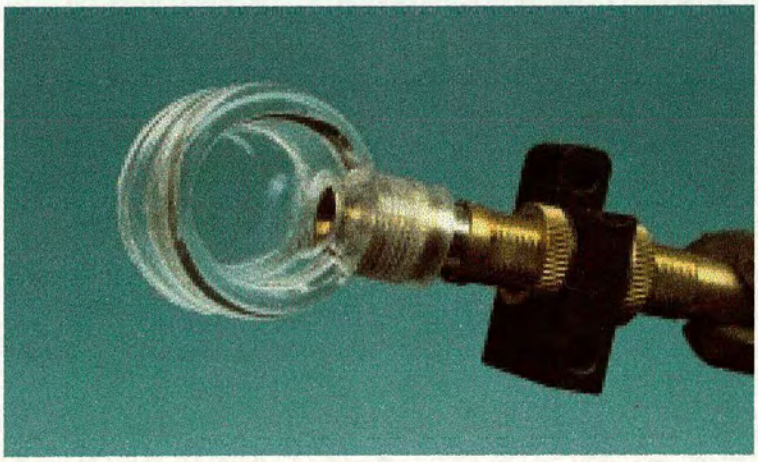

Figure 3.8: The transparent mouthpiece used to allow viewing of the lips, together with its mounting adapter.

and a thread carved to allow it to screw into the cup.

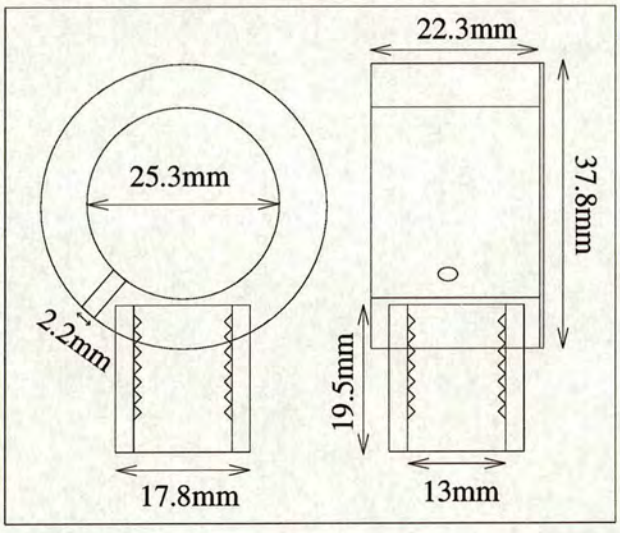

Figure 3.9: Schematic diagram of the transparent mouthpiece. The mouthpiece was made of three parts - the main barrel of the mouthpiece was made of polished perspex. The front window was made of glass, and the threaded adapter into which the mouthpiece shank was screwed was made of perspex. The perspex parts were glued together with perspex glue, and the glass window was glued to the barrel using silicon glue.

The mounting adapter was designed to allow the mouthpiece position relative

to the mounting rails to be accurately controlled. The adapter is shown in figure 3.10. It consists of two main pieces - a brass sleeve (Ma) that fits over the mouthpiece shank, and an aluminium block (Mb) that mounts onto the rails at the front of the mouth.

The internal bore of the adapter has two distinct sections, and was designed to have as small an effect as possible on the impedance of the instrument. The first section follows the external bore of the shank used in the transparent mouthpiece to provide a tight fitting seal. The ridge before the second section matches the internal diameter of the adapter to the internal diameter at the end of the mouthpiece shank, which ensures a smooth transition between the adapter piece and the additional length of pipe introduced by the adapter. The following section of internal bore is cylindrical - designed as such to have a minimum effect on the characteristic impedance of the mouthpiece. The outside of the adapter also has two sections. The first section is threaded, allowing the height of the mouthpiece relative to the face plate of the artificial mouth to be adjusted and firmly fixed. In order to further secure the mouthpiece, two sides of the external surface were flattened, and a PVC grub screw (Mc) was used to lock the adapter in place on the aluminium block, as well as two brass nuts (Md) and washers (Me) on either side of the block.

This mouthpiece behaves only slightly differently to a normal brass mouthpiece when playing the lower modes on the trombone. The volume of the cup of

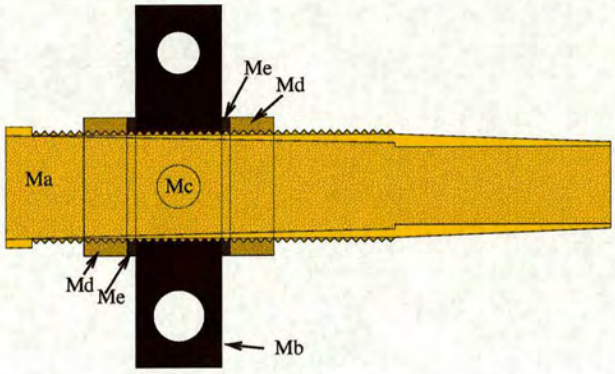

Figure 3.10: Cross-section of the transparent mouthpiece adapter.

the transparent mouthpiece was 12ml. This volume was not chosen by design, but was dictated by the physical restrictions imposed during the construction of the mouthpiece. The mouthpiece was chosen to have a rim size comparable to that of the Denis Wick 6BS mouthpiece, and the depth of the mouthpiece was chosen to provide enough material strength to safely mount the shank. The input impedance of the mouthpiece is shown in figure 3.11 (see section 3.4.2 for the experimental method used to obtain these data). This figure also shows the impedance of the Denis Wick 6BS mouthpiece from which the shank was obtained. This mouthpiece had a cup volume of 9ml. The input impedance of the J. Higham trombone with the two different mouthpieces attached is shown in figure 3.12.

In addition to the input impedance, tests by musicians have confirmed that the mouthpiece plays "as well" or even "better" than the standard mouthpiece in the lower modes, but the performance at the higher modes is poor. The input impedance reflects this impression - the lower modes have strong impedance val-

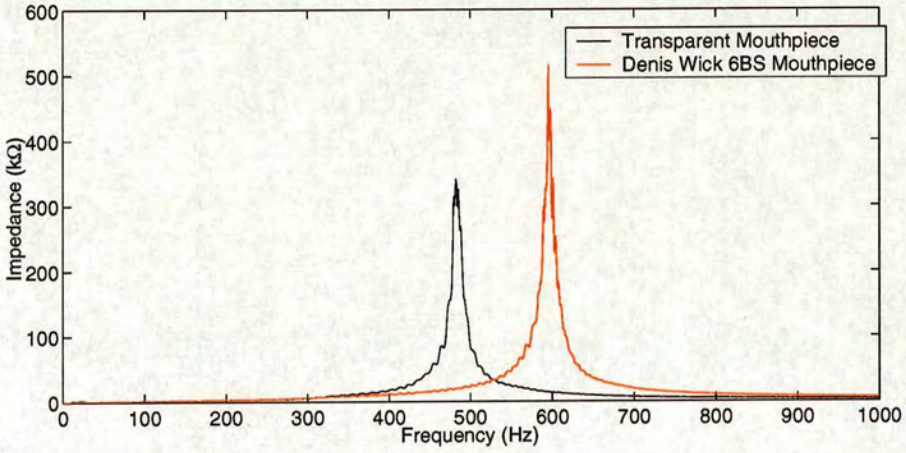

Figure 3.11: Input impedance of the transparent mouthpiece and the Denis Wick 6BS mouthpiece.

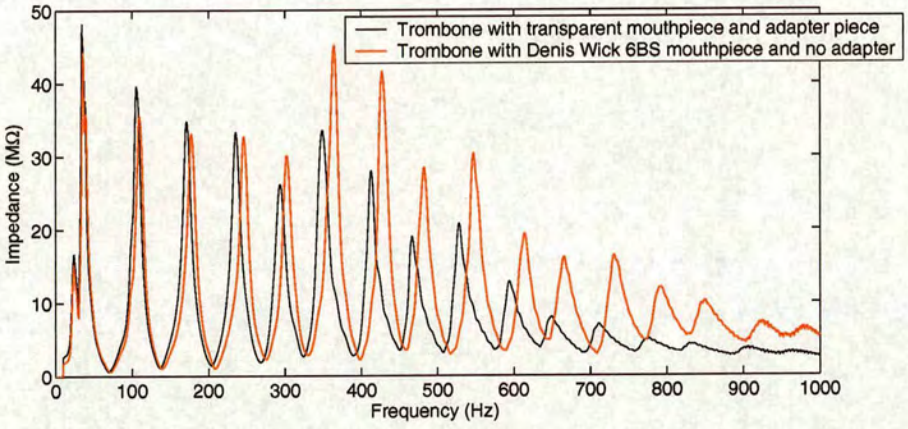

Figure 3.12: Input impedance of the J. Higham trombone with the transparent mouthpiece and with the Denis Wick 6BS trombone mouthpiece.

ues, whereas the higher modes have comparatively very weak impedance values, compared to those provided with the normal mouthpiece. The frequency shifts seen here are due to the presence of the extra length of tubing in the mouthpiece adapter.

3.4 Experiments

Using the artificial mouth, it is possible to create a broad range of playing situations, tailored to the problem in hand. The areas of interest are:

- Lip resonance properties - is is essential to know these properties for a full understanding of the system.
- Control parameters - how the behaviour of the is lips affected by changing the various settings available.
- Threshold playing behaviour - in order to reduce the complexity of the system, threshold measurements allow assumptions to be made about the linearity of the system.
- Non-linear behaviour - how the system changes as the relevant amplitudes are increased.
- Acoustic coupling - how the coupling between the lip reed and the acoustic resonator is controlled.
- Lip motion - how the lips move while playing a note. How does this behaviour vary across notes and musicians?

The artificial mouth was designed with these applications in mind. The experimental setup, a photograph of which is shown in figure 3.13, was designed so that

all these situations could be investigated with only small configuration changes. Detailed descriptions of the setup are given for each type of experiment in the following sections.

In order to obtain useful results, measurements were taken of:

- Lip motion
- Volume flow
- Mouth pressure - both static and oscillating
- Acoustic pressure in the mouthpiece
- Output acoustic pressure
- Water pressure in the lips

These parameters allow us to record the complete state of the system at any given time. There are two types of recording device used to capture the behaviour of the system:

- Microphone - Brüel and Kjær (B&K) microphones were used to record the pressure variations at various points in the system. An Audio-technica ATM31a cardiod response condenser microphone was used to record the radiated sound.
- Photodiode - the opening area between the lips was recorded by collecting the light admitted through them. A small laser was used to provide the

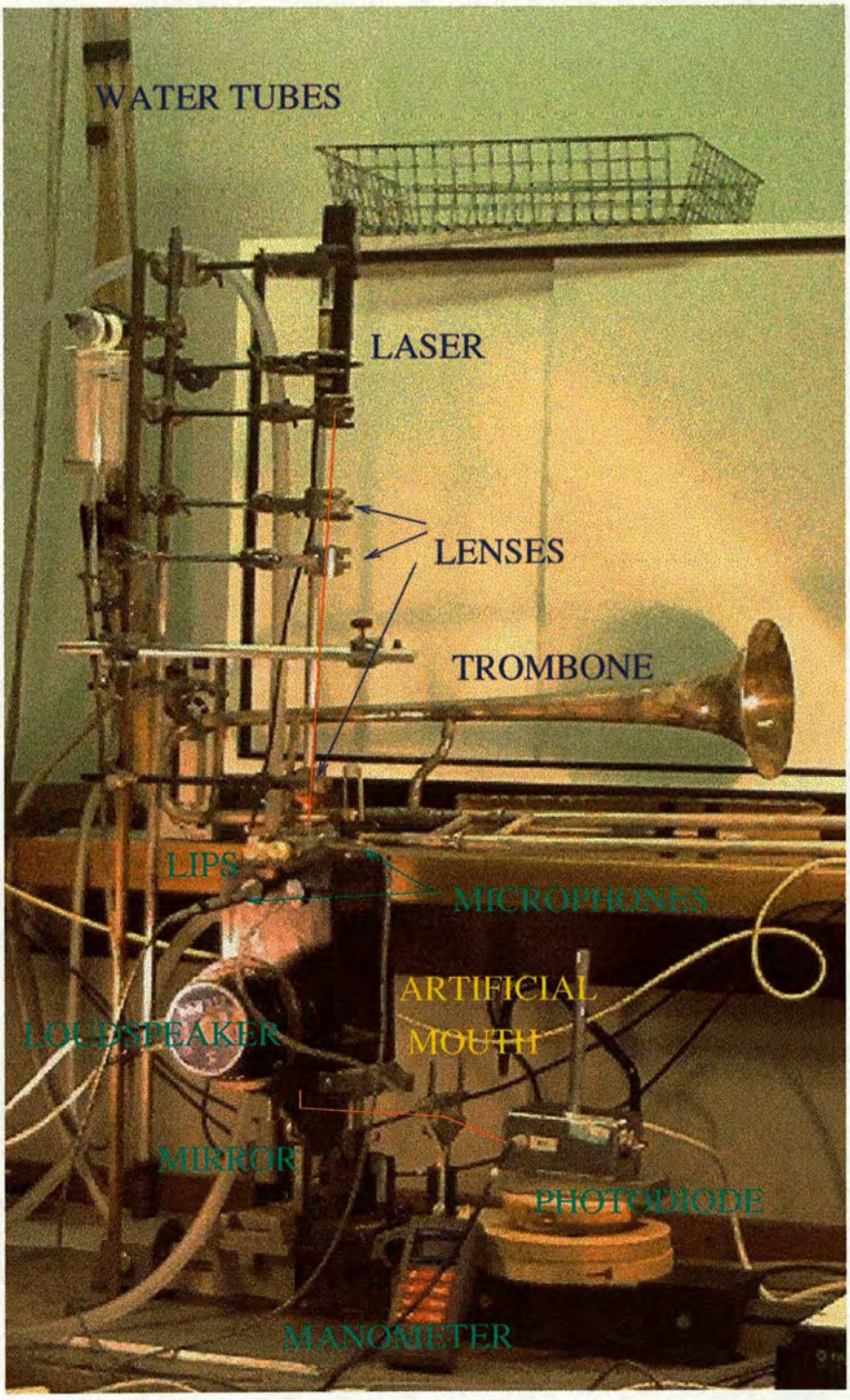

Figure 3.13: Photograph of experimental setup. This particular setup was used to measure the threshold playing frequencies of the system with various extensions of the trombone slide.

light source. The laser beam was expanded to flood the lip area, then focused down onto a type IPL10530DAL Hybrid Detector photodiode. This photodiode had a linear response up to 65kHz.

A static head of pressure was applied to the mouth from an Air Control Industries Ltd 8MS11 0.25kW pump. A Rotameter flow meter which measured flow rates between 0.05 and 0.5 ls^{-1} (with a resolution of 0.01 ls^{-1}) connected between the pump and the mouth gave the volume flow rate. In order to measure larger flow rates, a UCC flow meter was used, which could measure between 0.33ls^{-1} and 2.17 ls^{-1}, with a resolution of 0.08 ls^{-1}. The pressure was controlled using a variable valve which allowed smooth and continuous variation of the supply pressure. A Digitron p200UL manometer and a B&K Type 4938 $\frac{1}{4}''$ microphone measured the static and oscillating pressure inside the mouth cavity, respectively. A B&K Type 4192 $\frac{1}{2}''$ microphone with a short (31mm) probe was inserted into the mouthpiece to give the alternating component of mouthpiece pressure. A calibration curve for this probe adapter was produced and all results were filtered appropriately using a Matlab program. The Audio-technica ATM31a condenser microphone placed at the end of the instrument recorded the radiated acoustic pressure.

The instrument used in these experiments was a J. Higham tenor trombone, a trombone was chosen because it allowed smooth control over the resonance frequencies of the downstream resonator. The mouthpiece used was the trans-

parent mouthpiece presented in section 3.3. This allowed a laser to be shone through the transparent mouthpiece to illuminate the lips. The amount of light passed through the lips was recorded using the photodiode, providing a signal that was directly proportional to the opening area between the lips. This was checked by measuring the voltage change as the diode was exposed to laser light admitted through a variable slit of known width. These various signals were all collected and analysed using the B&K PULSE system. The PULSE system and the analysis and aquisition tools used in this study are described in appendix A. The PULSE system served as both a data acquisition device and as an analysis tool. The system was set to perform real-time FFTs of the relevant signals and, where appropriate, deconvolution of signals. The configuration of these functions was chosen separately for each experiment. The PULSE system makes use of pre-existing calibration data for B&K microphones, but using probe adapters or other microphones required further adjustment to the data. In order to compensate for phase and amplitude shifts, the recorded data was exported from PULSE into Matlab. Matlab programs were written to perform this phase inversion and further analyse the recorded data.

Calibration was performed by using a B&K Type 4134 $\frac{1}{2}''$ microphone as the reference microphone. For probe adapters, a calibration vessel with mounting holes for both the $\frac{1}{2}''$ and probe adapters was used which allowed both microphones to record the signal from a small speaker simultaneously without any external sound field. For other microphones, a free-field measurement was made

in an anechoic chamber. For the frequency range typically examined in this study, there was little distortion on any microphone, and even the probe adapter required only small adjustment of phase and amplitude. This adjustment was also performed by a Matlab program, using calibration data shown in figure 3.14

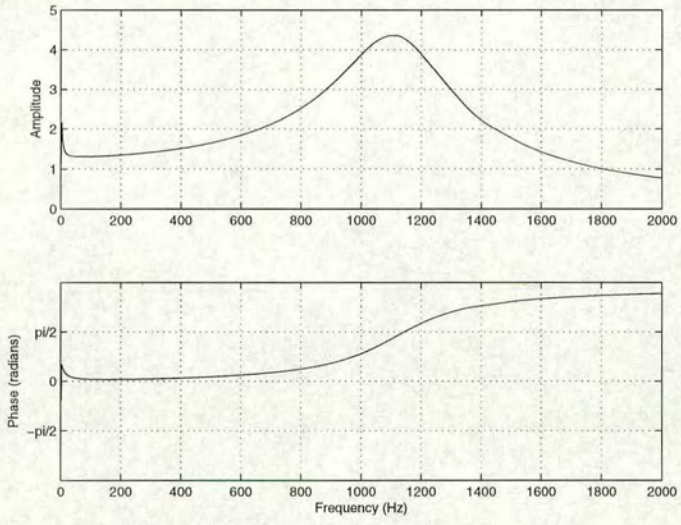

Figure 3.14: Calibration data for the probe microphone

As can be seen, the phase shift below 500Hz is small (less than 8°), but significant enough to be taken into account. Consequently, all data recorded with the probe microphone was adjusted appropriately before final analysis.

3.4.1 Lip Response Measurement

Experimental Setup

Frequency domain analysis is one of the most useful methods for investigating any oscillating system. In this case the response of the lips is measured by recording the lip opening area as it is excited by an acoustic pressure signal.

The experimental setup is shown in figure 3.15. This setup was similar to that used by Cullen [18] and Neal [48], with two key differences:

- The PULSE system was used as the data aquisition device. This allowed real time analysis of the data, as well as a great deal of extra flexibility in terms of the recorded and reproduced signals.
- The transparent mouthpiece was used instead of the standard style mouthpiece. This allowed the entire lip area to be viewed instead of the small section viewable through the mouthpiece shank. This also meant that the entire opening area could be recorded, rather than just the opening height at the centre of the lips.

The loudspeaker mounted on the mouth cavity provided the excitation signal, which was measured by the B&K Type 4938 $\frac{1}{4}''$ microphone inserted into the cavity. The resulting motion of the lips gave a varying area of opening that allowed an amount of laser light proportional to that area to pass through the

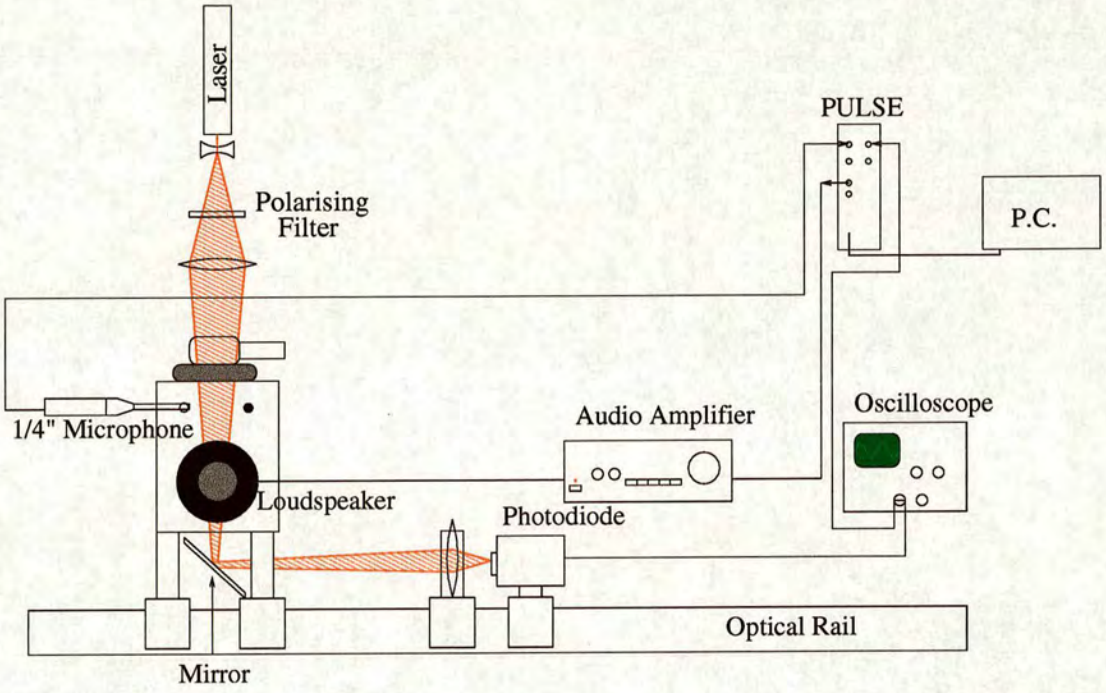

Figure 3.15: Diagram of experimental setup.

lips and be collected by the photodiode. The resulting microphone and diode signals were recorded and analysed by the PULSE system. The excitation signal was generated by a Matlab program. This program generated a swept sine wave signal that could make use of a calibration curve to provide an input signal with an almost flat spectrum over the frequency range of interest. The calibration curve was obtained with the same apparatus, using only the microphone signal to provide the scaling data.

The PULSE system was set to deconvolve the input signals from the microphone and the diode, and report the resulting FFT magnitude and phase. These data showed the frequency response of the lip opening area for any choice of input signal. The input signal had to provide energy to the system at the frequencies of

interest, but any signal could be used provided it met this condition. A swept sine wave was chosen because it could provide enough energy to give a measurable lip response, and could be easily customised to include the frequencies of interest.

It should be noted that driving the lips with an oscillating pressure in the mouth cavity is the opposite of what happens during a normal playing situation. During playing, the oscillating driving force is predominantly provided by the resonant air column of the musical instrument. However, when one considers that the driving force is provided not by any absolute pressure, but by the pressure difference across the lips, it becomes clear that the two different driving situations are equivalent. Figure 3.16 shows a diagram with the relevant pressures. If we assume a sinusoidal driving pressure, P, given by:

$$P = P_0 sin(\omega t + \phi), \tag{3.1}$$

it is clear that ΔP, the pressure difference across the lips, will be simply phase shifted by π when switching from a driving pressure inside the mouth to a driving pressure downstream.

In some situations, it was inconvenient to drive the lips from the mouth cavity, so a device was constructed which allowed the loudspeaker to be attached to the mouthpiece to provide an oscillating pressure from the downstream side. This device, shown in figure 3.17, was simply a plastic cylinder with a loudspeaker mounted on one end, and two holes cut into the sides to allow the mouthpiece

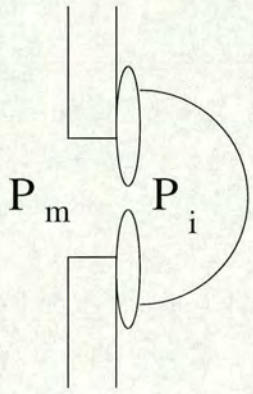

Figure 3.16: The lips are driven by the pressure difference $\Delta P = P_m - P_i$

and a tail pipe to be attached. When this device was used, the reference signal

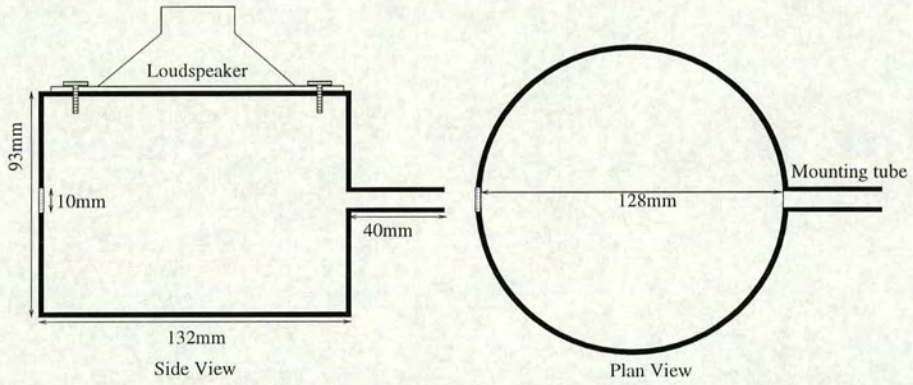

Figure 3.17: The loudspeaker coupling device. This device applies the driving pressure from the downstream side of the lips. The mouthpiece shank fits into the hole on the left side of this diagram. The speaker box is held in place using the mounting tube on the right hand side of this diagram.

was provided by a B&K Type 4192 $\frac{1}{2}''$ microphone with a short (31mm long) probe attachment, inserted into the mouthpiece cup. This microphone and probe were calibrated against a B&K Type 4134 $\frac{1}{2}''$ microphone, as described in section 3.4.

In order to obtain a lip response measurement, the following steps were carried

out:

- An embouchure was set up (with the trombone in place) that would play within the desired frequency range.
- The trombone was carefully removed.
- The mouth was left playing for an extended period of time (approximately 20 minutes) to ensure that the embouchure was stable. The playing frequency was recorded, as well as any time domain samples required.
- The supply pressure was turned off and the supply valve closed.
- All signal levels were set to ensure maximum signal strength without saturation.
- The excitation signal was played on a continuous loop through the loudspeaker.
- After a pause of 1 second, the PULSE system began recording (see appendix A for details).
- Once a stable response curve had been obtained (ie, there was no additional reduction in the signal noise from successive signal sweeps - typically obtained after three sweeps) the recording and playback were simultaneously halted.

EX BIBL. UNIV. EDINBURGH

In order to obtain the desired embouchure, there were several key parameters that had to be adjusted simultaneously:

- Lip water pressure
- Area of opening between the lips
- Mouthpiece position

These parameters are dependant on one another. Increasing the lip water pressure decreases the area of opening as the lips expand. Similarly, decreasing the area of opening by adjusting the lip guides increases the water pressure slightly due to the increased external pressure on the lips. Pushing the mouthpiece closer to the face plate increases the water pressure, and at the same time changes the area of opening between the lips.

Obtaining an embouchure that would play within a desired frequency range was very much a case of trial and error, based on adjusting the three key parameters mentioned above. However, certain guidelines can be used to give a starting point. For a low note, the water pressure in the lips should be low (approximately 1kPa) and the mouthpiece should be relatively far back from the face plate (approximately 4mm). For higher notes, the water pressure should be high (approximately 6kPa) and the mouthpiece closer to the faceplate (approximately 2mm). In either case, the embouchure would not play if the area of opening between the lips was set incorrectly. Too wide an opening and the air would flow

through the channel unhindered, applying little force to the lips. Too narrow an opening would cause the flow of air to be too slow, again reducing the force on the lips to a negligible level. The embouchure would typically play if the the height between the lips was approximately 0.5mm – 1mm.

Experimental Results

Figure 3.18 shows a typical mechanical lip response obtained using the methods described above. Further mechanical lip response data are given in appendix C.

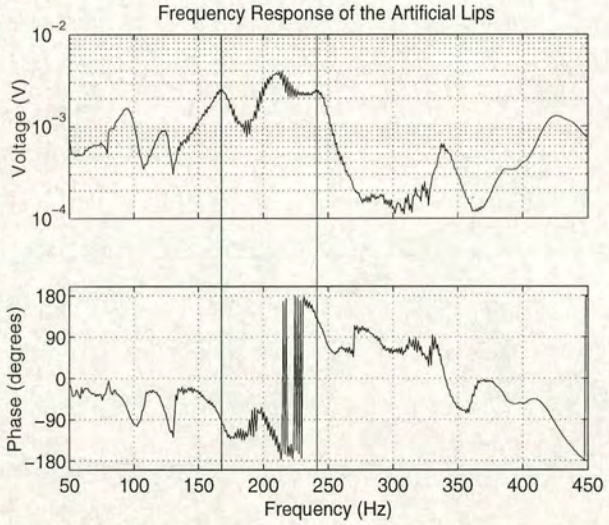

Figure 3.18: Frequency response of a typical configuration. The voltage of the diode signal is proportional to the area of opening between the lips. The vertical lines show the destabilising outward and inward striking resonances, at 167Hz and 242Hz respectively.

Immediately it is clear that this system is very complicated, with several resonant peaks showing in the response curve. Note that this experiment used only the mouthpiece, with no instrument on the downstream side of the lips. The

role of the resonator is examined in section 3.4.3. On either side of the playing frequency there are consistently two resonances – with phases of $-\pi/2$ and $+\pi/2$. These phases classify these resonances as outward striking and inward striking respectively, as shown in section 2.3. Previous work by Cullen [18] and Neal [48] have shown similar results, particularly the presence of an outward/inward pair of resonances between which the reed will always play. Another consistent feature is the presence of a resonance which is π radians out of phase with the driving pressure. These key features are always present in the lip response measurements, although occasionally they are so close together in frequency that they become indistinguishable. This is especially true if the resolution of the data is low, as in the results obtained by Cullen and Neal.

Repeated measurements of the same embouchure produce consistent data sets, and the main shape of a response will typically be retained if the mouth is reconfigured in the same way in subsequent sessions. Achieving this in practice is difficult due to the inter-dependence of the parameters of the embouchure, as well as some currently uncontrollable parameters – such as the angle at which the mouthpiece sits in its adapter. Such parameters are discussed in section 6.1, together with some possible modifications that could be made to the apparatus.

From these results, it is possible to derive numerical measurements of the resonance characteristics of the reed. The resonant frequencies are trivially determined; in the case of the response curve shown in figure 3.18 the frequencies

of the two highlighted resonances are 167Hz and 242Hz. Determining the quality factor of the resonances is a less trivial process, because this curve clearly does not describe a linear simple harmonic oscillator. The most useful method is to apply curve fitting to the well defined parts of the curve. As can be seen from figure 3.18, the curves can be distinctly lacking in useful data for this purpose, so an approximation is all that can be made. A quality factor of between approximately 3 and 8 is consistently measured using curve fitting methods. These measurements can be used as parameters in mathematical models of the lip reed. The resonant frequency can be measured with great accuracy, and as such can be easily transferred to a model. However, the quality factor measurements are less well defined, and as such provide nothing more or less than an order of magnitude estimation for model parameters. This is discussed further in chapter 5, where it also becomes clear that an order of magnitude estimation is all that is desired for modelling purposes.

The additional data sets presented in appendix C show the main features seen in figre 3.18 are consistent – namely, the presence of outward/inward pairs of resonances. Figure C.4 shows two such pairs – and this embouchure would play two different notes on the trombone (each within one of these pairs) with minimal adjustment of the system.

3.4.2 Input Impedance Measurements

The measurement of the input impedance of an object provides particularly useful information on the resonances of that object. The resonances of the object can be categorised by three parameters:

- Resonance frequency.
- Quality factor.
- Impedance magnitude and phase.

One method of measuring the input impedance is to apply a signal with a known acoustic volume velocity to the entrance of the instrument, and measure the resulting pressure inside the instrument (see equation 2.3). This technique is well established using stepped sine waves as the input signal [6] [7] [56].

This study uses the BIAS system (version 5.1), developed at the Institut für Wiener Klangstil [40], This is a compact hardware and software package that can measure the input impedance of an object [1]. This package uses a chirp signal instead of a stepped sine wave, and can therefore produce results in just a few seconds, rather than the several minutes required for the use of a stepped sine wave signal.

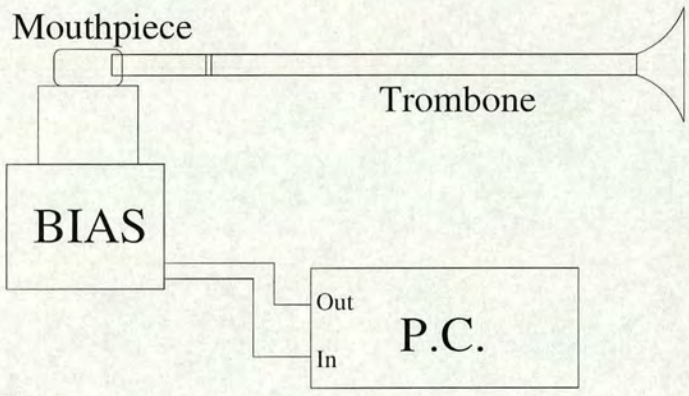

Figure 3.19: Experimental setup for the measurement of input impedance using the BIAS system.

Experimental Setup

In order to obtain the input impedance of an object, the setup shown in figure 3.19 was used. The BIAS head was attached to the mouthpiece of the object to be measured and clamped firmly in place, ensuring an airtight seal. The object and head were placed on a carpet tile to reduce background noise levels, and a measurement was made. In order to obtain all the data required for this study, several different object configurations were measured. These included:

- the trombone with the standard Denis Wick 6BS mouthpiece;
- the trombone with the standard Denis Wick 6BS mouthpiece and the adapter piece (see figure 3.10);
- the trombone with the transparent mouthpiece (see figure 3.8);
- the trombone with the transparent mouthpiece and the adapter piece, with

the slide extension varied in 5cm steps;

- the Denis Wick 6BS mouthpiece; and
- the transparent mouthpiece.

Experimental Results

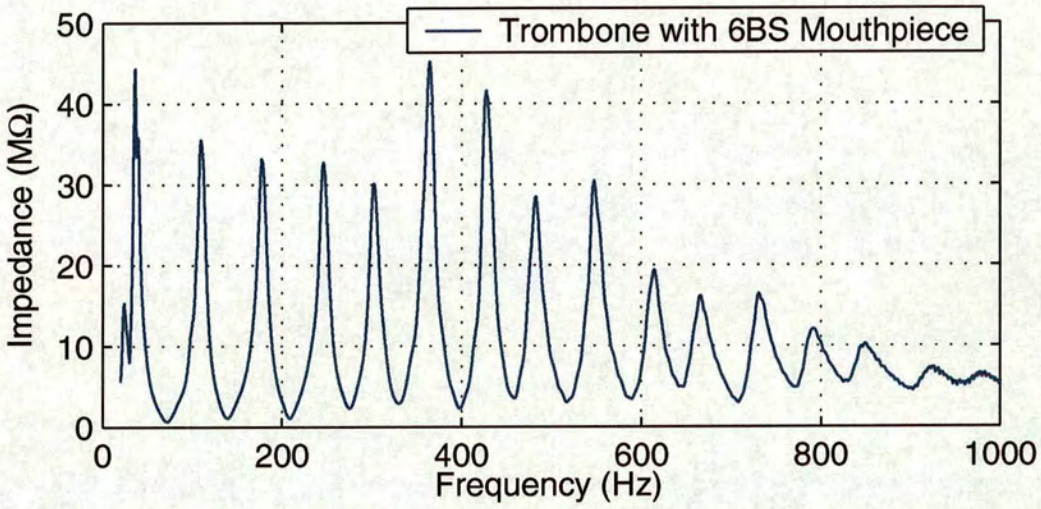

Figure 3.20: Input impedance curve for the trombone and Denis Wick 6BS, with the slide unextended.

Figure 3.20 shows a typical input impedance measurement, in this case for the J. Higham trombone with the Denis Wick 6BS mouthpiece attached. The frequency, quality factor and amplitude of each resonant peak are given in appendix B.

3.4.3 Threshold Playing Behaviour

In order to investigate the fundamental behaviour of the lip reed, it is convenient to examine its behaviour in a linear regime. This is possible by looking at the behaviour near threshold, defined as the point at which the system enters self-sustained oscillation. This point is typically defined by a blowing pressure, and is characterised by the resulting playing frequency. Analysing how the system destabilises allows the type of reed to be defined, using the inward and outward striking reed definitions given in section 2.3.

Experimental Setup

In order to investigate this threshold behaviour, the experimental setup shown in figure 3.21 was used. In this setup, the trombone was attached to the mouthpiece using the adapter piece. The trombone was firmly clamped in place to prevent changes to the sensitive embouchure caused by the potentially large forces applied by the trombone to the mouthpiece. The slide was left unclamped so that it was free to move, but it was supported along its length.

The lips were configured to play a given mode on the trombone, the frequency of which was determined from the input impedance measurements described in section 3.4.2. The frequency response of this embouchure was measured as described in section 3.4.1. In order to measure the threshold behaviour, the supply

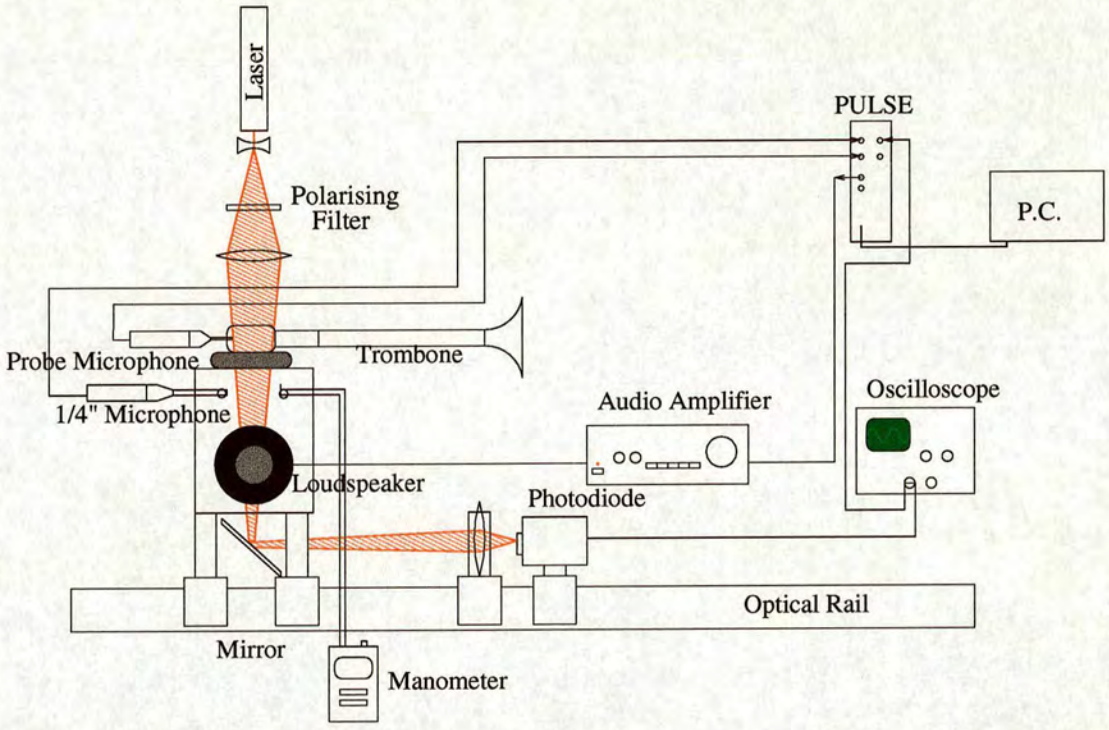

Figure 3.21: Experimental setup for measuring the threshold playing behaviour.

pressure was slowly increased until the lips began to play the trombone. Often the note was too quiet to hear initially, so the oscilloscope was used to monitor the diode signal. The pressure was then reduced to the minimum level required to sustain the note. The frequency of the played note was recorded. It should be noted that in many cases the pressure required to sustain the note was less than that required to initiate oscillation. The flow was then stopped and the slide of the trombone extended by 5cm, and the process repeated. Thus measurements showing the threshold playing frequency as a function of the trombone slide extension, and consequently of the resonance frequency of the instrument, were obtained. The data obtained in section 3.4.2 were used to give the values of the trombone resonances for a given slide extension. The frequencies of the lip

resonances were taken from the lip response data obtained at the begining of the experiment.

Experimental Results

Figure 3.22 shows one set of data. As can be seen, this data is qualititavely similar to data obtained in similar experiments by Cullen [18] and Neal [48]: the playing frequency crosses from below to above the trombone's resonance frequency as the slide is extended (and consequently the resonance frequency reduced). Playing below the instrument resonance is characteristic of inward striking reed types, whereas playing above the instrument resonance is characteristic of outward striking reed types, as shown in section 2.3.

Clearly inward striking and outward striking regimes cannot individually account for this behaviour. At either extreme of the data set, the reed could be classified as either inward striking (short pipe length, playing below the instrument and reed resonances) or outward striking (long pipe length, playing above the instrument and reed resonances). However, such reed types cannot play exactly on the instrument resonance, nor can they cross over it.

Note that altering the instrument resonance is equivalent to "lipping" a note, where the pitch is smoothly changed by the musician around a single instrument resonance by adjusting the embouchure. In the "lipping" case, it is the resonance frequencies of the lips that are changed, rather than the resonance frequencies of

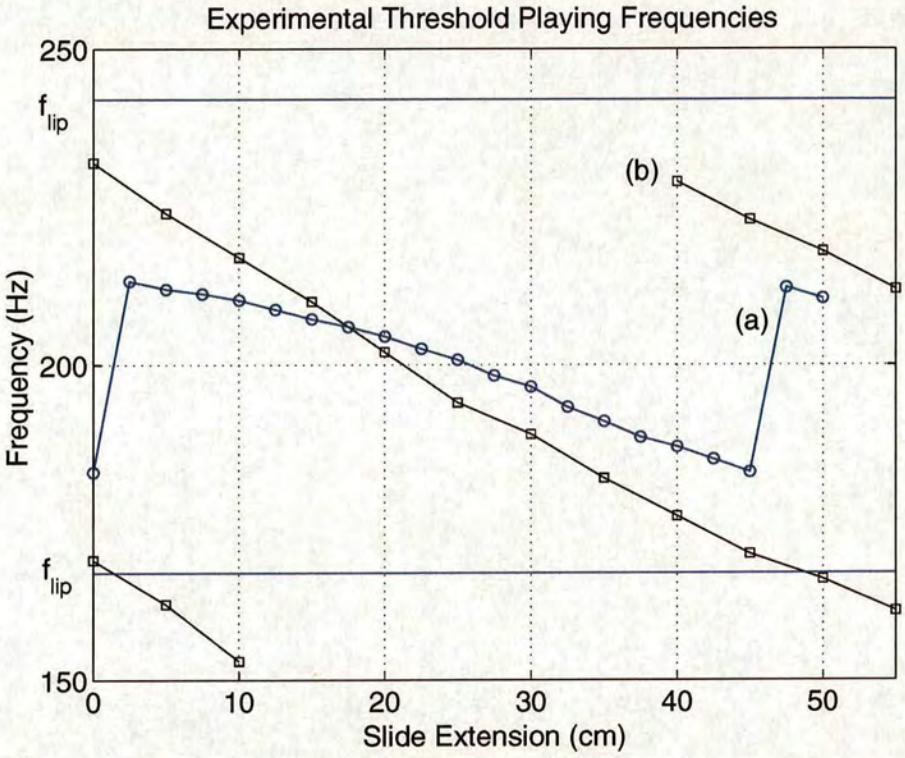

Figure 3.22: Experimentally measured threshold behaviour. Line (a) shows the threshold playing frequency. Lines (b) show the instrument resonances. The horizontal lines show the relevant lip resonance frequencies, identified in figure 3.18

the instrument. This study uses a variable instrument resonance because it was easier to control systematically than the resonance frequencies of the lips.

The system can also be seen to "jump" between the modes of the trombone at the extreme slide extensions (0cm extension and 47.5cm extension). The threshold playing frequencies suggest that there is a limited range of notes that the embouchure used in this experiment will play – in this case between 183Hz and 213Hz. This jump between modes corresponds to a switch between outward striking type behaviour on the lower mode, where the threshold playing is above

the local instrument resonance, and inward striking on the higher mode where the threshold playing frequency is below the instrument resonance. The point at which the threshold playing frequency crosses from below to above the same instrument resonance (at slide extension 17.5cm in figure 3.22) clearly does not exhibit such a sudden change in reed behaviour, but rather represents a continuous transition between the two modes of oscillation. Consequently, the use of such well defined, and opposing, reed types is clearly not appropriate for the description of this reed – such definitions do not allow for this kind of continuous change in the threshold playing frequency from below to above the instrument resonance. Instead, it is worth considering what kind of reed would allow this observed behaviour, and this is investigated in chapter 5.

3.4.4 Mouth Cavity Effects

Experimental Setup - Radiated Sound Investigation

Section 2.4 presents a description of the brass musician in terms of a set of coupled oscillators - the lips and the instrument. However, there is also a third resonator in the system - the vocal tract. This section investigates the effect that this has on the system.

The artificial mouth was designed to have a large cavity volume behind the lips so that the Helmholtz resonance of the cavity was sufficiently low as to be

insignificant. However, it is possible to alter the cavity volume by adding water. The Helmholtz resonance ω_H of a rigid-walled object with a cavity volume V and an outlet of length l and area S is given by [28]:

$$\omega_H = c\sqrt{\frac{S}{(l + 1.5\sqrt{\frac{S}{\pi}})V}}. \tag{3.2}$$

This equation is based on several assumptions. First, that the wavelengths of interest are much greater than the dimensions of the resonator. Thus the resonator can be treated as a series of lumped elements, specifically the neck and body of the object. Another assumption is that viscous losses are negligible compared with the acoustic radiation impedance. For systems where the neck has an area of approximately πcm^2 or greater this assumption is valid. However, in the typical playing situation the lip channel has an area of opening much smaller than this ($\sim 10^{-2}\text{cm}^2$). The effect is that the system has a much greater damping coefficient, which reduces the quality factor and the calculated resonance frequency. The final assumption is that the body of the resonator has rigid walls. This is largely true when using the artificial mouth, but in the case of the human vocal tract this is not the case - the soft walls mean that the damping of the system is further increased.

The maximum cavity volume of the artificial mouth was 1800ml. This could be reduced by adding water to the cavity to reduce the volume of air. A maximum of 1500ml of water could be added in this way. The position of the air inlet

fitting – part (p) in figure 3.4 – marked the maximum water level. Taking the approximate values $l = 10\text{mm}$ $(= 0.01\text{m})$ (the approximate length of the lip channel), $S = 6\text{mm}^2$ $(= 6 \times 10^{-6}\text{m}^2)$ (the approximate opening area of the lip channel) and $V = 1300\text{ml}$ $(= 0.013\text{m}^3)$ (the volume of the mouth cavity) we get an indication of the Helmholtz frequency of this system: $\omega_H \approx 550\text{rad/s}$. If the volume of air in the mouth cavity is reduced to its minimum value of 300ml, this value becomes $\omega_H \approx 1160\text{rad/s}$. These angular frequencies convert to approximately 87Hz and 185Hz respectively. Consequently, we expect to see a Helmholtz resonance for the mouth cavity of between $\approx$ 50Hz and $\approx$ 200Hz, depending on the configuration. The second and third modes of the trombone, with the slide unextended, fall into this region. In order to investigate the effect of the cavity on the played note, the radiated sound was recorded using the setup shown in figure 3.23. The mouth was mounted pointing upwards towards the ceiling to allow the cavity to be filled to its maximum level with water. The artificial mouth was reconfigured from the setup shown in figures 3.3 to 3.7. The 'speaker' plate (B) was inverted so that the small microphone holes (j) were at the bottom of the mouth. The speaker hole (k) was sealed with a rubber bung, as was one of the microphone holes. The other microphone hole acted as an outlet for the water, through a piece of tubing which was sealed in the hole. A Hoffmann clip was placed on the end of this tube, acting as a valve.

In order to observe subtle changes in the sound, 1 second samples were sequentially captured and analysed in a Matlab program. The Fourier transforms

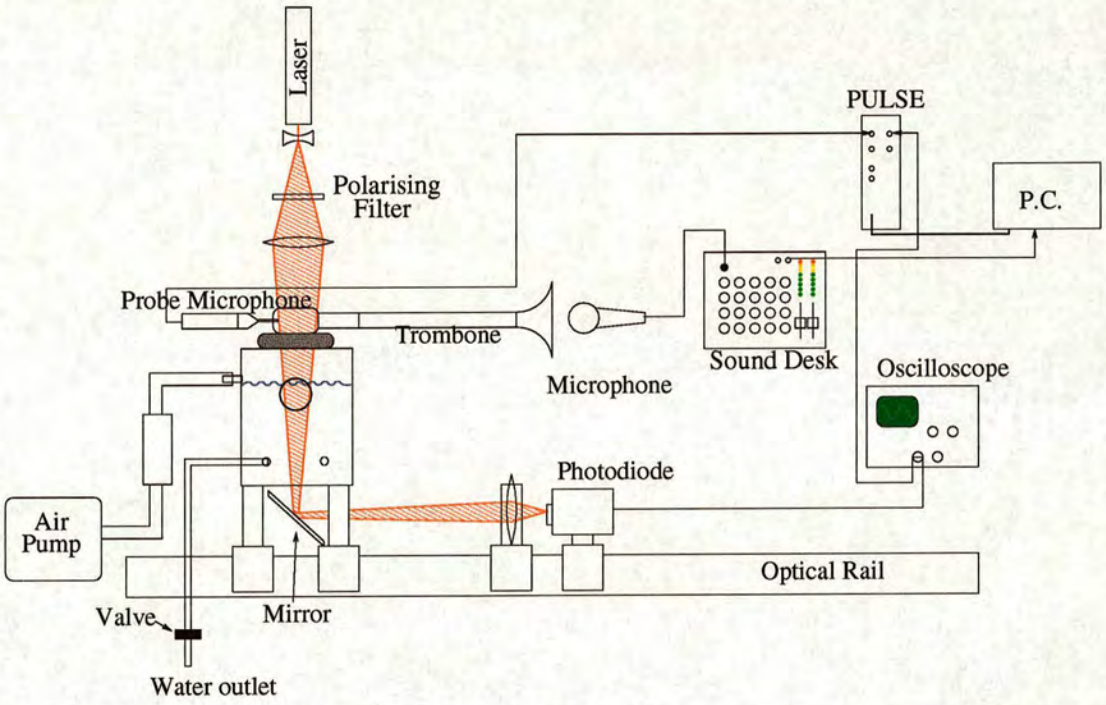

Figure 3.23: Experimental setup for measuring the radiated sound from the trombone, with varying mouth cavity volume. Water was added to the system through the air inlet to which the pump is attached in this diagram. Water was slowly removed by opening the valve on the water outlet a small amount. The radiated sound was recorded by the PC running Matlab, and analysed at the same time.

of these samples were analysed to determine the amplitudes and frequencies of the spectral peaks. The system was set up as in figure 3.23 with the maximum possible level of water (1500ml) in the mouth cavity. This gave a remaining cavity volume of 300ml. The system was set playing the second mode of the trombone, with the slide unextended, and the data acquisition started. In order to eliminate any changes in radiated sound due to transient behaviour in the system, no changes were made to the system for a significant length of time (approximately 20 minutes). This ensured that the system had settled into a steady state. Once it was established that the radiated sound was constant, a valve was opened at

the base of the mouth allowing the water to leave the mouth cavity slowly. The flow rate was held constant at 7.6ml per second.

Experimental Results - Radiated Sound Investigation

The results of these experiments showed very little variation in the timbre, pitch or amplitude of the radiated sound as the cavity volume was changed. The largest change in the radiated spectrum was observed as the volume of air in the mouth cavity was increased from 300ml to 550ml, as shown in figure 3.24. The steady state before the water valve was opened is shown in the first section of this figure. The valve was open during the second section, where the water steadily and slowly flowed out from the mouth cavity. The final section shows the system after the valve had been resealed.

The variation in the amplitude of each peak in this case was less than 1dB, except the 5th peak, which varied by 1.5dB. These variations are negligible when compared with the variations typically seen during normal playing.

Experimental Method - Self Oscillation

The role that the mouth cavity plays in 'buzzing' the lips - where the lips oscillate without any downstream resonator (ie, with a mouthpiece rim) is also uncertain [31]. Without the periodic driving force provided by the downstream resonator, the model represented by equation 2.24 can not sustain oscillation. However, a

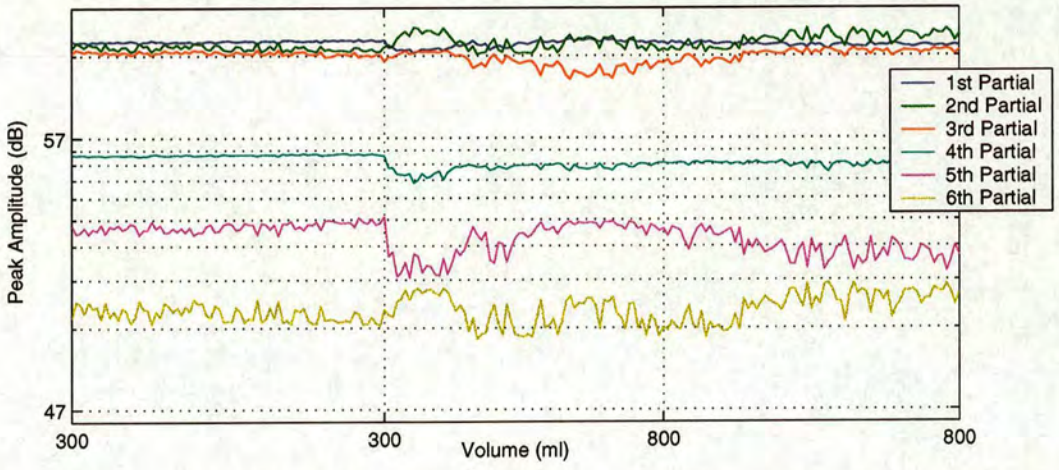

Figure 3.24: Amplitude of the components of the radiated sound from the trombone as the water volume is changed. The three sections of the graph show the steady state before and after the release of the water and the dynamic state as the water was released and the cavity volume went from 300ml to 800ml at a rate of 7.6ml/sec.

widely used practice technique for human players is to place their lips to a brass mouthpiece rim and buzz their lips as if they were playing an instrument, showing that equation 2.24 does not adequately describe the system.

One possible explanation for this phenomenon is that the impedance of the mouth cavity and vocal tract provides the oscillating driving force. In order to investigate this, the artificial mouth was set up to play a mouthpiece rim, with no downstream resonator. The mouthpiece rim was represented by a device which was originally designed to hold a normal brass mouthpiece in the mouthpiece holder – item (m) shown in figure 3.4. This component had a diameter and rim thickness similar to a trombone mouthpiece. Additionally, previous experience indicated that using a thinner grade of latex for the lips would make self-oscillation

easier, and so the 0.3mm thick latex lips were replaced with 0.2mm thickness lips, whilst keeping the other dimensions the same (16mm diameter, 120mm length, 70mm effective lip length). Aside from these changes, the experimental setup was the same as used in the previous section. Instead of analysing the radiated sound spectrum, the parameters of interest were the threshold pressure and threshold playing frequency. The mouth cavity was filled with 1500ml of water, leaving an air volume of 300ml. An embouchure was then found that played in this configuration, and the threshold playing frequency and pressure were measured. The air supply valve was then closed and 25ml of water extracted from the mouth cavity. The new threshold playing frequency and blowing pressure were then measured, and this process repeated in 25ml steps until the lips would not buzz even with the maximum supply pressure applied. Once this stage had been reached, the water was reintroduced in 25ml steps until the cavity volume was reduced to its 300ml starting point. A second embouchure was then established that played at a comparatively low frequency (98Hz) and the process repeated for this new embouchure.

Experimental Results - Self Oscillation

The initial investigations quickly showed that the lips would only sustain oscillaions if the mouth cavity volume was small - ie, there was a large amount of water in the cavity. Consequently threshold results were only obtainable for cav-

ity volumes up to 425ml, whereas the maximum cavity volume was 1800ml. The air in the cavity can be thought of as a 'spring'. The strength of this 'spring' increases in value as the volume of air decreases. In order for it to be a useful part of the oscillating system, the spring must provide a force which is comparable to, or greater than, the other forces acting on the system. Assuming that the force will be strong enough if the magnitude of the impedance provided by the air cavity is close to the peak of the impedance of a trombone mouthpiece it is possible to estimate at what cavity volume an effect will be observed.

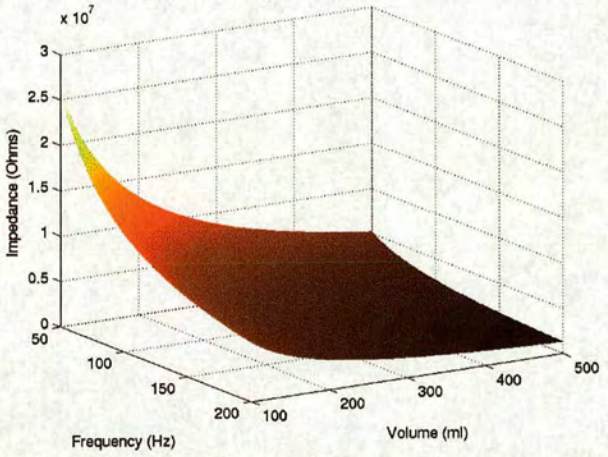

Figure 3.25: Impedance of a volume of air as a function of frequency and volume.

The impedance of a volume of air is given by [28]:

$$Z_c = \left(\frac{\rho c^2}{V}\right)\frac{1}{j\omega}, \tag{3.3}$$

where V is the volume of the cavity, c is the speed of sound in air and ρ is the density of air. This function is shown graphically in figure 3.25. For a playing

frequency of 100Hz (628rad/sec), an impedance of $5 \times 10^5 \Omega$ would be provided by a volume of 1040ml. This is only a first approximation, because of the presence of the large over pressure in the cavity coming from the feed pipe and air pump, and the fact that the volume of air is not completely sealed by the lips, which therefore allows air which has been acousically compressed to leak out through the lips, reducing the effective impedance of the cavity.

A small volume provides a larger impedance, which suggests that the embouchure would be easier to play. The results of the two data sets (playing at 121Hz and 98Hz in the first instance) are shown in figure 3.26. As can be seen, there is a steady rise in threshold pressure as the cavity volume is increased, and a corresponding drop in frequency.

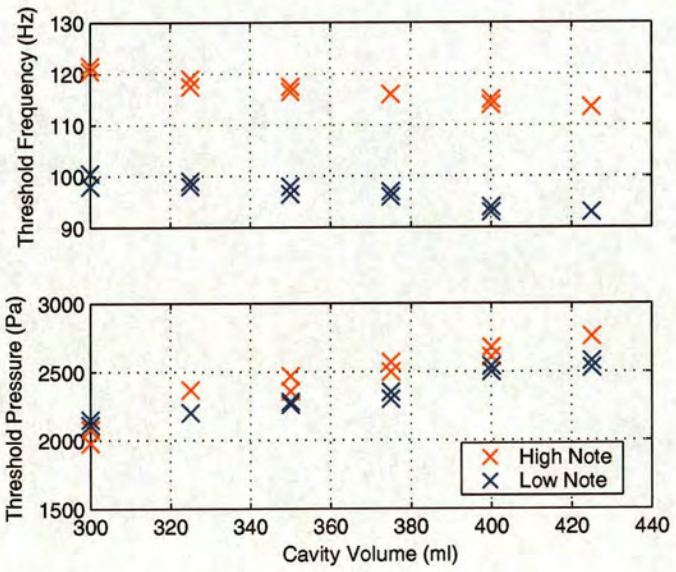

Figure 3.26: Threshold playing frequencies and pressures for varying mouth cavity volumes.

The source of the frequency change as the cavity volume was increased was

not due to changes in the upstream cavity, but due to the increased air flow and pressure. This was established by a quick measurement – the lips were buzzed with a small cavity volume near threshold and played at a frequency of 89Hz. The pressure was increased, and the new playing frequency was 85.5Hz. A final increase to the maximum pressure resulted in a playing frequency of 84Hz. For comparison, the pressure was then set to a constant value and the cavity volume was increased in steps of 25ml between 300 and 475ml. This produced a spread in frequency of just 1.25Hz. Clearly the main frequency changes were due primarily to the pressure increase. The data for these tests are shown in figure 3.27.

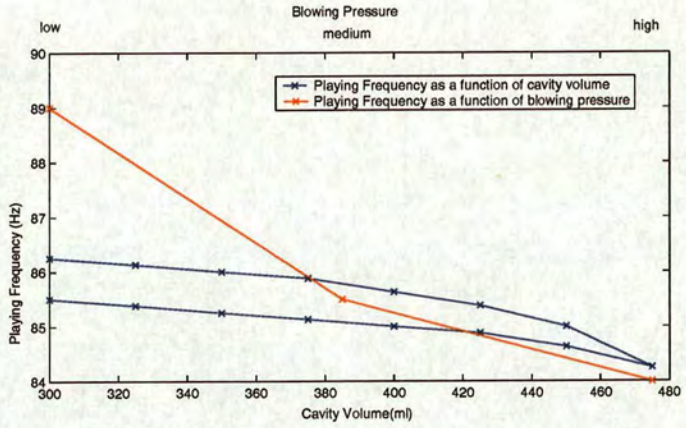

Figure 3.27: The effect of blowing pressure and cavity volume on the playing frequency. The much larger shift in frequency due to the blowing pressure changing implies that the playing frequency is largely independent of the cavity volume.

Conclusions - Mouth Cavity Effect

It has been shown that the volume of the mouth cavity has very little effect on the radiated sound from the trombone. However, in the case of the 'buzzing lips', the

cavity volume plays a very important part by providing the impedance against which the lips can play. In this experiment, it was found that a cavity volume of approximately 425ml or less was required for the examined embouchures to destabilise. This experiment did not investigate the effect of vocal tract shape on the radiated sound. For example, in the case of didjeridu playing the vocal formants have an enormous effect on the radiated sound [27]. However, in the case of the trombone, and other common brass instruments, unlike the didjeridu the input impedance of the instrument is far greater than that of the vocal tract, so the effects are very subtle. Where the impedance of the instrument is particularly low, as with the didjeridu, and also the pedal note of the larger brass instruments (including the trombone), the effect is quite obvious. The characteristic impedance Z_c is given by:

$$Z_c = \frac{\rho c}{S}, \tag{3.4}$$

and so it is immediately obvious that this value will be far larger for an instrument, where $S \approx 0.25\pi$ cm^2, than for a human vocal tract where $S \approx \pi$cm^2 to $S \approx 9\pi$cm^2. Performing experimental investigations of this nature on human players is very difficult, because the embouchure of the player cannot be controlled separately from the configuration of the vocal tract and the mouth cavity. Using an artificial mouth solves this problem.

3.4.5 Conclusions

Measurement of the response of the area of opening between the lips to an oscillating pressure difference across the lips shows that the artificial lips exhibit a complex response, but there are two distinct resonances present. One of these shows outward–striking characteristics and the other shows inward–striking characteristics. The lips will destabilise at a frequency between these two resonances.

The artificial mouth can, like a human player, play at threshold both below and above the resonance of an instrument. This is at odds with the outward–striking model of the lips proposed by Helmholtz which predicts that only playing *above* the instrument resonance is possible.

The volume of air in the mouth cavity has no discernible effect on the radiated sound. However, in order for the lips to self–oscillate when playing without a downstream resonator (ie, a musical instrument), the volume of air in the mouth cavity plays a key role.

Chapter 4

Investigation of the two-dimensional motion of the lips

4.1 Introduction

Photographic analysis of the lip motion of brass players was first performed by Martin in 1942 [45]. Using a strobe light and a movie camera, Martin took a series of images at different phases of lip motion of a cornet player. He used a special mouthpiece designed for this purpose, which had a viewing window in the plane of the player's lips. Martin's results showed the opening height between

the lips as a function of phase, and investigated the relationship between the lip opening height and lip opening area. Subsequent studies by Copley and Strong [16] and Yoshikawa [68] extended the original investigations by looking at the three-dimensional motion of the lips. These studies also used strobe photography to obtain information throughout a complete cycle of lip motion.

The information that can be derived from these studies is critical to the development of accurate simulations of lip behaviour. As one example, Msallam et al [47] demonstrated the effect of using an appropriate relationship between the height between the lips and the overall area between them. Instead of using the simplistic rectangular function $Area = Length \times Height$, where $Length$ is constant, Msallam used a quadratic function:

$$Length/Height = constant, \tag{4.1}$$

and therefore:

$$Area = constant \times Height^2. \tag{4.2}$$

This change greatly enhanced the stability and continuity of the model, and removed much of the undesirable high frequency components from the flow spectrum. A similar method described by Vergez and Rodet [63] results in equivalent behaviour, which was further enhanced by their considerations of the fluid flow at small areas of opening between the lips. Experimental visualisations of em-

bouchures, both of the artificial mouth and human players, provide the opportunity to verify or improve this relationship.

4.2 Experimental investigation of the self-sustained oscillation of the lips using a high-speed camera

Use of a modern high-speed video camera eliminates many of the negative effects of using strobe photography. Particularly, any long term variations (ie, variation over many cycles) in the playing situation are effectively removed from the sample - for instance slight changes in frequency and timbre that occur over the time period required for strobe photography. This method also allows transient effects to be observed - such as the starting and stopping of notes, or changes in pitch. In this study, a Vision Research, Inc. [64] Phantom v4.1 camera was used, which was capable of taking up to 32,051 digital images per second at varying resolutions. The mimimum useful resolution in this study was 256x128 pixels, which allowed a maximum frame rate of 7142 frames per second. The resolution was not the only limit on the frame rate - the exposure time was also an important factor. An 800W halogen lamp was used to illuminate the lips, but even this source was not sufficiently bright for exposure times below approximately 100μs. This is perhaps the main drawback of using high-speed photography. However, the

playing frequencies studied here reach a maximum of 268Hz, so there is sufficient bandwidth to analyse the lip motion accurately.

4.2.1 Experimental Setup

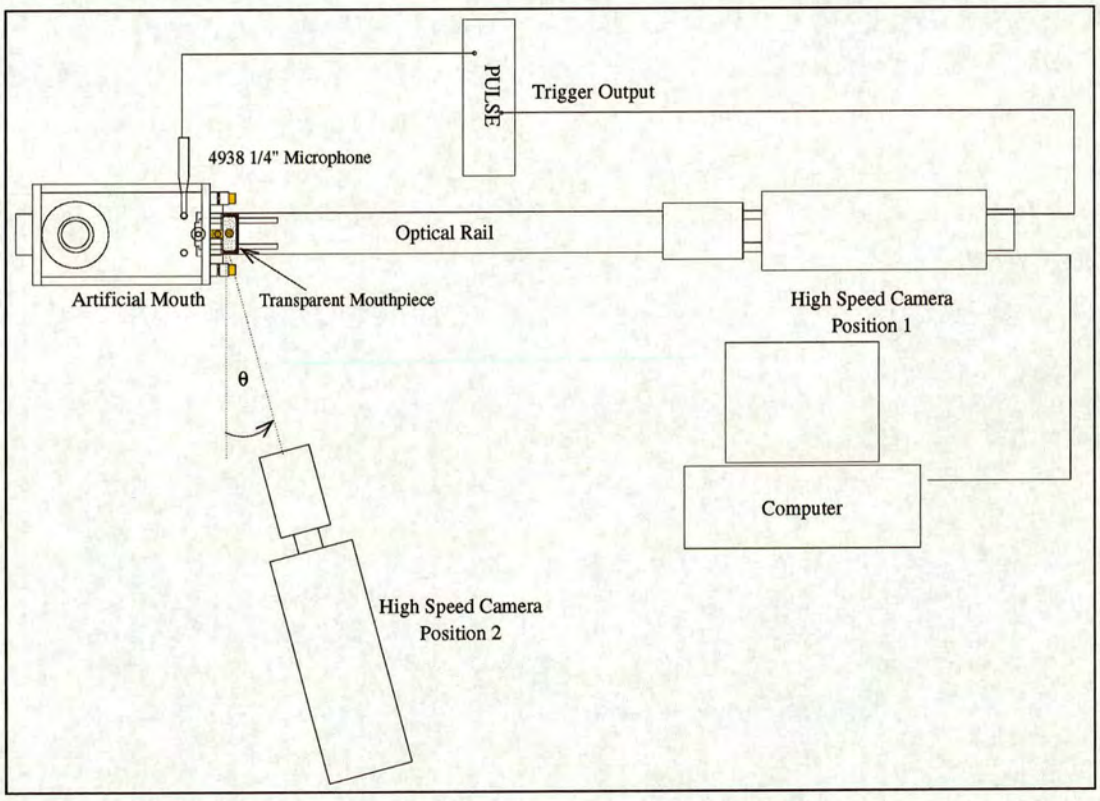

Figure 4.1: Experimental setup for the high speed camera experiments. θ was set to 15° for this study.

In order to analyse the lip motion, it is desirable to have a setup which can simultaneously record the audio and video signals. To this end, the PULSE system was configured to record the pressure variation in the mouth cavity, and also to provide a trigger to the high speed camera. The trigger used was a 5 Volt positive pulse, with a duration of 1/65536 seconds. The equipment was set

up as shown in figure 4.1. The high speed camera was placed in position one initially - pointing along the axis of the artificial mouth (so that the axis of the camera was perpendicular to the front of the artificial mouth). The camera was aligned so that only half of the lip opening was in shot. This allowed a greater resolution in the height measurements, but only measured the area of opening of one side of the lips. The measurements therefore assume that the area of opening is symmetrical about the middle point of the lips. This is approximately true for most configurations of the artificial mouth, but less so for some human players. A typical image captured from this setup is shown in figure 4.2. The artificial mouth was set playing for several minutes to be sure that the played note was fully stable, and then the recordings were taken.

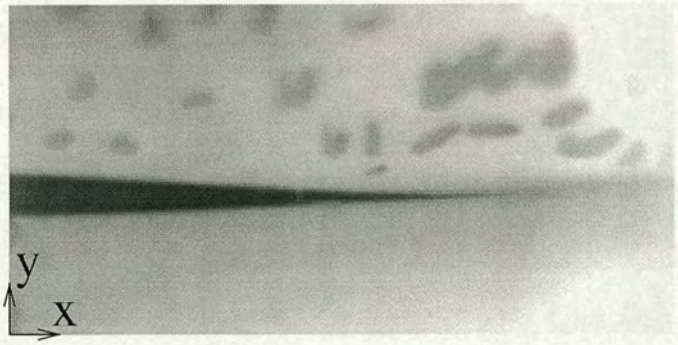

Figure 4.2: Typical image taken with the high speed camera showing half of the lip opening. The marks on the upper lip were drawn on with a fine tipped marker pen to provide some texture to the otherwise smooth lip surface.

The PULSE system was designed to send the trigger and simultaneously start recording the audio signal at a sampling rate of 65536Hz. The camera was set to start recording when it received the trigger from the PULSE system. The data

was then exported as a series of uncompressed jpeg format images for processing in Matlab.

In order to measure the motion in the z–direction, the camera was moved to position 2 while the lips were still playing the recorded note, and a second measurement was taken. The system was set playing for several minutes before taking any measurements to ensure that the note would be stable over the period between taking measurements in the two camera positions. This effectively allowed the motion of a single point on the lips to be tracked in two dimensions. For this purpose, small marks were drawn on the upper lip with a fine tipped marker pen. Without these marks, there would be no easily distinguishable point on the lips to track. In these recordings, the front and side views were phase locked using the oscillating pressure signal recorded in the mouth cavity. A typical pair of synchronised images is shown in figure 4.3.

4.2.2 Image Analysis

In order to analyse the images obtained, each series was imported into Matlab. For the recordings taken from position 1, the x and y ranges over which the lips were open were derived by visual inspection. A script was written to calculate the lip opening area by assigning a threshold intensity value, below which a pixel would be classed as "open", above which it would be "closed". The number of "open" pixels in the given area were counted and recorded. In addition, the

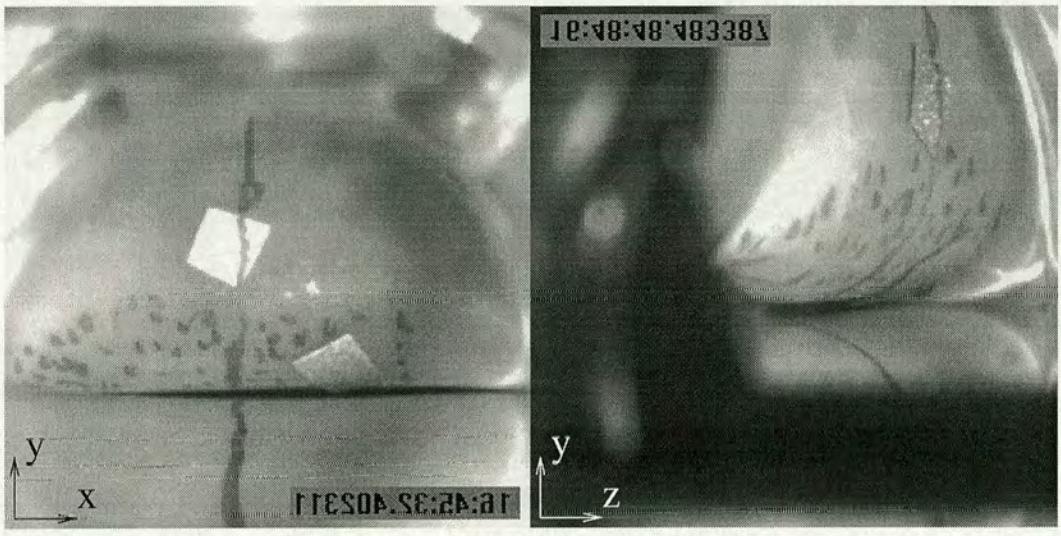

Figure 4.3: An example of a pair of images captured using the high speed camera from two different angles. These recordings were synchronised using the oscillating pressure signal in the mouth cavity. The images have been mirrored and rotated to account for the changes imposed by the camera setup – the left image is mirrored about the y-axis to compensate for to the camera lens inversion, and the right image is inverted about the z-axis because the camera was mounted upside down on the tripod. The squares of reflective tape seen here were used for the vibrometer experiments presented in section 4.3.

opening height was also recorded. This was defined as the maximum open height within a certain band. This band was chosen to be in the centre of the lips, and was again chosen by visual inspection. Once the relevant boundary conditions had been set, the full data set was analysed in this fashion.

For the recordings taken from position 2, the images had to be analysed by hand. There was no simple way of automatically analysing the images. For this experiment, dots were drawn on the upper lip with a fine tipped permanent marker. This allowed individual points on the lip to be tracked. It was also very difficult to get a viewing angle that allowed the full tracking of an individual

point over a lip cycle.

The images were scaled by placing a flexible ruler over the lips and recording a few images of the ruler. These images were then loaded into Matlab and a pixels/mm scale was derived for each camera position.

A series of measurements was taken with a selection of amplitudes and pitches. The amplitudes were chosen to be either just above threshold (data sets 2, 3, 11 and 12), at the maximum supply pressure (data sets 5, 6, 9 and 10), or approximately halfway between the two (for data set 4). The frequencies used were around 170 Hz or 270 Hz - which were two notes that were easily and repeatably achievable with only small adjustments to the embouchure. The parameters for each recording are given in table 4.1

4.2.3 Analysis of Aquired Data

X–Y Plane Analysis (Camera Position 1)

Data sets 2 - 6 were analysed using the pixel counting method described in section 4.2.2. This analysis produced the lip areas and lip opening heights for these data sets. Data set 2 was analysed to find the scale for these data sets. Short sections of the waveforms of the lip opening area and lip opening height are presented in

Data Set	Amplitude	Frequency (Hz)	Frame Rate frames/sec	Angle
1	Calibration	–	7100	front
2	Threshold	177	7100	front
3	Threshold	268	7100	front
4	Medium	257	7100	front
5	Maximum	262	7100	front
6	Maximum	173	7100	front
7	Calibration	–	3700	front
8	Calibration	–	3700	side
9	Maximum	167	3700	front
10	Maximum	167	3700	side
11	Threshold	166	3700	front
12	Threshold	166	3700	side

Table 4.1: Table of high speed recordings. Data sets 1 - 6 were face on recordings. Data set 1 provided the calibration for these data sets. Data sets 7 - 12 were sets of front and side recordings. Data sets 7 and 8 provided the calibration for these data sets. The *Amplitude* of each data set was either just above threshold (data sets 2, 3, 11 and 12) or at the maximum blower pressure – approximately 1.5kPa (data sets 5, 6, 9 and 10). Data set 4 used a blowing pressure approximately halfway between threshold and maximum.

figure 4.4.

It is worth noting the behaviour evident in data set 6 (large amplitude, low frequency) which clearly demonstrates a "bump" near the peak of the area plot (indicated by the arrow). This behaviour is also evident in data sets 2 and 5, although it is much less obvious.

From these results, we can see that the relationship between lip opening height and lip opening area is not a linear function. If we try a solution of the form:

$$A = \alpha H^n, \tag{4.3}$$

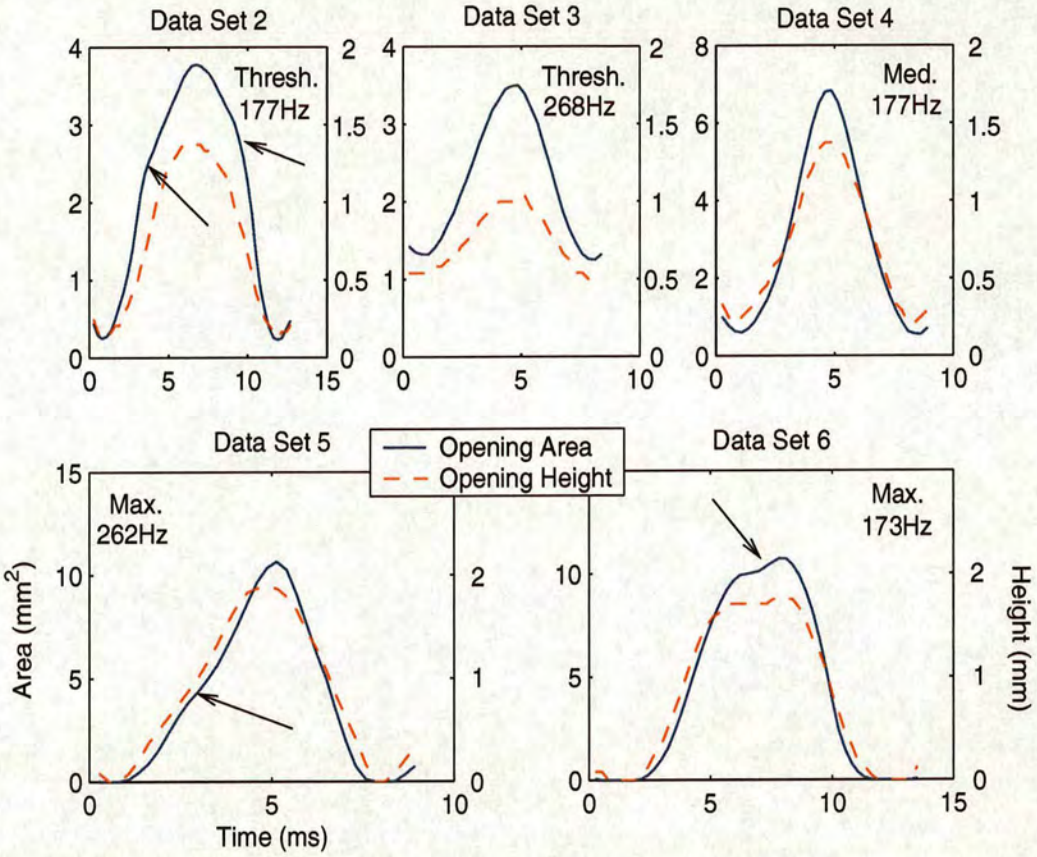

Figure 4.4: The waveforms of the lip opening height and lip opening area functions for each data set recorded with the high speed camera. The arrows point to the non-linear phenomena.

where A is the total open area between the lips, H is the maximum height of the opening, and α is a constant with dimensions $\text{mm}^{(2-n)}$. This solution can be considered by plotting the Area versus Height with logarithmic axes - as shown in figure 4.5. If the solution is valid, the data should form a straight line

This figure shows that for all data sets except data set 2, the solution form given in equation 4.3 is valid for the majority of the cycle. The value of n is given

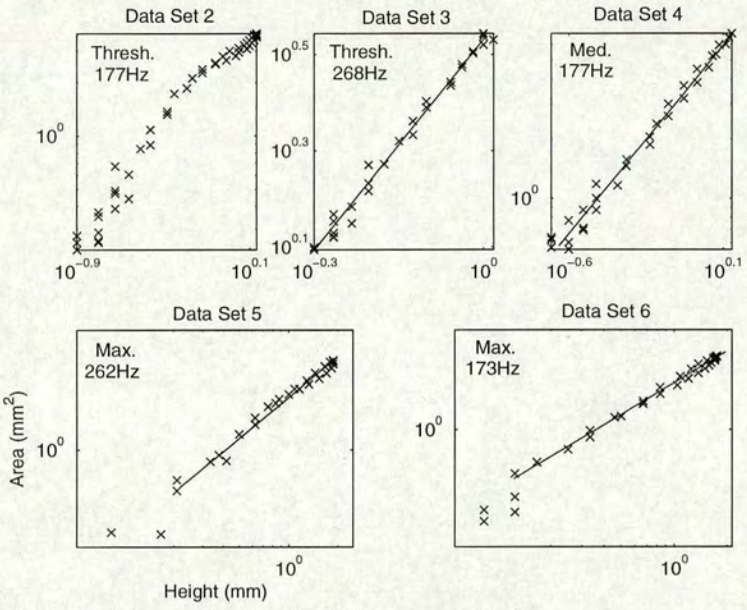

Figure 4.5: Log/Log plot of Area (vertical axis) versus Height (horizontal axis), with straight line fits where appropriate.

by the gradient of the line of best fit for the graph of:

$$ln\left(\frac{A}{A_0}\right) = nln\left(\frac{H}{H_0}\right) + c, \tag{4.4}$$

where A_0 is the unit area constant (1mm^2) and H_0 is the unit height constant (1mm). The value of α is given by:

$$\alpha = \alpha_0 e^c, \tag{4.5}$$

where c is the intercept of the best fit line and α_0 is the scale unit constant ($1\text{mm}^{(2-n)}$). These values are shown in table 4.2 for each data set. Thus the area of opening is given as a function of the height between the lips for each note. For

Data Set	Gradient (n)	Intercept ($ln(\alpha)$)	α
2	n/a	n/a	n/a
3	1.48	1.22	3.39
4	1.35	1.47	4.35
5	1.47	1.40	4.06
6	1.72	1.45	4.26

Table 4.2: Table of the calculated values of n and α for the solution given in equation 4.3 for the different recordings of lip motion.

data set 6, representing a loud note at 173Hz, the area is given by:

$$A = \alpha_6 H^{1.72}, \tag{4.6}$$

where $\alpha_6 = 4.26\text{mm}^{0.28}$.

This relationship is similar to that used by Msallam et al [47], where the authors used $n = 2$ for simplicity. In the case where $n = 2$ the width of the lip opening increases directly as the height increases. Where $n = 1$, the width of the lip opening remains constant throughout the cycle of lip motion. These results lie somewhere between these two cases - clearly the width of the lip opening does not remain constant, but equally it is not directly proportional to the opening height.

Y-Z Plane Analysis (Camera Position 2)

Data sets 7 to 9, which were recorded using the two different camera angles shown in figure 4.1, were analysed as described in section 4.2.2. The images

recorded from the front were analysed in the same way as data sets 2-6, but the images recorded from the side view were analysed manually by viewing the image series and recording the co-ordinates of a single point on the lip. The motion of the lip measured in this fashion is shown in figure 4.6 This figure

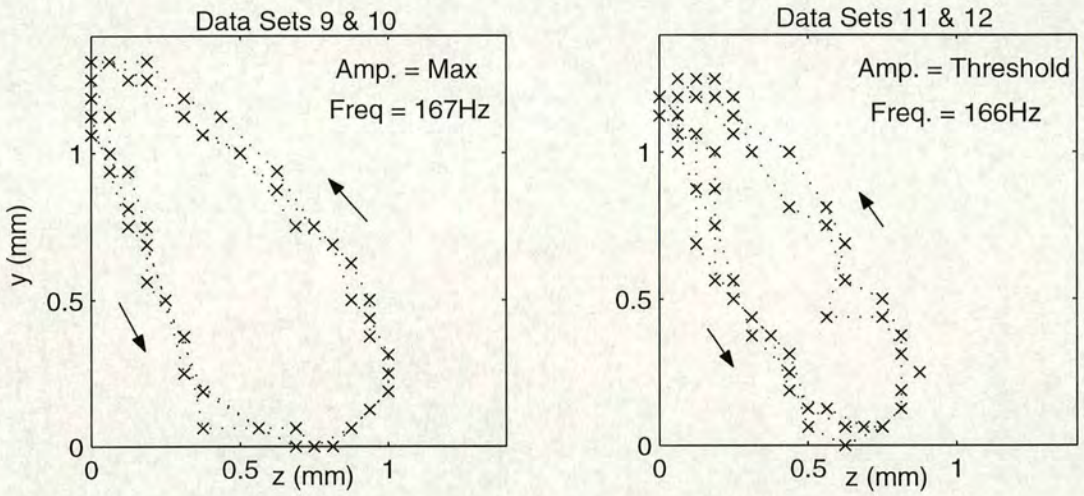

Figure 4.6: Outward (z) and Upward (y) motion of the lips. $y = 0$ is defined for each data set as the minimum opening height.

represents the motion of an individual point on the lip. In contrast, a recent study by Yoshikawa and Muto [68] tracked the motion of specific "features" on the lip surface – the "lip tip" and the "wave crest". However, what is clear is that there is motion in both the y and z directions (as defined in figure 4.3), and that these motions are out of phase with one another, which agrees with the findings of previous research [16] [68]. Copley and Strong [16] showed that there was significant variation in the phase difference between the longitudinal (z) and transverse (y) displacements. The motion observed in this study does not exhibit such large variation, but the range of amplitudes and pitches produced here is

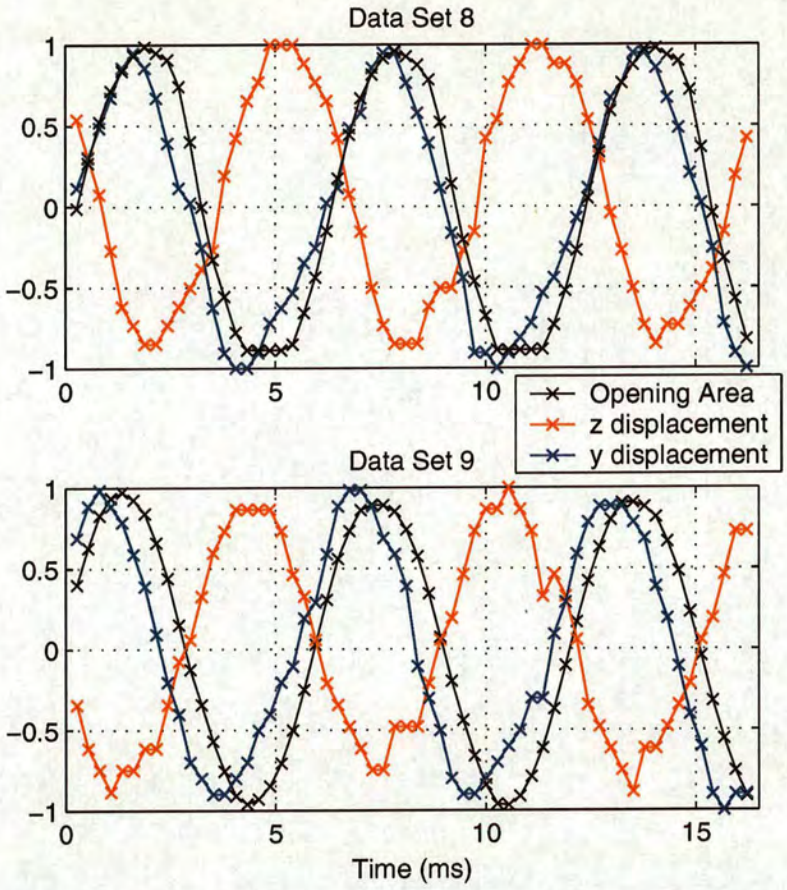

Figure 4.7: Waveforms of the motion in the y and z directions, and the opening area. These data have been normalised for clarity. Data set 8 was a high amplitude tone with a fundamental frequency of 167Hz. Data set 9 was a low amplitude tone with a fundamental frequency of 166Hz.

much smaller than those investigated by Copley and Strong. The frequencies used here (166Hz and 167Hz) are closest to the F3 pitched notes used by Copley and Strong. The amplitude of the displacements of the upper lip as measured by Copley and Strong for this note were approximately 2.1mm and 3.0mm for the "soft" and "loud" notes respectively, with maximum areas of opening of 22.5mm^2 and 41mm^2. The amplitude of displacement of the artificial lip was 1.25mm and 1.3mm for the "threshold" and "maximum" notes, and the areas of

opening opening were 3.8mm^2 and 11mm^2. As can be seen, there was significantly more motion measured by Copley and Strong for the motion of the human lips.

Figure 4.7 shows the normalised waveforms for displacement in the y and z directions, as well as the lip opening area. Note that the lip opening area presented here is the full lip opening area, rather than half the lip opening area as used for data sets 2-6. As can be seen, the lip opening area is almost in phase with the y-displacement, but approximately π radians out of phase with the z-displacement.

4.3 Measurements of the frequency response of the artificial lips using laser Doppler vibrometry

4.3.1 Introduction

The experiments described in the previous section were appropriate for investigating the large-amplitude motion of the lips during oscillation, but to look at the frequency response of the lips requires a much more sensitive system. In section 3.4.1 a photodiode is used to record the light from a laser as it passes through the area between the lips. This system provides the sensitivity necessary to examine

the mechanical response of the lips, but can only produce one-dimensional results. In order to investigate the lip response more fully, a Laser Doppler Vibrometer can be used to record the motion of a given area of the lip surface in a given direction. The background physics and techniques of Laser Doppler Vibrometry (LDV) are well established (for a concise summary, see [51]).

4.3.2 Experimental Setup

The areas of interest are the front and back of the upper lip, in the y and z directions. Figure 4.8 shows the experimental setup used, with the three different vibrometer positions shown.

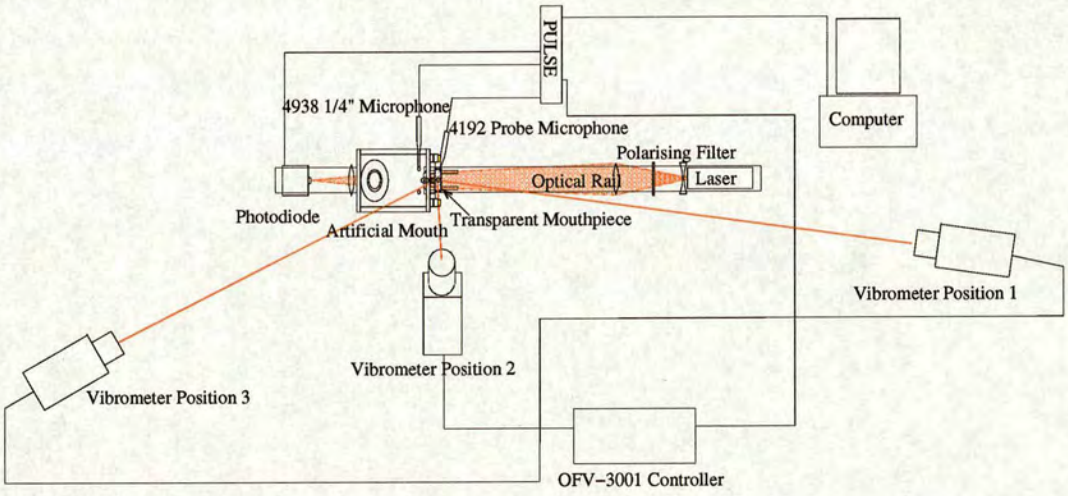

Figure 4.8: Experimental setup used for the vibrometer experiments. The vibrometer was placed in three different positions.

In this study a Polytec OFV-303 vibrometer head with a Polytec OFV-3001 controller is used. This vibrometer produced a positive going voltage for a reduc-

tion in the distance to the target. In order to obtain sufficient reflections from the lip surface, several small pieces of reflective tape were adhered to the lips. These pieces of tape were positioned so as to allow the vibrometer beam to measure the displacement at the front and back of the lips, in both the y–direction and z–direction (see figure 4.3). The vibrometer was set in one of the three positions shown in figure 4.8. Position 1 allowed the displacement of the front of the lip in the positive z–direction to be measured. Position 2 allowed the positive y–displacement of the front of the lip to be measured. Position 3 allowed the negative z–displacement of the rear of the lip to be measured. A fourth position was also used, where the vibrometer was pointed from below the mouth up through the side window, focusing on the rear of the lip. This view was intended to record the motion of the rear of the lip in the vertical (y) dimension. However, due to the shape of the mouth box, this position proved to be impossible to achieve.

These positions were chosen in order to investigate the relative phase behaviour between the motion of individual points on the lip. Many two–dimensional lip models [3] include motion in both the y and z directions. However, a model of the vocal folds presented by Lous et al [43] used two vertical degrees of freedom – one at the front of the lips and one at the rear of the lips. This vocal fold model is adapted to represent the lip reed and investigated in section 5.4. The chosen camera positions ought to provide data to help determine which degrees of freedom are important in describing the motion of the lip reed. The relative phases of the motion in these degrees of freedom will also help in the understanding of

the overall behaviour of the system.

The displacement signal from the vibrometer controller was input into the PULSE system, along with the signals from the photodiode, 4938 microphone (recording the pressure in the mough cavity) and the 4192 microphone with the probe attachment (recording the pressure in the mouthpiece). In order to excite the lips, the speaker box shown in figure 3.17 was attached to the mouthpiece. The PULSE system delivered a calibrated swept sine wave signal through this speaker, which was recorded using the probe microphone. Using this setup, it was possible to obtain simultaneous recordings of both the 'standard' lip response (as used in chapter 3, and by Neal [48] and Cullen [18]) by measuring the amount of light admitted between the lips, and the response of the area of the lip surface as measured by the vibrometer.

In order to obtain the lip response (using both the vibrometer and photodiode signals) the methods used in section 3.4.1 were used. The probe microphone signal was used as the reference signal.

The artificial mouth was set up, with the speaker box attached to the mouthpiece, and set playing for a long period of time (approximately 20 minutes) to ensure a stable embouchure. The threshold playing frequency was then measured. The air supply was then switched off (and the supply valve closed) before taking the measurements. Measurements were taken with the vibrometer in the three different positions shown in figure 4.8. The exact position of the camera is best

described in spherical co–ordinates (r,θ,ϕ). We define the origin as the centre of the lip surface, and r, θ, and ϕ as given in figure 4.9. Thus position 1, which

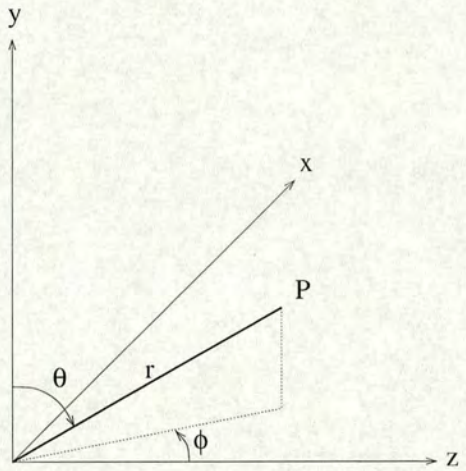

Figure 4.9: Spherical polar co–ordinate system used to map the camera positions. With respect to figure 4.8 the y–axis is rising out of the page, the z–axis goes from the lip centre towards the laser source, and the x–axis goes up the page perpendicular to the optical rail.

pointed at the front of the lip, had co–ordinates $(3\text{m}, 90°, 5°)$, position 2 pointed at the bottom of the front of the lip, had $(0.5\text{m}, 165°, -75°)$ and position 3, which pointed at the rear of the lip, had $(2\text{m}, 90°, -160°)$.

4.3.3 Experimental Results

Each experiment produced a set of data that contained the following measurements:

- Area of opening response (as presented in section 3.4.1).

- Displacement response in vibrometer position 1, corresponding to the motion of the front lip surface in the z–direction (ie, outwards from the face).
- Displacement response in vibrometer position 2, corresponding to the motion of the front lip surface in the y–direction (ie, upwards).
- Displacement response in vibrometer position 3, corresponding to the motion of the rear lip surface in the z–direction. This signal was inverted to account for the fact that a positive motion in the z–direction would result in a decreasing voltage signal from the vibrometer.

Note that all the signals were also inverted due to the inversion of the B&K microphone signal.

Figure 4.10 shows one complete set of results. This figure shows the response curves described above. The playing frequency is shown by the vertical red line at 240Hz. The vertical black lines show the resonances observed in the area response measurement. These include the outward resonances at 92Hz, 122Hz and 145Hz, and the inward resonance at 251Hz, and as can be seen the threshold playing frequency lies between the outward and inward resonances. There are also a number of other resonances seen. Of particular interest are the peaks at the higher frequencies (334Hz and 444Hz for instance), where there is no corresponding peak in the response curves measured with the vibrometer. There is another of these resonances at 173Hz.

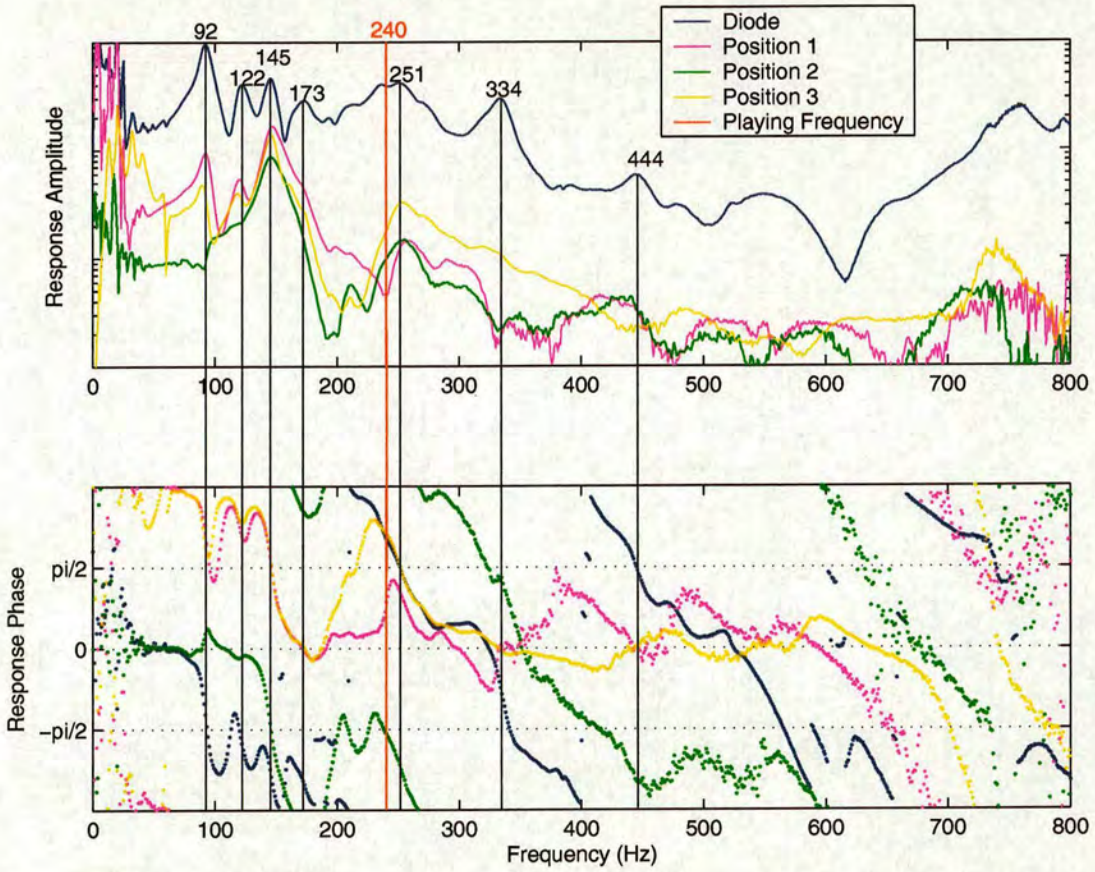

Figure 4.10: Response of the opening area (diode signal) and the point displacements (Positions 1–3). The red vertical line shows the threshold playing frequency (240Hz), the vertical black lines show the resonances identified in the opening area response. The key resonances are the outward striking resonances at 92Hz, 122Hz and 145Hz, and the inward striking resonance at 251Hz.

The vibrometer data shows far fewer resonances. The data from positions 1 and 3 show mainly the motion of the lip in the z–direction. There are clearly peaks in these responses corresponding to the outward striking resonances identified in the area response. The first two of these peaks are conspicuously absent from the measurement taken in position 2, which implies that these low frequency peaks are due solely to motion in the z–direction. The presence of peaks in all four data

sets at 145Hz implies a strongly coupled resonance at this frequency. The strength of this resonance in all signals suggests that it is the dominant outward–striking resonance in this embouchure. Similarly, the presence of the peak at 251Hz in all data sets shows it is a significant resonance. This resonance has inward–striking characteristics. The variations in the frequency of this resonance throughout the data sets implies that it is not strongly coupled in the dimensions observed here.

The motion in the y–direction is out of phase with the motion in the z–direction, which agrees with the time-domain oscillation measurements obtained using the high speed camera (see figure 4.7).

4.3.4 Conclusions

The interpretation of these results in a quantitive manner is difficult. One of the main problems lies with the fact that the lips are oval shaped, and consequently when using a Cartesian co–ordinate system the displacement of the surface in one direction results in a displacement in another direction also. What is more, the restrictions on the positioning of the vibrometer mean that there will inevitably be some 'leakage' between the different motions - particularly for position 2, where the angles were not ideal ($\theta = 165°$ instead of $\theta = 180°$). However, the data does provide some very interesting insights into the mechanics of the system.

The fact that there are several peaks in the area response function that are

not present in the vibrometer signals suggest one of two things:

- The vibrometer measurements failed to record some of the modes of oscillation of the lips. However, because the points chosen for the vibrometer measurements cover all degrees of the lip motion, we can assume this is not the case.

- These peaks are created by non–linearities in the area function itself. This will be discussed further in chapter 5.

The presence of four resonance peaks in the vibrometer data suggests a four degree–of–freedom model is needed to fully represent the lip motion. However, it is not clear how important each of these degrees of freedom is to the overall behaviour of the reed. The two low frequency modes in the z–direction (positions 1 and 3), for instance, do not appear to be coupled to the motion in the y–direction. This implies that this motion is not critical in determining the behaviour of the air flow through the lip channel, which is controlled by the open area between the lips.

Chapter 5

Lip Modelling

5.1 Introduction

One of the most useful tools in understanding the lip reed system is computational modelling. By creating a simulation of the lips, it is possible to investigate the effect of the relevant control parameters on the behaviour of the system. This can lead not only to a greater understanding of the dynamics of the system, but can also assist in the creation of an easily controllable sound synthesis device. In this study, time domain simulations are used to investigate the behaviour of a number of models. Simple models of the lips are used, with just one or two degrees of freedom. Vocal folds have very similar characteristics to the lips - both in terms of their physiological characteristics and in terms of the fluid mechanics involved. Vocal fold research is a much more advanced field than lip reed research, and

consequently it is very beneficial to use methods developed for voice modelling [37] [41] [44] [59] [65] and see how applicable they can be to lip reed modelling [42].

Several lip models of varying complexity exist. The most common model is the simple "mass on a spring" type of model [2] [24] [47] [38] [61]. One such model is presented in section 2.4. Due to its simplicity, this model proves to be very useful for sound synthesis. However, important aspects of the lip behaviour are not reproducible using this model. Of particular importance is the fact that a model of this nature can not play both above and below the instrument resonance (see section 3.4.3). A one degree of freedom model has only one mode of oscillation - either inward or outward striking, depending on the parameters of the model, and as such can only enter self sustained oscillation either below or above the instrument resonance respectively [18] (see section 2.3).

There are two methods used in this chapter to investigate the behaviour of several lip models. The first is Linear Stability Analysis (LSA) [4] [17] [36] [58]. This technique is comparable to the experimental threshold measurements described in section 3.4.3, and is presented in section 5.2.2. The second method used is time domain synthesis, presented in section 5.2.1. This method is used to obtain the impulse response data for the various models, similar to the experimental measurements presented in sections 3.4.1 and 4.3.

5.2 Computational Methods of Modelling

5.2.1 Time Domain Modelling

Time domain modelling is perhaps the most intuitive method of simulating a dynamic system. The process involves deriving the equations of motion for the system, providing expressions for the acceleration of the discrete components under investigation, and then calculating the movement of these components in a digitised time space. The general equation of motion used is:

$$\frac{\partial^2 \mathbf{x}}{\partial t^2} = \frac{\mathbf{F}(\mathbf{x})}{m}. \tag{5.1}$$

This equation is then discretised, so ∂t becomes ΔT, where T is the sampling period, and $\mathbf{x}$ becomes $\mathbf{x_n}$, where n is the sample number. We make the assumption that the acceleration is approximately constant over the sampling period T to obtain the equation for the acceleration $\mathbf{a_{n+1}}$, the velocity $\mathbf{v_{n+1}}$ and the displacement $\mathbf{x_{n+1}}$:

$$\mathbf{a_{n+1}} = \frac{1}{m}\mathbf{F}\left(\mathbf{x_n}, \frac{\partial \mathbf{x_n}}{\partial \mathbf{t}}\right), \tag{5.2}$$

$$\mathbf{v_{n+1}} = \mathbf{v_n} + \mathbf{a_{n+1}}\Delta T, \tag{5.3}$$

$$\mathbf{x_{n+1}} = \mathbf{x_n} + \mathbf{v_{n+1}}\Delta T + \frac{1}{2}\mathbf{a_{n+1}}\Delta T^2. \tag{5.4}$$

This method provides an accurate description of the system only if the sampling rate ν_s is high enough. The accuracy of a given simulation is frequency dependant [60]. In order to obtain accurate results, a sampling rate of ν_s of 22.05kHz was chosen. This provides good accuracy within the frequency range of interest (approximately 20–500Hz), as well as being a standard sampling rate used in digital audio applications.

In order to obtain the frequency response of the digitised model, an impulsive pressure difference is applied across the "virtual lips". This takes the form of an upstream (mouth) pressure which has a finite value for the first sample in the simulation and zero at all other times. This provides energy to the system equally at all frequencies up to the Nyquist frequency (half the sample frequency) with zero phase, which means that it is not necessary to deconvolve the response signal from the input signal. The resulting time domain motion is Fast Fourier Transformed to give the complex impulse response in the frequency domain. This is then plotted as the magnitude and phase of the response, in a comparable format to the experimental data presented in chapters 3 and 4.

There are two methods used to obtain the threshold playing frequency. The first is simply to apply a static upstream pressure large enough to produce a sustained oscillation, but small enough that it is just above threshold. The other method is linear stability analysis, which is vastly more economic, computationally, and therefore requires far less computational time to determine the threshold

point. This technique is discussed in section 5.2.2.

The Matlab language was used in this study to code and perform the simulations. This package was chosen because of its integration with a large number of signal processing tools and graph plotting packages, as well as the benefits of having all data stored as matrices in the workspace. Matlab is not a very efficient programming language however, and so it was prudent at times to use C code for simulations. This was particularly advantageous when using "`for`" loops, which form the core of any time-domain simulation. Despite the large speed advantage though, most code was written in Matlab because of the flexibility and accessibility associated with it. In order to further improve the manageability of the code, large programs were written as a collection of modules. This allowed the code to be easily changed to represent a different model, at the expense of some computational time, as well as making it much simpler to make functional modifications to the code.

5.2.2 Linear Stability Analysis

Doing a time domain simulation of the lips is very computationally demanding – each simulation can take anywhere from between one minute and one day, depending on the complexity of the model and the number of samples used. A far quicker method is to use Linear Stability Analysis [17] [18] [58]. The analysis of the stability of the system about an equilibrium point is particularly useful

for examining how the system will destabilise [44]. This involves linearising the model to reduce it to a relatively simple set of equations. These equations are then represented in matrix form, and the eigenvalues of this matrix describe the important aspects of the lip motion.

The matrix is recalculated for a number of different mouth pressures, and so we can determine if a given model will destabilise and obtain the threshold pressure and threshold playing frequency. This information is enough to categorise a given configuration of the model as either inward or outward striking. It is also a simple task to perform "experiments" on the model by varying its parameters. The computer time required for each run is nominal compared to a time domain simulation: the time requirements are dictated by the number of pressure steps and the complexity of the model. A 500 point simulation will take just a few seconds on a typical computer, which allows a large number of "experiments" to be carried out in a reasonable time.

The process of linearising the model involves discarding any term which is not a linear function of an alternating variable. Each oscillating variable is assumed to be separable into a small dynamic component oscillating around a static component, so variable X becomes:

$$X = \overline{X} + x, \tag{5.5}$$

where $\overline{X}$ is the static component of the variable and x is the oscillating component. This situation is similar to measuring threshold oscillations in the lab (see section 3.4.3) – in cases where the threshold point is well defined – or exciting the lips with small acoustic pressures (see section 3.4.1) resulting in small displacements about equilibrium. The static component is calculated by evaluating the equations of motion in a steady state (ie, finding the equilibrium position). The equations are then linearised, around the calculated equilibrium position, as a function of the oscillating components of the lip displacement and air pressure in the instrument mouthpiece, resulting in a matrix equation with dimensions equal to the number of degrees of freedom in the lip model, plus the degree of freedom of the acoustic resonator. The resonator is represented by a single mode oscillator - a significant simplification of the true system, which is justified by investigating only near-threshold behaviour [33]. The equation of motion for the resonator is given by equation 2.5, and repeated here for convenience:

$$\frac{\partial^2 \psi}{\partial t^2} + \frac{\omega_i}{Q_i}\frac{\partial \psi}{\partial t} + \omega_i^2 \psi = \frac{Z_i \omega_i}{Q_i} u, \tag{5.6}$$

where ω_i is the instrument resonance frequency of interest, Z_i is the amplitude of the impedance at this frequency, Q_i is the quality factor of this resonance, $\frac{\partial \psi}{\partial t}$ is the pressure in the instrument mouthpiece and u is the oscillating component of the volume flow injected into the instrument through the reed [18]. The equations of motion for the coupled mechanical and acoustical oscillators (equations 2.22

and 2.23) can be linearised and written in matrix format:

$$\mathbf{MX} = \frac{d}{dt}\mathbf{X}, \tag{5.7}$$

where $\mathbf{M}$ is the matrix of coefficients:

$$\mathbf{M} = \begin{bmatrix} \mathbf{0} & \mathbf{I} \\ \mathbf{K_x} & \mathbf{B_x} \end{bmatrix}, \tag{5.8}$$

where $\mathbf{0}$ is the n-dimensional zero matrix, I is the n-dimensional identity matrix, and $\mathbf{B_x}$ and $\mathbf{K_x}$ are the effective damping and effective spring coefficients (as introduced in equation 2.22) and $\mathbf{X}$ is the vector containing the displacement and velocity components for each degree of freedom:

$$\mathbf{X} = \begin{bmatrix} x_1 \\ x_2 \\ \vdots \\ x_n \\ \dot{x_1} \\ \dot{x_2} \\ \vdots \\ \dot{x_n} \end{bmatrix} \tag{5.9}$$

The solutions of this equation take the form:

$$x = Ae^{\lambda t}, \tag{5.10}$$

where λ is a complex eigenvalue of the matrix $\mathbf{M}$ and A is a constant (with units of length). Equation 5.10 can be written as:

$$x = A\left(e^{Re[\lambda]t}e^{Im[\lambda]jt}\right). \tag{5.11}$$

Therefore, the real part of the eigenvalue dictates the overall amplitude behaviour of the system. If the real part of λ is negative, the amplitude will exponentially decay. However, if the real part is positive the amplitude will exponentially grow – and this is how the threshold point is decided. The threshold playing frequency is given by the imaginary part of the eigenvalue.

5.3 Lip Models

5.3.1 One degree of freedom model

The basic model presented in section 2.4 provides the first subject for investigation. This type of model is popular in sound synthesis applications because of its simplicity. Figure 2.5 is repeated here, with the further simplification of the area

between the lips having a rectangular cross section.

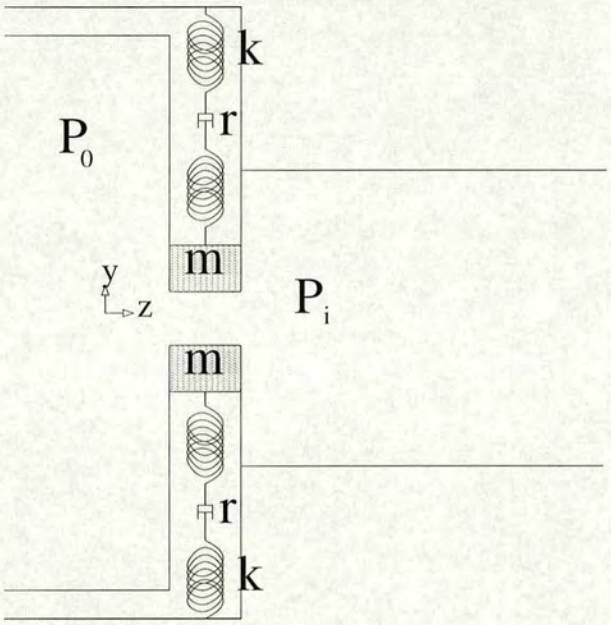

Figure 5.1: The simple lip model presented in section 2.4, with a rectangular cross sectional area between the lips.

The equation of motion for this model was given in equation 2.24:

$$\frac{\partial^2 y}{\partial^2 t} + \frac{\omega_l}{Q_l}\frac{\partial y}{\partial t} + \omega_l^2 y = \frac{F(y, \frac{\partial \psi}{\partial t}, P_0)}{m_l}. \tag{5.12}$$

The force term on the right hand side of the equation defines how the model responds to the fluid forces at work on the lip. These forces come in the form of air pressures applied to the surface of the lip. Therefore, the force applied to the lip will be proportional to the surface area over which the individual pressures apply. Since the model is constrained to move only in the y–direction, we can say that any pressure will act either to increase or decrease y, depending on the

configuration of the surface area of the lip. If a positive pressure difference across the lips results in a positive force (ie, forcing the lips open) the model will behave as an outward striking reed. If a positive pressure difference across the lips draws the lips closer together, the model will behave as an inward striking reed. As a result, we can say that this model will behave as an inward or outward striking reed (see section 2.3) depending on the phase difference between the forcing term on the right hand side of the equation and the pressure difference across the reed, without making any statements about the shape of the lip or the specific characteristics of the fluid forces involved.

Assuming the flow through the lip channel is quasi–stationary, frictionless and incompressible, the fluid velocity in the lip channel V_l is given by the Bernouilli equation [18]:

$$P_0 = P_l + \frac{1}{2}\rho V_l^2, \tag{5.13}$$

where P_0 is the mouth pressure, and P_l is the pressure in the lip channel. The assumption is made that the cross-sectional area of the mouth cavity is much larger than the cross-sectional area in the lip channel, and so the velocity of the fluid in the mouth cavity is negligible. It is also assumed that the fluid forms a jet as it exits the lip channel, and that there is no downstream pressure recovery. As a result, the pressure in the instrument mouthpiece, P_i, can be assumed to be the same as the pressure in the lip channel. The pressures generated by the fluid flow through the lips will act on the surface area of the lip. If it is assumed

that there are two separable forces – one generated the pressure difference across the lips and the other by the Bernoulli effect of the flow through the lip channel [17] [18] – then it is clear that these pressures will act on different surface areas of the lips. The force created by the pressure difference across the lips will result in outward striking behaviour – the lips will be pushed open by an overpressure in the mouth cavity. This force acts over an effective surface area on an effective mass, and the ratio of these two parameters can be lumped into the parameter μ_{out}:

$$\mu_{out} = \frac{S_{out}}{m_{out}}, \tag{5.14}$$

where m_{out} is the effective mass driven by this force (rather than the absolute mass – the simplicity of the model means that it is not possible to equate the parameters of the model with physical parameters of real lips) and S_{out} is the effective surface area over which the pressure difference across the lips acts.

The equivalent parameter for an inward striking force is defined by the surface area in the lip channel over which the Bernoulli pressure acts, and is given by:

$$\mu_{in} = \frac{S_{in}}{m_{in}}, \tag{5.15}$$

where m_{in} is the effective mass driven by the inward striking force, and S_{in} is the effective surface area over which the pressure is applied.

Using the parameters μ_{in} and μ_{out}, equation 5.12 becomes:

$$\frac{\partial^2 y}{\partial^2 t} + \frac{\omega_l}{Q_l}\frac{\partial y}{\partial t} + \omega_l^2 y = (\mu_{out} - \mu_{in})(P_0 - P_i). \tag{5.16}$$

Separating P_0, P_i and V_l into their static and oscillating components (as per equation 5.5), equation 5.13 becomes:

$$\overline{P_0} + p_0 = \overline{P_i} + p_i + \frac{1}{2}\rho\left(\overline{V_l} + v_l\right)^2. \tag{5.17}$$

Assuming that the area of the mouth cavity is large compared with the area of the lip channel and instrument, the oscillating component of the mouth pressure is negligible (ie, the input impedance of the mouth cavity is small compared to the input impedance of the instrument). Furthermore, assuming that the cross sectional area of the lip channel is small compared with the cross sectional area of the mouthpiece throat, it can be assumed that the static component of the mouthpiece pressure $\overline{P_i}$ is negligible. Thus equation 5.17 becomes:

$$\overline{P_0} = p_i + \frac{1}{2}\rho\left(\overline{V_l} + v_l\right)^2. \tag{5.18}$$

By applying the law of conservation of volume flow, it is possible to derive an equation for the volume flow through the lip channel, U:

$$U = \overline{U} + u = 2d\left(\overline{Y} + y\right)\left(\overline{V_l} + v_l\right), \tag{5.19}$$

where d is the width of the lip opening area (in the x–direction), as shown in figure 2.5, and Y is the displacement of the lip from the origin (defined as the centre point between the two lips in equilibrium position). Again, the notation presented in equation 5.5 has been used to denote the static and oscillating components of the variables used here – ie, $Y = \overline{Y} + y$.

By assuming that the two lips move symmetrically, the height between the lips, H, is given by:

$$H = \overline{H} + h = 2Y = 2\left(\overline{Y} + y\right). \tag{5.20}$$

To linearise these equations, any term that is not a linear function of an oscillating variable is discarded. Thus, equation 5.18 becomes:

$$p_i + \frac{1}{2}\rho\left(2\overline{V_l}v_l\right) = 0, \tag{5.21}$$

and therefore

$$v_l = -\frac{p_i}{\rho\overline{V_l}}. \tag{5.22}$$

Similarly, equation 5.19 gives:

$$u = 2d\left(\overline{Y}v_l + \overline{V_l}y\right). \tag{5.23}$$

Substituting equation 5.21 into equation 5.23 gives:

$$u = 2d\overline{V_l}y - 2d\overline{Y}\frac{p_i}{\rho\overline{V_l}}. \tag{5.24}$$

Given that $p_i = \frac{d\psi}{dt}$, the oscillating component of the flow can now be defined as a function of the two variables of the system:

$$u = 2d\overline{V_l}y - 2d\overline{Y}\frac{1}{\rho\overline{V_l}}\frac{\partial\psi}{\partial t}. \tag{5.25}$$

Substituting this into the equation of motion of the one-mode acoustic resonator (equation 5.6) gives the equation of motion as a function of y and ψ:

$$\frac{\partial^2\psi}{\partial t^2} + \frac{\omega_i}{Q_i}\frac{\partial\psi}{\partial t} + \omega_i^2\psi = \frac{Z_i\omega_i}{Q_i}\left(2d\overline{V_l}y - \frac{2d\overline{Y}}{\rho\overline{V_l}}\frac{\partial\psi}{\partial t}\right). \tag{5.26}$$

Rearranged, this gives:

$$\frac{\partial^2\psi}{\partial t^2} + \left(\frac{\omega_i}{Q_i} + \frac{Z_i\omega_i}{Q_i}\frac{2d\overline{Y}}{\rho\overline{V_l}}\right)\frac{\partial\psi}{\partial t} + \omega_i^2\psi - \frac{Z_i\omega_i}{Q_i}2d\overline{V_l}y = 0. \tag{5.27}$$

The linearised version of equation 5.16:

$$\frac{\partial^2 y}{\partial^2 t} + \frac{\omega_l}{Q_l}\frac{\partial y}{\partial t} + (\mu_{out} - \mu_{in})\frac{\partial\psi}{\partial t} + \omega_l^2 y = 0, \tag{5.28}$$

completes the set of equations of motion for this model for small oscillations around an an equilibrium position.

These equations of motion can be written as:

$$\frac{\partial^2}{\partial t^2}\begin{bmatrix} y \\ \psi \end{bmatrix} + \mathbf{C}\frac{\partial}{\partial t}\begin{bmatrix} y \\ \psi \end{bmatrix} + \mathbf{K}\begin{bmatrix} y \\ \psi \end{bmatrix} = 0, \tag{5.29}$$

where

$$\mathbf{C} = \begin{pmatrix} \frac{\omega_l}{Q_l} & (\mu_{out} - \mu_{in}) \\ 0 & \left(\frac{\omega_i}{Q_i} + \frac{Z_i\omega_i}{Q_i}\frac{2d\overline{Y}}{\rho\overline{V_l}}\right) \end{pmatrix}, \tag{5.30}$$

and

$$\mathbf{K} = \begin{pmatrix} \omega_l^2 & 0 \\ -\frac{Z_i\omega_i}{Q_i}2d\overline{V_l} & \omega_i^2 \end{pmatrix}. \tag{5.31}$$

Equation 5.29 can be written in the same form as equation 5.7:

$$\frac{\partial}{\partial t}\begin{bmatrix} y \\ \psi \\ \frac{\partial y}{\partial t} \\ \frac{\partial \psi}{\partial t} \end{bmatrix} = \begin{bmatrix} \mathbf{0} & \mathbf{I} \\ -\mathbf{K} & -\mathbf{C} \end{bmatrix}\begin{bmatrix} y \\ \psi \\ \frac{\partial y}{\partial t} \\ \frac{\partial \psi}{\partial t} \end{bmatrix} \tag{5.32}$$

It is now possible to investigate the stability of this model by examining the eigenvalues of the matrix

$$\mathbf{M} = \begin{bmatrix} \mathbf{0} & \mathbf{I} \\ -\mathbf{K} & -\mathbf{C} \end{bmatrix} \tag{5.33}$$

as a function of a control parameter. Of particular interest is the stability as a

function of supply pressure, which allows the threshold playing frequency of the model with a given a set of parameters to be calculated.

A Matlab program was written to calculate the threshold playing frequencies as a function of blowing pressure. The procedure was as follows:

- Choose values of μ_{out} and μ_{in} to give either an inward or outward striking reed type.
- Calculate the equilibrium positions for a given mouth pressure (starting from well below threshold pressure).
- Calculate the matrix $\mathbf{M}$ (eq. 5.33) for the calculated equilibrium state.
- Calculate the eigenvalues of the matrix.
- Increment the supply pressure and repeat until the pressure is well above the threshold pressure.
- When the pressure limit is reached, increment the resonator length (by means of changing the resonance frequency, ω_i) and repeat.

The model parameters were taken from experimental measurements with the artificial mouth. The resonance frequencies and quality factors of the lips were taken from the response measurements performed in section 3.4.1. The μ_{out} and μ_{in} parameters were based on those obtained by Cullen [18] in the first instance. These parameters were adjusted somewhat to produce useful results - ie, a "virtual

embouchure" that could play over the whole range of resonator frequencies under investigation.

The parameters of the acoustical resonator (equation 5.6) were taken from experimental measurements of the trombone used in the experimental investigations, as described in section 3.4.2.

The equilibrium position, y_0 is calculated by setting all time derivatives to zero, thus:

$$y_0 = \frac{\mu P_0}{\omega_l^2}. \tag{5.34}$$

Figure 5.2 shows the threshold playing frequencies as a function of resonator length, similar to the threshold experiments discussed in section 3.4.3, for an inward striking parameter choice (with resonance frequency of 162Hz) and an outward striking parameter choice (with resonance frequency of 118Hz). As can be seen, the model will only play below the instrument and reed resonances (inward striking case) or only play above the instrument and reed resonances (outward striking case). The requirements for regenerative feedback stated in section 2.3 explain why this is the case. However, the threshold experiments performed using the artificial mouth in section 3.4.3 showed that the reed would play both above *and* below the instrument resonance, so clearly the one degree of freedom model used here does not adequately model the lip reed.

In addition to the linear stability analysis techniques, which are comparable

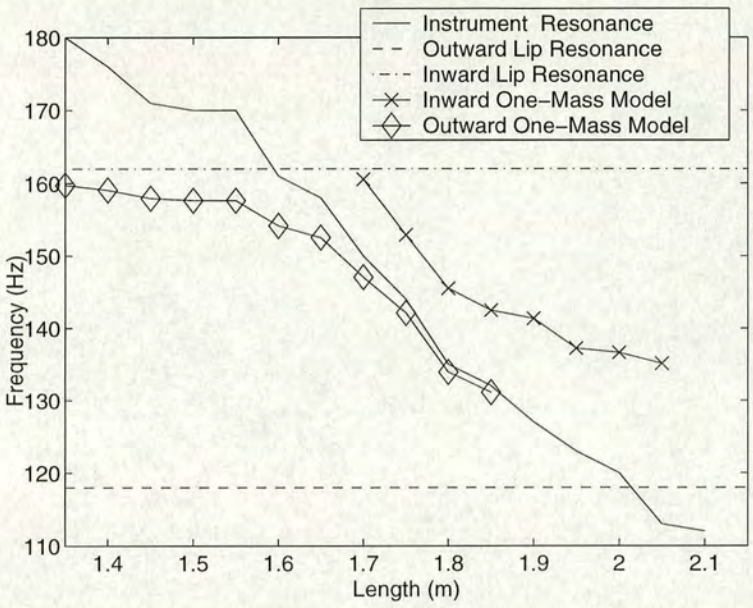

Figure 5.2: The threshold playing frequency of two different one-mass models. The cross symbols show an inward striking model, playing only *below* the instrument and reed resonances. The diamond symbols show an outward striking model, playing only *above* the instrument and reed resonances.

to the threshold playing experiments performed in the lab, it is also useful to examine the response of the lip model to a known small pressure difference. This gives comparable results to the response measurements presented in section 3.4.1. In order to obtain the response, a 1Pa impulsive pressure difference was created across the reed. The FFT of the resulting time domain motion gives the frequency response.

Figure 5.3 shows the response of a one-mass inward striking model. As expected, there is only one resonance. This model clearly does not accurately describe the response of the lip reed as shown in figure 3.18.

This one degree of freedom model is clearly unable to reproduce the exper-

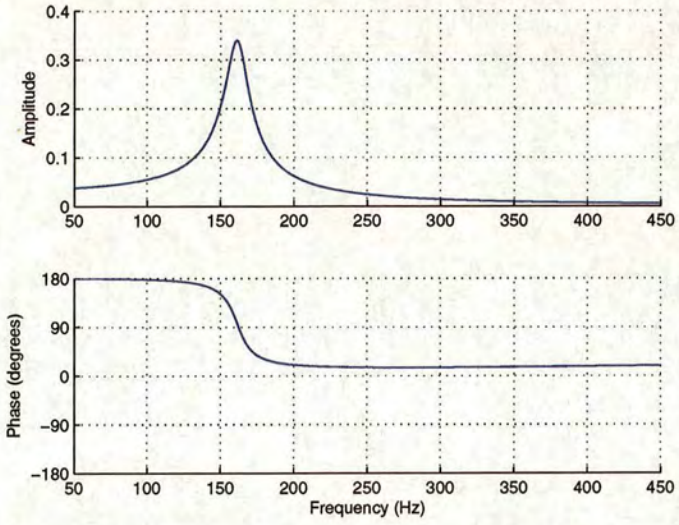

Figure 5.3: Frequency response of a one degree of freedom inward striking lip model. The response is as expected for a linear one-mode oscillator, and contains none of the complexity seen in experimental response measurements.

imentally observed behaviour. A more complex, but still very simple, model is investigated in the following section.

5.3.2 Two degree of freedom model

It is clear from the previous section that the one degree of freedom model is insufficient to explain the experimentally observed behaviour presented in chapter 3. Particularly, the model failed to play both above and below the resonance frequency of the instrument in a given configuration, and the response of the reed was very simple compared to the experimental response shown in figure 3.18.

The experimental measurements indicated that there were two significant resonances present in the lip reed that had an effect on its destabilisation. These

two resonances formed an outward and inward striking pair on either side of the threshold playing frequency. Based on this, it seems sensible to extend the model used in the previous section - using two degrees of freedom instead of just one. This is simple to do in a very general manner for the linear stability analysis.

Instead of a model free only to move in one dimension, y, we now use a model capable of moving in two dimensions: x_1 and x_2. No assumptions are made at this point as to the specifics of these dimensions – thus this model remains general enough to cover a large number of simple two–dimensional models, such as those presented by Adachi and Sato [3], Federico and Borin [23]

However, in order to provide a coupling between the displacements and the resulting flow admitted through the reed, the assumption is made that the opening height is just the average of the two displacements:

$$h = \frac{h_1 + h_2}{2} = x_1 + x_2. \tag{5.35}$$

The modes of oscillation are also coupled by arbitrary coupling constants C_1 and C_2. Making the same assumptions about flow separation as used in the previous section, the two dimensional equivalent of equation 5.16 is given by:

$$\frac{d^2x_1}{dt^2} + \frac{\omega_1}{Q_1}\frac{dx_1}{dt} + \omega_1^2(1 + C_1)x_1 - C_1\omega_1^2 x_2 = \mu_1(P_0 - P_i), \tag{5.36}$$

$$\frac{d^2x_2}{dt^2} + \frac{\omega_2}{Q_2}\frac{dx_2}{dt} + \omega_2^2(1 + C_2)x_2 - C_2\omega_2^2 x_1 = \mu_2(P_0 - P_i), \tag{5.37}$$

where μ_1 is the effective surface area/effective mass ratio relevant to motion in the direction x_1, and μ_2 is the effective surface area/effective mass ratio relevant to motion in the direction x_2. The equation of motion for the air resonator is still given by equation 5.6:

$$\frac{\partial^2 \psi}{\partial t^2} + \frac{\omega_i}{Q_i}\frac{\partial \psi}{\partial t} + \omega_i^2 \psi = \frac{Z_i \omega_i}{Q_i} U, \tag{5.38}$$

but a new definition of the flow, U, in terms of x_1 and x_2 is required:

$$U = \overline{U} + u = d\left(\overline{X_1} + \overline{X_2} + x_1 + x_2\right)\left(\overline{V_l} + v_l\right). \tag{5.39}$$

Using the same arguments as in the previous section, and assuming that $h = x_1 + x_2$, the linearised equation of motion for the resonator is given by:

$$\frac{d^2 \psi}{dt^2} + \left(\frac{\omega_i}{Q_i} + \frac{Z_i \omega_i}{Q_i}\frac{d\overline{H}}{\rho \overline{V_l}}\right)\frac{d\psi}{dt} + \omega_i^2 \psi - \frac{Z_i \omega_i}{Q_i} d\overline{V_l}(x_1 + x_2) = 0. \tag{5.40}$$

The equilibrium state is calculated, as with equation 5.34, by setting all time deriviatives to zero:

$$x_1 = \frac{P_0}{(1 + C_1 + C_2)}\left(\frac{\mu_1 (1 + C_2)}{\omega_1^2} + \frac{\mu_2 C_1}{\omega_2^2}\right), \tag{5.41}$$

$$x_2 = \frac{P_0}{(1 + C_1 + C_2)}\left(\frac{\mu_2 (1 + C_1)}{\omega_2^2} + \frac{\mu_1 C_2}{\omega_1^2}\right). \tag{5.42}$$

In the uncoupled case ($C_1 = C_2 = 0$), each of these equations becomes equivalent to equation 5.34:

$$x_1 = \frac{\mu_1 P_0}{\omega_1^2}, \tag{5.43}$$

$$x_2 = \frac{\mu_2 P_0}{\omega_2^2}, \tag{5.44}$$

The linearised equations are again calculated by removing any static or non-linear components from the equations, giving:

$$\frac{d^2x_1}{dt^2} + \frac{\omega_1}{Q_1}\frac{dx_1}{dt} + \frac{1}{\mu_1}\frac{d\psi}{dt} + \omega_1^2(1 + C_1)x_1 - C_1\omega_1^2 x_2 = 0, \tag{5.45}$$

$$\frac{d^2x_2}{dt^2} + \frac{\omega_2}{Q_2}\frac{dx_2}{dt} + \frac{1}{\mu_2}\frac{d\psi}{dt} + \omega_2^2(1 + C_2)x_2 - C_2\omega_2^2 x_1 = 0, \tag{5.46}$$

$$\frac{d^2\psi}{dt^2} + \left(\frac{\omega_i}{Q_i} + \frac{Z_i\omega_i}{Q_i}\frac{d\overline{H}}{\rho\overline{V_l}}\right)\frac{d\psi}{dt} + \omega_i^2\psi - \frac{Z_i\omega_i}{Q_i}d\overline{V_l}(x_1 + x_2) = 0. \tag{5.47}$$

These linearised equations can be written in matrix form (see equation 5.7):

$$\mathbf{M}\mathbf{x} = \frac{d}{dt}\mathbf{x}, \tag{5.48}$$

where:

$$\mathbf{M} = \begin{bmatrix} \mathbf{0} & \mathbf{I} \\ -\mathbf{K} & -\mathbf{C} \end{bmatrix}, \tag{5.49}$$

$$\mathbf{x} = \begin{bmatrix} x_1 \\ x_2 \\ \psi \\ \frac{dx_1}{dt} \\ \frac{dx_2}{dt} \\ \frac{d\psi}{dt} \end{bmatrix}, \tag{5.50}$$

$$\mathbf{K} = \begin{bmatrix} \omega_1^2(1+C_1) & -C_1\omega_1^2 & 0 \\ -C_2\omega_2^2 & \omega_2^2(1+C_2) & 0 \\ -\frac{Z_i\omega_i}{Q_i}d\overline{V_l} & -\frac{Z_i\omega_i}{Q_i}d\overline{V_l} & \omega_i^2 \end{bmatrix}, \tag{5.51}$$

$$\mathbf{C} = \begin{bmatrix} \frac{\omega_1}{Q_1} & 0 & \frac{1}{\mu_1} \\ 0 & \frac{\omega_2}{Q_2} & \frac{1}{\mu_2} \\ 0 & 0 & \left(\frac{\omega_i}{Q_i} - \frac{Z_i\omega_i}{Q_i}\frac{d\overline{H}}{\rho\overline{V_l}}\right) \end{bmatrix}. \tag{5.52}$$

The eigenvalues of the matrix $\mathbf{M}$ can then be derived as a function of mouth pressure, and the computation is repeated with varying parameters, most importantly the parameters of the resonator, as in section 5.3.1. Using the parameter set given in table 5.1, the threshold parameters as a function of tube length are obtained, as shown in Figure 5.4. This graph has a similar form to the experimentally obtained results shown in figure 3.22, playing below the air column resonance at short slide extensions (0cm – 15cm) and smoothly changing to playing above the air column resonance at longer slide extensions (20cm – 45cm).

Parameter	Value
ω_1	1018 rad s^{-1}
ω_2	1520 rad s^{-1}
Q_1	3.68
Q_2	3.6
μ_1	0.19 m^2kg^{-1}
μ_2	-0.19 m^2kg^{-1}
d	7mm
$\overline{H}$	1mm
C_1	0
C_2	0

Table 5.1: Parameters used to obtain the data in figure 5.4. The angular frequencies correspond to the measured resonance frequencies obtained from the data shown in figure 3.22 – 167Hz and 242Hz. Similarly, the values of d and $\overline{H}$ were measured experimentally. The remaining parameters were chosen to give suitable results, obtained by iteration around values obtained from experimental measurements.

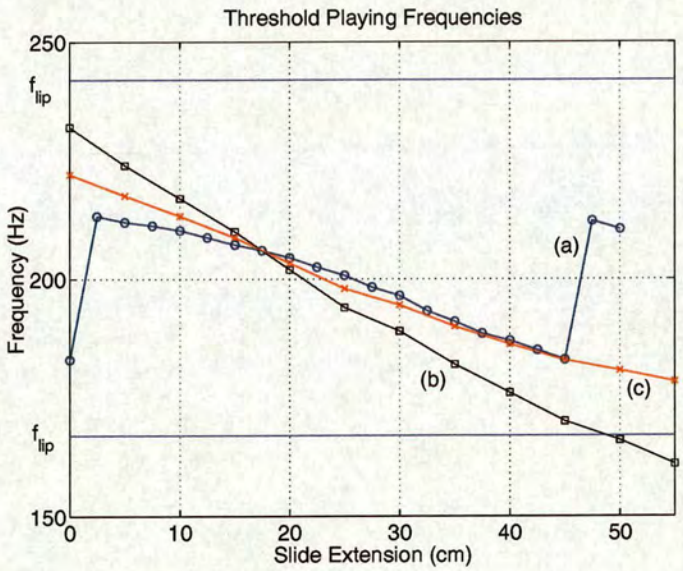

Figure 5.4: Threshold behaviour of the model. Lines (a) and (b) are the same as those recorded experimentally and shown in figure 3.22. Line (c) shows the simulated threshold playing frequencies, as obtained from linear stability analysis.

In this instance, the two lip resonance frequencies were taken from experimental lip response measurements. The quality factors were estimated from

these measurements, and the μ_1 and μ_2 parameters were based on those used by Cullen [18]. The quality factors and μ_1 and μ_2 parameters were then adjusted around their initial values to create a "virtual embouchure" that would destabilise within the given range.

Figure 5.5 shows the threshold playing frequency of both the one degree of freedom model used in section 5.3.1 and the two degree of freedom model used here. As can be seen, the one degree of freedom model can model the cases where the threshold playing frequency is relatively far from the instrument resonance, but the two degree of freedom model smoothly crosses from playing below to playing above the instrument resonance.

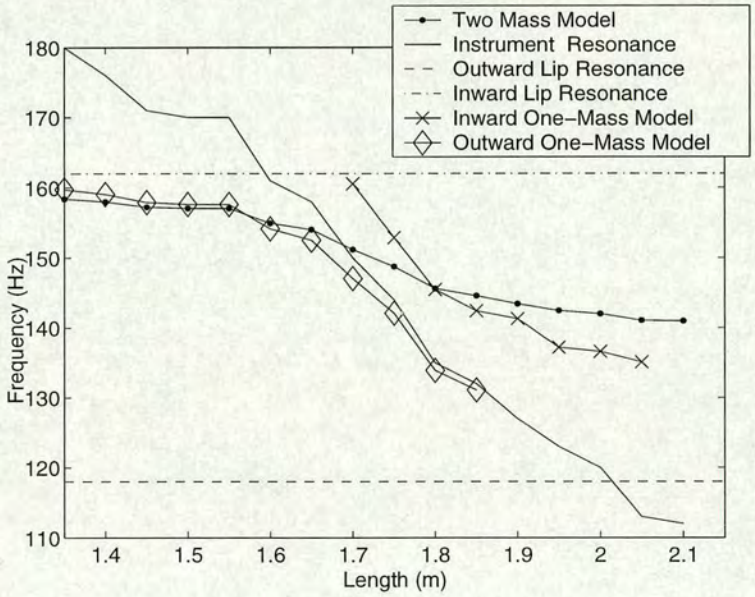

Figure 5.5: Linear stability results for the one degree of freedom and two degree of freedom models. The threshold playing frequency of the one degree of freedom models does not cross over the resonance frequency of the air column, but the two degree of freedom model smoothly crosses over.

5.4 A non–linear two degree of freedom lip model

The human vocal folds share many similar characteristics with the human lips. Both are made up of a similar structure of tissue and muscle, and both are made to oscillate by forcing air through the constricted area of opening. As such it is possible to translate models used in voice synthesis to model the lips of the brass player. One such vocal fold model, presented by Lous et al [43] and based on a model originally described by Ishizaka and Flanagan [37], is used here to represent the lips. Figure 5.6 shows the model.

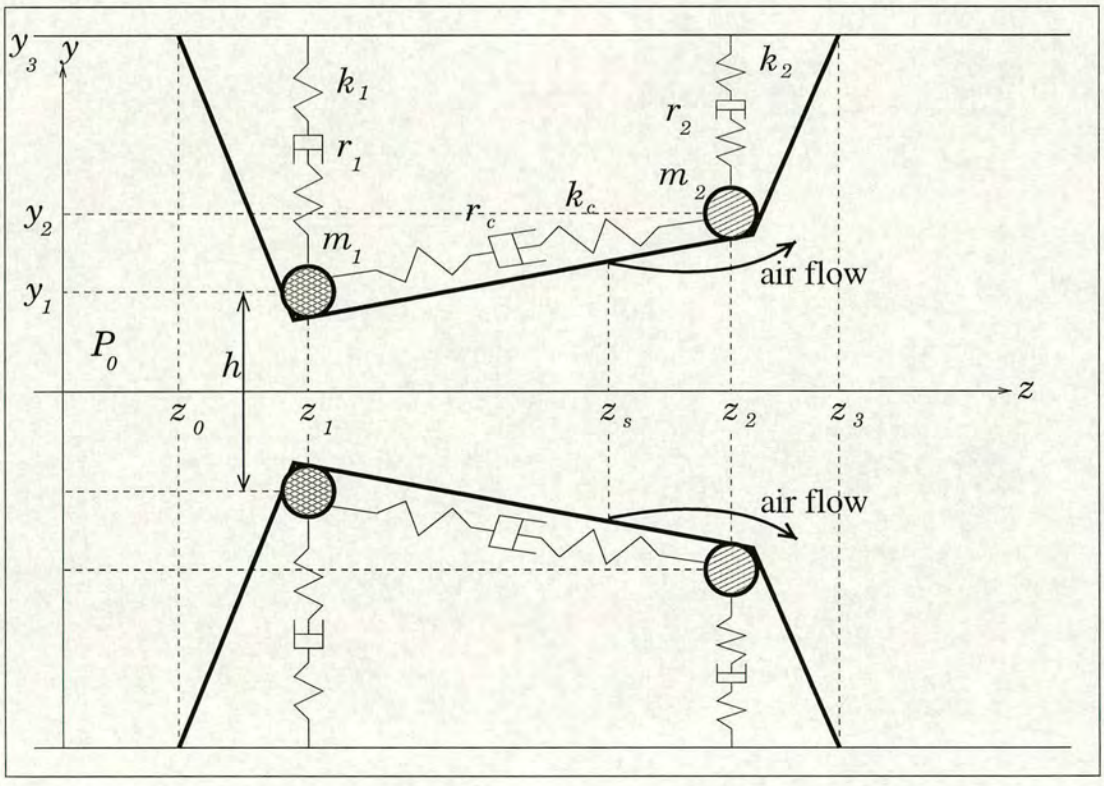

Figure 5.6: Lous model of the vocal folds. Through appropriate parameter choice this model can be adapted to represent the brass players' lips.

It is useful to make the assumption at this early stage that the motions of the top and bottom lips are symmetrical. This assumption was also used in the previous models presented in this chapter. In practice, there is a wide variation in the symmetry of motion of the lips – both between players and between different notes played by the same player. The spread of playing styles encompasses motion where the top and bottom lips behave in a similar fashion, but also where the bottom lip is almost stationary. Each lip is represented by a pair of coupled masses on springs. Each of the two masses is constrained to move in only one dimension (the y–direction), so the model has only two degrees of freedom. If one of these dimensions has inward–striking characteristics and the other outward–striking, this model will have the potential to fulfil the behaviour seen both experimentally (section 3.4.3) and in the linear stability analysis of a two degree of freedom model presented in section 5.3.2.

The parameters of the model shown in figure 5.6 are listed in table 5.2. The parameters are mirrored for the upper and lower lips due to the assumed symmetry. These parameters should be thought of as "effective" parameters - ie, "effective mass" - because they do not necessarily directly reflect actual physical measurements. Due to the simplification implicit in using a model of this nature, these parameters are representative of "lumped" physical parameters. For instance, the inner point mass used here is representative of the distributed mass of the inner portion of the lip.

Parameter	Description
m_1	Effective mass of the inner point mass.
m_2	Effective mass of the outer point mass.
k_1	Effective spring constant for the inner spring.
k_2	Effective spring constant for the outer spring.
k_c	Effective spring constant for the coupling spring.
γ_1	Effective damping co–efficient for the inner spring.
γ_2	Effective damping co–efficient for the outer spring.
γ_c	Effective damping co–efficient for the coupling spring.
d	Effective width of the lip channel (in the x–direction).
z_0	Left–most point of the movable part of the lip geometry.
z_1	x–co–ordinate of the inner point mass.
z_2	x–co–ordinate of the outer point mass.
z_3	Right–most point of the movable part of the lip geometry.
z_s	Point at which the flow of air separates from the lip surface.
y_1	Vertical displacement from the centre of the lips of the inner point mass.
y_2	Vertical displacement from the centre of the lips of the outer point mass.
y_3	Height of the upstream and downstream channels.

Table 5.2: Descriptions of the parameters of the lip model shown in figure 5.6. The upper and lower lips are assumed to move symmetrically, so the parameters are equivalent for both lips.

In order to investigate the characteristics of this lip model, time domain simulations were used to analyse both the response of the lips in the frequency domain, and the steady state oscillation behaviour. A Matlab program was written for this purpose, which allowed a variety of model parameters to be used and data extracted from the simulation at any and all relevant points. Of specific interest were the calculated displacements of the individual point masses – which were examined to provide the response of the model.

The equations of motion were derived by Lous et al. [43], in terms of the y–displacements of each point mass.

$$m_1\ddot{y_1} + R_1\dot{y_1} + K_1y_1 + K_{12}(y_1 - y_2) = F_{h1} \tag{5.53}$$

$$m_2\ddot{y_2} + R_2\dot{y_2} + K_2y_2 + K_{12}(y_2 - y_1) = F_{h2} \tag{5.54}$$

where

$$F_{h1} = \int_{z_0}^{z_1} \left(\frac{z - z_0}{z_1 - z_0}\right) p(z,t)dz + \int_{z_1}^{z_2} \left(\frac{z_2 - z}{z_2 - z_1}\right) p(z,t)dz, \tag{5.55}$$

and

$$F_{h2} = \int_{z_1}^{z_2} \left(\frac{z - z_1}{z_2 - z_1}\right) p(z,t)dz + \int_{z_2}^{z_3} \left(\frac{z_3 - z}{z_3 - z_2}\right) p(z,t)dz, \tag{5.56}$$

The pressure, $p(z,t)$ is given by the Bernouilli equation assuming a 1–dimensional,

quasi–stationary, frictionless and incompressible flow:

$$p(z,t) = p_0(t) + \frac{\rho_0}{2}\left(\frac{U_g(t)}{h_0 d}\right)^2 - \frac{\rho_0}{2}\left(\frac{U_g(t)}{h(z,t)d}\right)^2 \tag{5.57}$$

The program is structured as follows:

- Set initial conditions.
- Calculate pressure difference across the lips.
- Calculate the volume flow from the current geometry and pressure difference, using cartesian co–ordinates.
- Calculate the forces on the lips due to the fluid pressures.
- Calculate the resulting displacement of the point masses for a timestep Δt.
- Update the geometries of the lips (ie, calculate cartesian co–ordinates for calculation of the volume flow).
- Add current geometries to the "answer" data set.
- Update timestep and loop back to calculation of the pressure difference.
- Once the simulation has run for the desired period, organise the data sets and graph the results.

Initial investigations of the impulse response of the displacement in the y_1 and y_2 directions, of mass 1 and mass 2 respective produce the results expected of a

pair of coupled simple harmonic oscillators - namely, two resonant peaks. This is shown in figure 5.7. The phase behaviour of these resonances shows clearly that there are both inward $(+\pi/2)$ and outward $(-\pi/2)$ striking characteristics associated with the motions of these masses.

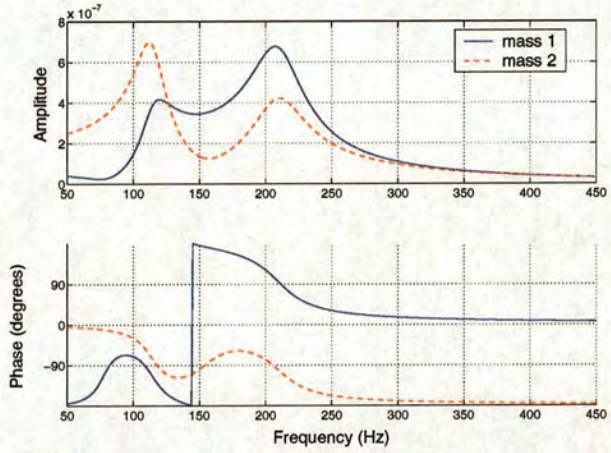

Figure 5.7: The impulse response (in the frequency domain) of the displacement of the individual point masses of the lip model. As expected, each of the two coupled point masses exhibits two resonances. What can also be seen is that there are clearly inward and outward striking characteristics present in these response curves.

This response curve is still far removed from those observed experimentally (see figure 3.18). The experimental response curves show a far more complex structure, with further peaks above, below and between the main resonances.

However, the experimental technique used to obtain the data shown in figure 3.18 (which is repeated here as figure 5.8 for reference) was designed to measure the area of opening between the lips, and not the individual displacements of point masses in the lip. Consequently, a direct comparison between the two data sets is not appropriate. Instead, this simulated response curve could be compared

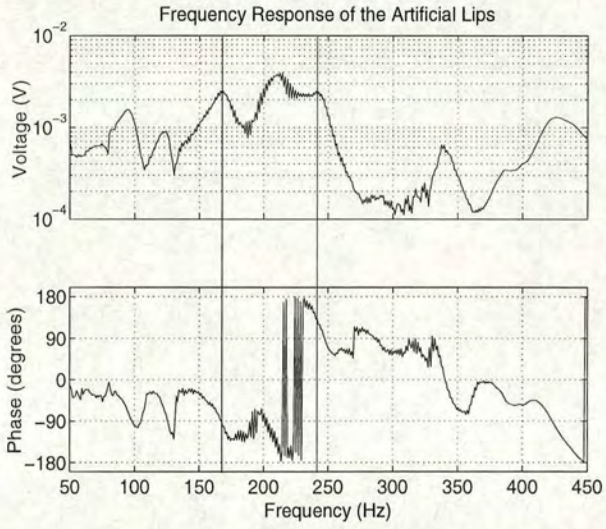

Figure 5.8: Frequency Response of a typical configuration. The vertical lines show the destabilising outward and inward striking resonances, at 167Hz and 242Hz respectively. This figure is a repeat of figure 3.18.

to experimental measurements of point displacements of the artificial mouth, or the experimental measurements of the area of opening could be compared to the equivalent function in the simulation data.

Comparison to experimentally obtained point displacements is the less accurate of the two techniques. The computational model is a highly simplified representation of the physical system. One of the main simplifications is the representation of the lips, which are a distributed system, as a pair of point masses. This makes direct comparisons between the displacement of these symbolic entities with the real physical system difficult. However, experiments performed using the laser Doppler vibrometer (presented in section 4.3) provide a possible source of data for these comparisons. This will be discussed later in this section.

Examining the computational model for the appropriate area of opening function is a much simpler comparison to make. In order to do this, the area of opening function needs to be defined. For the one degree of freedom model used in section 5.3.1 the area of opening was assumed to be rectangular, with a fixed width and a variable height, which depended solely on the displacement of the mass. The same assumptions are used here, except that the height no longer depends on the displacement of a single mass, but rather on the displacement of both masses in the model. In fact, the area of opening is dependant on the displacement of whichever mass is lower at the time of measurement. This can be described by saying:

$$Area = 2d \min[y_1, y_2], \tag{5.58}$$

where d is the fixed width of the lip opening, and $\min[y_1, y_2]$ is the lesser (minimum) of the displacements y_1 and y_2. Figure 5.9 shows the response of this function in the frequency domain.

The response clearly shows a more complex structure than the responses of the displacements of the point masses. The presence of two peaks above the resonance frequencies of the masses is similar to those seen in the experimental response measurement (figure 3.18). These peaks can be explained by considering the behaviour of the lip model if the inner and outer point masses are oscillating out of phase. Using the simple case of sinusoidal motion as an example, with the point masses oscillating at the same frequency and π radians out of phase with

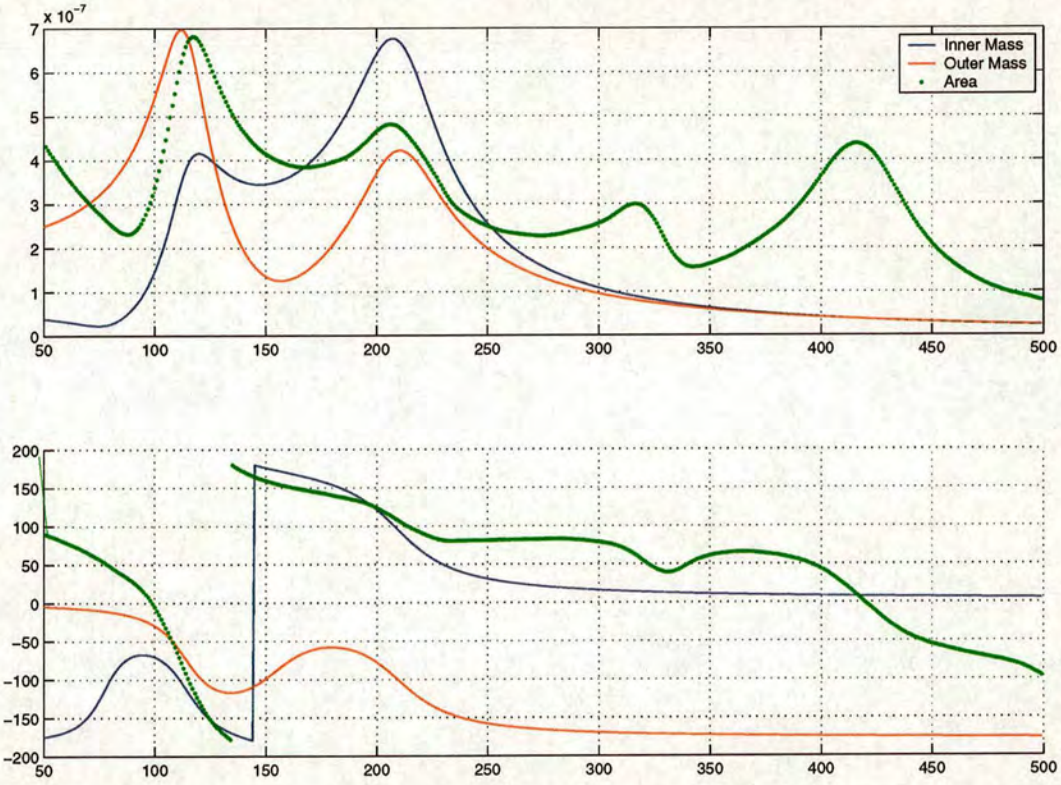

Figure 5.9: Response of the area of opening function of the lip model (green line). The red and blue lines show the response of the displacement of the two point masses (see figure 5.7). The higher two peaks form the "fingerprint" of the non-linear height function. The lower two resonances form a pair of outward and inward striking resonances.

one another, the height function will take the form of a rectified wave (figure 5.10), with a fundamental period which is half that of the individual sinusoidal motions.

The phase of the area of opening function shows that the two main resonances form an outward striking and inward striking pair, as seen in the experimental studies [17] [18] [48] [49] [50] [54]. Thus the evidence is strong that the area of opening function in the model used here behaves in a similar fashion to the areas

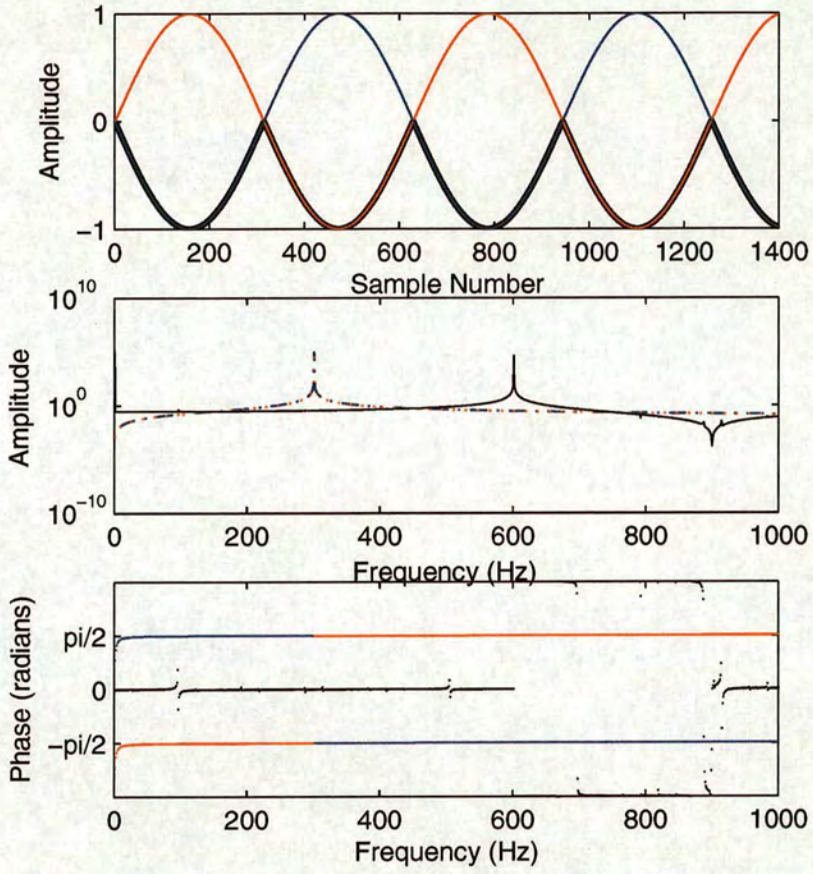

Figure 5.10: When two out of phase sine waves (blue and red lines) are superposed the resulting waveform (black line) has twice the frequency of the original sine waves

of opening measured experimentally.

In order to examine how well this model describes the motion of the lip, it is useful to look at how the motion of individual points on the lip surface compares to similar measurements performed in the lab. The measurements made using the laser Doppler vibrometer (LDV), presented in section 4.3, are repeated here for convenience (figure 5.11).

It is reasonable to compare the displacements of the point masses calculated

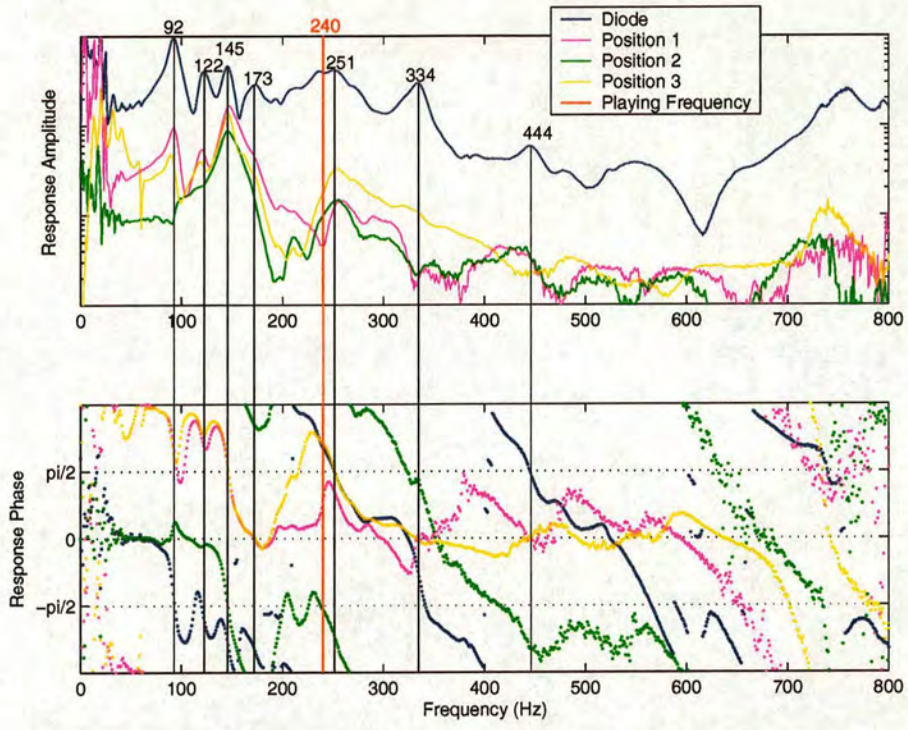

Figure 5.11: Response of the opening area (diode signal) and the point displacements. The red vertical line shows the threshold playing frequency (240Hz), the vertical black lines show the resonances identified in the opening area response. The key resonances are the outward striking resonances at 92Hz, 122Hz and 145Hz, and the inward striking resonance at 251Hz. This figure is a repeat of figure 4.10.

in the simulations with the measured displacements of points on the lip surface measured with the LDV. In particular, the measurements taken in position 2 (green line) can be approximated as a measurement of the displacement in the vertical direction of the front of the lip – equivalent to the front point mass in the model (the red line in figure 5.9). The similarity between this curve and that obtained for the point mass is quite striking. Particularly, the presence of two main resonances (at 145Hz and 251Hz) with outward striking phase ($-\pi/2$ radians) in the experimental curve matches with the simulated data. In addition,

the lack of any significant response above the main responses in the experimental vibrometer data suggests that these resonances (seen in the diode signal, the blue line in figure 5.11) are indeed non–linear phenomena resulting from the area of opening function. Unfortunately, the physical constraints of working with the artificial mouth meant that it was not possible to measure the vertical displacement of the inner part of the lip surface, which would correspond to motion of mass 1 in the y_1 direction.

The low frequency lip resonances seen in the experimentally observed area of opening response (figure 3.18) are also present in the vibrometer measurements in figure 5.11. Their presence in the measurements of displacement in the direction of the lip channel (positions 1 and 3, shown by the magenta and yellow lines in figure 5.11) suggests that these resonances are solely related to the motion of the lip in this direction. This would be equivalent to displacement in the z–direction in the model presented above. However, these resonances do not appear in figure 5.9 because the model was prohibited from moving freely in this direction.

Figure 4.4 shows the time domain waveforms of the area of lip opening for a number of different notes, recorded using the high speed camera. These waveforms have features where the velocity suddenly changes. This effect can be reproduced when looking at the "switching" behaviour of the lip model, where the waveform of the area of opening can be seen to exhibit discontinuities where the displacement of one mass becomes lower than the other. This is shown in

figure 5.12.

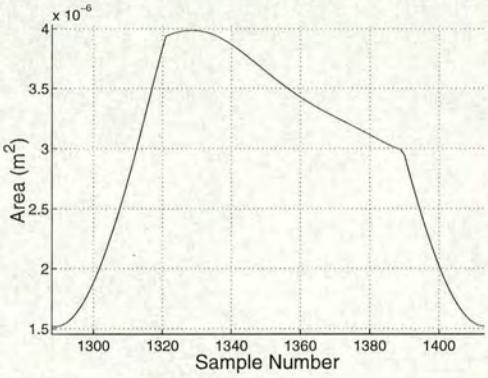

Figure 5.12: Opening area waveform produced by the Lous model. The discontinuities occur where the y-displacement of one mass becomes less than the other.

This model is capable of producing results which are qualitatively similar to those seen in the experimental studies, when looking at the non–linear function that defines the area of opening between the lips. Specifically, it demonstrates a pair of outward/inward striking resonances, and some of the non–linear responses at higher frequencies. However, it fails to reproduce the low frequency responses seen in the experimental data.

In order to investigate whether these resonances were due to the motion in the z–direction, the model was adapted to allow for motion in this dimension. The most convenient way of doing this was to change the co–ordinate system to that shown in figure 5.13 – ie, using the co–ordinates r_1, r_2, ϕ_1 and ϕ_2 to describe the system. This involved the addition of the control parameters k_{ϕ_1}, k_{ϕ_2}, γ_{ϕ_1} and γ_{ϕ_2}, which represent the effective spring constants and damping factors of

the two new springs associated with motion in the ϕ_1 and ϕ_2 dimensions, as well as re–defining the springs that previously acted in the y_1 and y_2 directions to now act in the r_1 and r_2 directions.

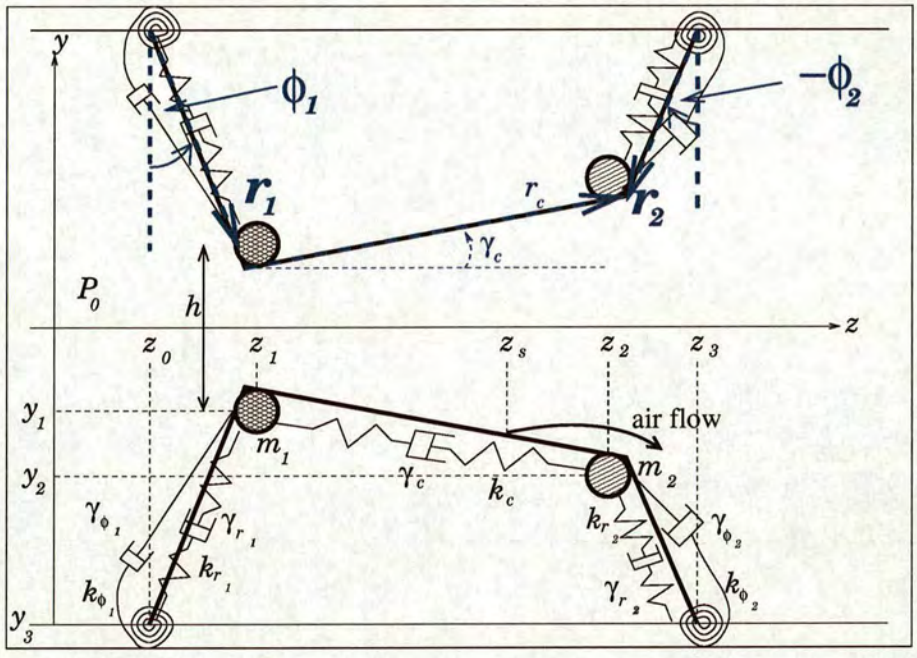

Figure 5.13: The co–ordinate system used for analysis of the lip model. Using circular co–ordinates instead of cartesian co–ordinates allows for simple extension of the model into a four degree–of–freedom model. The ϕ_2 co–ordinate is negative in this diagram because ϕ is defined as being positive in the clockwise direction.

Equations 5.53 to 5.56 adapted to calculate the displacement in circular co–ordinates for each point mass (ie, using r and ϕ instead of x and y) are given here. The equation of motion for r_1 is given by:

$$\frac{\partial^2 r_1}{\partial t^2} - \frac{\gamma_{r_1}}{m_1}\frac{\partial r_1}{\partial t} + \frac{k_{r_1}}{m_1}(r_1 - r_1(0)) + \frac{k_c}{m_1}(r_c - r_c(0))sin(\phi_1 + \phi_c) = \frac{F_{r_1}}{m_1}, \quad (5.59)$$

where r_1, r_2, ϕ_1 and ϕ_2 are the dimensions as given in figure 5.13, the parameters

γ and k refer to the damping and spring co–efficients in the given (subscript) dimension, with γ_c and k_c giving the coupling damping and spring co–efficients, and $r_1(0)$ and $\phi_1(0)$, and $r_2(0)$ and $\phi_2(0)$ are the equilibrium positions of mass 1 and 2 respectively. $r_c(0)$ and $\phi_c(0)$ are the equilibrium co–ordinates of the coupling spring. F_{r_1} is given by:

$$F_{r_1} = d\frac{sin(\phi_1 + \phi_c)}{cos(\phi_c)} \int_{z_1}^{z_2} \left(\frac{z_2 - z}{z_2 - z_1}\right) p(z,t)dz. \tag{5.60}$$

The equation of motion for r_2 is given by:

$$\frac{\partial^2 r_2}{\partial t^2} - \frac{\gamma_{r_2}}{m_2}\frac{\partial r_2}{\partial t} + \frac{k_{r_2}}{m_2}(r_2 - r_2(0)) + \frac{k_c}{m_2}(r_c - r_c(0))sin(\phi_c + \phi_2) = \frac{F_{r_2}}{m_2}, \tag{5.61}$$

and the driving force, F_{r_2} is given by:

$$F_{r_2} = d\frac{sin(\phi_c)}{sin(\phi_2)} \int_{z_1}^{z_2} \left(\frac{z - z_1}{z_2 - z_1}\right) p(z,t)dz. \tag{5.62}$$

The equation of motion for ϕ_1 is given by:

$$\begin{aligned} &\tfrac{\partial^2 \phi_1}{\partial t^2} - \tfrac{\gamma_{\phi_1}\phi_1 r_1^2}{I_1}\tfrac{\partial \phi_1}{\partial t} + \tfrac{k_{\phi_1}}{4I_1}(\phi_1 r_1^2 - \phi_1(0)r_1(0)^2) \\ &+\tfrac{k_c r_1}{I_1}(r_c - r_c(0))cos(\phi_1 + \phi_c) = \tfrac{F_{\phi_1}}{I_1}, \end{aligned} \tag{5.63}$$

where the moment of inertia, I_1, is given by:

$$I_1 = \frac{1}{3}m_1 r_1^2 \tag{5.64}$$

and the driving force, F_{ϕ_1} is given by:

$$\begin{aligned} F_{\phi_1} &= d\frac{(z_1-z_0)}{sin^2(\phi_1)}\int_{z_0}^{z_1}\left(\frac{z-z_0}{z_1-z_0}\right)p(z,t)dz \\ &+d\frac{cos(\phi_1+\phi_c)}{cos(\phi_c)}r_1\int_{z_1}^{z_2}\left(\frac{z_2-z}{z_2-z_1}\right)p(z,t)dz. \end{aligned} \tag{5.65}$$

The equation of motion for ϕ_2 is given by:

$$\begin{aligned} &\frac{\partial\phi_2}{\partial t}-\frac{\gamma_{\phi_2}r_2^2}{I_2}\frac{\partial\phi_2}{\partial t}+\frac{k_{\phi_2}}{4I_2}\left(\phi_2 r_2^2-\phi_2(0)r_2(0)^2\right)- \\ &\frac{r_2k_c}{I_2}\left(r_2-r_c(0)\right)cos(\phi_2+\phi_c)=\frac{F_{\phi_2}}{I_2}, \end{aligned} \tag{5.66}$$

where the moment of inertia, I_2 is given by:

$$I_2=\frac{1}{3}m_2r_2^2, \tag{5.67}$$

and the driving force, F_{ϕ_2}, is given by:

$$\begin{aligned} F_{\phi_2} &= d\frac{z_3-z_2}{sin^2(\phi_2)}\int_{z_2}^{z_3}\left(\frac{z_3-z}{z_3-z_2}\right)p(z,t)dz+ \\ &d\frac{cos(\phi_c)}{cos(\phi_2)}r_2\int_{z_1}^{z_2}\left(\frac{z-z_1}{z_2-z_1}\right)p(z,t)dz \end{aligned} \tag{5.68}$$

With the addition of these parameters, and accounting for the fact that the geometric behaviour of the model becomes much more complex (instead of just two variable components to the geometry, there are now four), the model becomes very unwieldy and difficult to control. Nevertheless, preliminary results shown in figure 5.14 show that freeing up these extra dimensions brings forth further low frequency resonances.

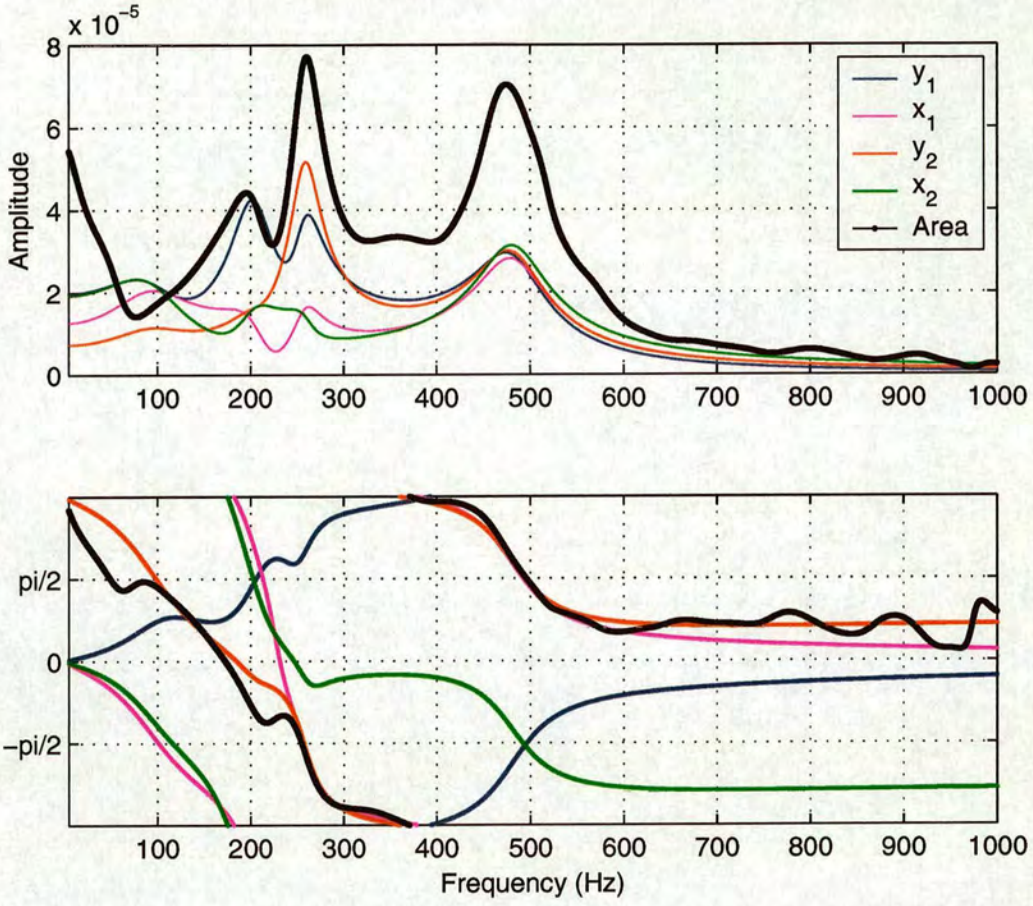

Figure 5.14: The response of the lip model in four dimensions, together with the response of the non–linear area of opening function. Of particular interest is the presence of additional low frequency resonances.

5.5 Conclusions

Linear stability analysis has shown that a one degree of freedom model cannot reproduce the phenomenon of "lipping" a note both above and below the resonance of the instrument being played. Analysis shows that a two degree of freedom model, with both an inward–striking and outward–striking modes, is capable of reproducing this experimentally observed behaviour.

Time domain simulations provide results that are comparable with experimental measurements of reed response. The response of the one degree of freedom model bears little similarity with the experimental results. The response of the displacements of the two degree of freedom model used here shows similarities with the experimental response data obtained using the laser Doppler vibrometry techniques – particularly with the data set that corresponds to the displacement of the lip in the vertical direction.

In order to compare the model response with the experimentally obtained measurement of the response function of the area of opening, the height function needs to be defined as:

$$h = \min[y_1, y_2], \tag{5.69}$$

corresponding to the "switching" motion that occurs when the point masses in the lip model move out of phase. The response of this function shows clear similarities to the response data obtained experimentally. Particularly, the peaks at the higher frequencies seen in the lab emerge from the non–linear function.

In order to display resonances at lower frequencies, the model needs to be extended to motion in four dimensions. Initial investigations of the four degree of freedom model show low–frequency resonances in the direction of the fluid flow (the z–direction in the co–ordinates used here).

Chapter 6

Conclusions and Future Work

6.1 Suggested changes to the Artificial Mouth

The artificial mouth used in this study has proved to be particularly well suited to a wide variety of measurements on the lip reed. However, during the course of this study, several potential improvements to the design have come to light. Throughout this section, the component labelling established in section 3.2 will be used.

6.1.1 Main Box Construction

The main mouth cavity volume was adjustable between 300ml and 1800ml. The experiments on mouth cavity volume presented in section 3.4.4 showed that the

influence of the mouth cavity on the destabilisation of the lips with no resonator attached increased as the cavity volume decreased. The volume had an effect at a cavity of 425ml or smaller. In order to investigate this phenomenon more thoroughly, it would have been convenient to have a cavity that was reducible to a much lower volume to more accurately model the range of volumes available to the human player.

6.1.2 Front Plate

The front plate of the artificial mouth hosts the majority of the key control devices. These devices were, on the whole, designed to be easily interchangeable with different pieces, provided those pieces were designed to fit the existing mount points. In particular, the lip guides(b) and lip retention blocks(d) were designed to be easily exchanged. Throughout the course of this study, only one set of these components was used, and no other components were constructed. An investigation of the effectiveness of different lip guides and lip retention blocks would be most useful. Of particular interest would be constructing a series of lip retention blocks with a different spacing of the holes. This would allow a greater control over the equilibrium position of the lips than can be offered by the lip guides alone. Additionally, the use of different lip guides could prove useful in obtaining "better" embouchures (where a stable note was easier to achieve, or with a greater dynamic and pitch range), especially when considering using a

different type of instrument mouthpiece. For instance, to allow a trumpet to be played well, it may prove useful to have lip guides that have a smaller raidus of curvature. Conversely, to aid in the playing of the didjeridu, much wider, shallower lip guides may prove useful.

6.1.3 Mouthpiece Holder

The method of securing the mouthpiece could also be improved. In this study, it was found that the height of the mouthpiece could not be easily reproduced between experiments. To facilitate this, a groove was cut in the shaft(o) of the mouthpiece holder (m). This allowed the height to be fixed, by locking the PVC locking bolt (p) into the groove. However, this restricted the mouthpiece to effectively one vertical position. What is more, the angular position of the mouthpiece was still uncontrollable. In order to overcome these obstacles, a regular series of "dimples" should be cut into the shaft. These should be spaced at regular intervals, and be at an angle on the shaft such that when the locking bolt (p) is fixed in place, the mouthpiece rim is parallel with the face plate(A).

6.1.4 Tongue Mechanism

The tongue mechanism was designed to simulate the effect of a human player starting a note on a brass instrument. However, although it could provide the

rapid transient opening equivalent to a brass player's "tonguing" of a note, the accompanying rise in blowing pressure can not be provided by this mechanism. Instead, the pressure behind the lips is held artificially high by the pump, and the consequent release when the tonge mechanism is opened is quite explosive. In order to investigate this area further, the supply pressure would need to be controlled in an appropriate manner, perhaps by the use of a quickly opening valve (although slower speed than the tongue valve) – controlled either manually or by computer. The specifics of the behaviour of the supply pressure could be easily investigated using human players.

6.2 Investigation of threshold behaviour

The experiments investigating the threshold playing frequency as a function of instrument resonance (varied by changing the slide extension of a trombone) confirmed that the artificial lips used in this study could, like human players and previous artificial lip setups [18] [48], smoothly "lip" a note from below to above the resonance frequency of the instrument, with a constant embouchure. This behaviour is at odds with the *outward–striking* model used by Helmholtz [34] to describe the motion of the lip reed.

Using linear stability analysis to investigate the stability of a lip model around an equilibrium point, which is comparable to experimental measurements of

threshold playing, it was shown that a model with two degrees of freedom – one outward–striking and one inward–striking – could reproduce this smooth "lipping" behaviour. Linear stability analysis of a simple one dimensional model shows that such a model has the ability to play only below, in the case of an inward–striking model, or above, in the case of an outward–striking model, the instrument resonance, but not both.

6.3 Mouth Cavity

A brief investigation into the effect of the mouth cavity on the ability of the lips to self–oscillate (ie, play a mouthpiece rim only, with no air resonance attached downstream), showed that the ability of the artificial lips to self oscillate, without an air resonance, was influenced by the size of the air volume in the mouth cavity. As the volume of air in the mouth cavity was increased in 25ml steps from 300ml, the threshold pressure (required for self–sustained oscillation) also increased, until at a cavity volume of 450ml the pressure supplied by the pump was no longer enough to destabilise the lips.

6.4 Response Measurement

Measurements of the lip response in previous studies of the lip reed [17] [18] [49] [50] [48] [53] recorded the opening height or area of opening between the lips. The results of these measurements revealed a complicated response structure that could not be explained by a simple linear model. Further consideration of the nature of the experiments, while considering a type of lip model such as that presented in section 5.4, suggests that the measurement of the area of lip opening is not a linear function of the displacement of individual points on the lip surface, but is a non-linear function of these displacements.

Investigations of the lip response in two dimensions, using a laser doppler vibrometer, provided more insight into the behaviour of the reed. The recording of the reed response in the vertical direction showed that this response was far more linear in nature than the measurements of the opening height response, and bore characteristics of a system made up of two coupled oscillators – ie, two distinct resonances, with very little "non–linear" response at frequencies above these resonances – suggesting that the measurements of the area of lip opening correspond with the "switching" behaviour described by equation 5.58. Motion in the direction of the flow (ie, outwards from the face) was also recorded. This data showed additional resonances that were not present in the upward motion, suggesting that these resonances exist solely in the "outward" direction.

6.5 High speed video recordings

Recordings of the reed motion during self–sustained oscillation (with a resonator attached) using a high speed camera and motion tracking techniques showed that a point on the lip engages in rotational motion – ie, moving both upwards and outwards with a phase difference between the upward displacement and outward displacement between $\frac{\pi}{2}$ and $\frac{3\pi}{2}$.

The area of opening between the lips was analysed during oscillation, and provided confirmation that the opening area between the lips was not rectangular (a simplification used in many models), but rather followed a power law:

$$A = \alpha H^n, \tag{6.1}$$

where A is the area of opening between the lips (in units of mm^2), H is the maximum opening height between the lips (in units of mm), and α is a constant (with dimensions of $\text{mm}^{(2-n)}$). The values of n observed here ranged from 1.35 to 1.72, and the values of α ranged from $3.39\text{mm}^{0.52}$ to $4.35\text{mm}^{0.65}$ (see table 4.2).

6.6 Computational Lip Modelling

The response of a linear, one degree of freedom model (figure 5.3) showed that this model is inadequate for describing the experimentally observed lip response.

However, the response of the displacement of the point masses in the two degree of freedom model of the lips based on the Lous model of the vocal folds [43] produced a two–mode system with outward–striking and inward–striking characteristics. This response data had striking similarities to the experimentally measured response of the displacement of the front of the artificial lips in the vertical direction, recorded using the laser doppler vibrometer. Comparison with the vertical motion of the rear part of the lips was not possible due to the inaccessibility of that part of the lip in the experimental setup used.

When considering the specifics of the experimental measurements of lip response, it becomes clear that the function being measured is the area of opening between the lips, and not the opening height. Simple models make the assumption that the area of opening is directly proportional to the opening height. However, when the area of opening between the lips of the model used in section 5.4 was examined, it was seen that the area of opening is defined by a non–linear function of the height between the separate masses of the lips. Thus a direct comparison between the experimental measurements of the response of the area of opening between the artificial lips was made. This showed further similarities between the experimental and comptational results. In particular, non–linear peaks were evident in the response curve at frequencies above the fundamental resonances of the system, which matched similar peaks seen in the experimental results.

Extension of the model into four degrees of freedom suggested that the low

frequency resonances seen in the measurements taken with the laser doppler vibrometer of motion in the "outwards" direction could be explained by modelling "swinging" motion in the lip model. Such a model is, however, very difficult to control – a particularly important point when considering the implementation of physical modelling sound synthesis, for instance.

The methods used in this thesis focus on the low–amplitude playing near threshold. This only encompasses the lower end of the dynamic range of brass players. Consequently, further investigation of the high–amplitude behaviour of the lip reed is important for sound simulation purposes.

6.7 Future work

In order to further investigate the motion of the lips during oscillation, measurements of the motion of both artificial and human lips using the high speed cameraIn particular would be useful. Such an investigation should also investigate the differences between the artificial lips and human lips, as well as variations within human players.

It may be possible, using a high speed camera or laser Doppler vibrometry, to investigate the mechanical response of a human player's embouchure. Such an investigation would be unlikely to produce measurements with similar accuracy to the measurements of the response of the artificial lips, but would likely pro-

vide further information as to the similarities, or otherwise, between human and artificial lips.

Understanding what makes a "bad" embouchure – one that does not play a stable note, or that will not play at all – could be investigated by further measurements of the response of such embouchures. Such an investigation could easily encompass an investigation of how best to control the parameters of the embouchure – particularly the amplitude, quality factors and frequencies of the lip resonances.

Additional investigation of lip models with similar characteristics to those two and four degree of freedom models used here, with a particular focus on their stability and controllability, could yield results that not only further the understanding of the lip reed, but could also lead to development of the "next generation" of physical model based sound synthesis devices.

6.8 Conclusions

Clearly, the lip reed is far more complex than Helmholtz' initial description suggests. A two–mode oscillator is required to explain the flexibility in the threshold playing frequency of the lip reed.

Many of the experimentally observed features of the artificial lip reed can be explained by the model of the lips based on the Lous model of the vocal fold.

- The non–linear function that describes the area of opening between the reed shows similar characteristics to the experimentally measured mechanical response of the artificial lips.

- The mechanical response of the displacement of individual points on the surface of the artificial lips in the "upward" (y) direction (and the "outward" (z) direction when the model is given four degrees of freedom), shows strong similarities to the equivalent response in the model.

Appendix A

The PULSE System

The Brüel and Kjær (B&K) PULSE system is a hardware and software package that provides two main services:

- It acts as an amplifier for the B&K microphones.
- It provides a data acquisition system.
- It can perform a large number of analysis and signal processing functions.
- It can generate a wide range of signals at high sampling frequencies.

The deconvolution was performed using an average of a configurable number of samples. The averaging was done using the "exponential" averaging method provided by the PULSE software, with the samples overlapping by 75%. This method weighted the contribution of each sample towards the average by an

exponentially decaying curve with a time constant equal to the number of averages taken (N_a) multiplied by the time between sample triggers ($0.25T$ for a 75% overlap).

$$A(t) = e^{\frac{4t}{N_a T}} \tag{A.1}$$

This meant that a driving signal where the frequency components were spread out over a long time would not be appropriate. When using a frequency sweep, this means that the signal length must be short enough that the exponential weighting coefficient be close to unity for the whole length of the sweep. However, since the averaging algorithm is applied to both the reference signal and the response signal equally, the resulting deconvolution is unaffected by this averaging method, except in the manifestation of reduced background noise. If one were to look at the individual FFT of one of these signals though, the averaging method does need to be considered. For a sample period of 1 second and averaging over 2500 samples, a 2 second excitation signal will have a deviation of 0.3% from start to finish. A 10 second signal would have a 1.6% deviation. This number can be reduced by including more averages in the set, increasing the sample period or decreasing the excitation signal duration.

Appendix B

Input Impedance Measurements

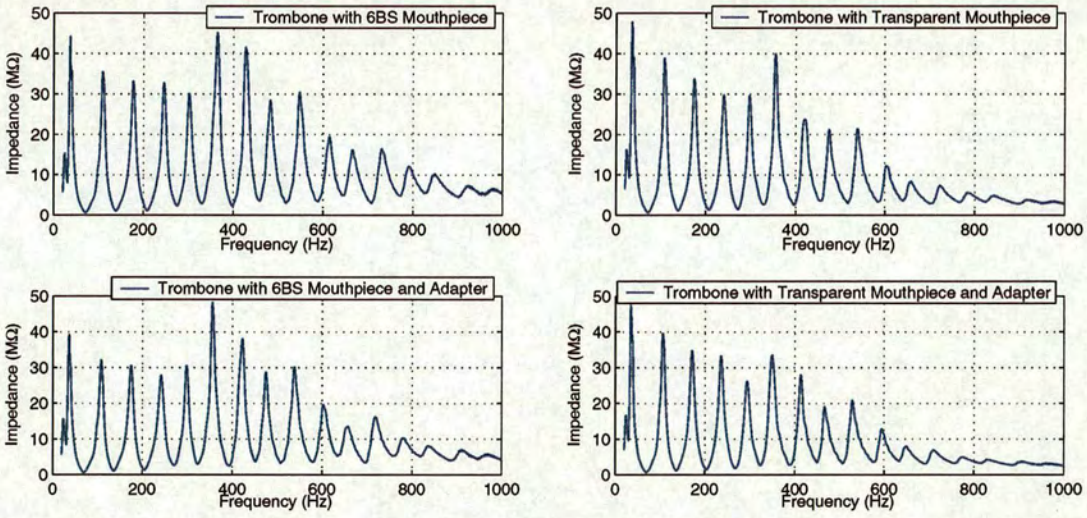

Figure B.1: Input impedance measurements for the trombone with various mouthpiece configurations.

Configuration	Description
A	Trombone with Denis Wick 6BS mouthpiece
B	Trombone with Denis Wick 6BS mouthpiece and adapter piece
C	Trombone with transparent mouthpiece
D	Trombone with transparent mouthpiece and adapter piece

Table B.1: Description of the various configurations of trombone and mouthpieces.

Configuration		Frequency (Hz)	Impedance ($M\Omega$)	Quality Factor
A	Mode 2	110	36	13.5
	Mode 3	177.5	34	20
	Mode 4	246	33	26
	Mode 5	302.5	30	30
B	Mode 2	108	33	12.5
	Mode 3	175	31	16.5
	Mode 4	241.5	28	21
	Mode 5	298.5	31	32.5
C	Mode 2	108	40	14
	Mode 3	174.5	34	19.5
	Mode 4	240	30	23
	Mode 5	298	30	33
D:	Mode 2	106.5	40	13.5
	Mode 3	171.5	35	19
	Mode 4	235.5	34	24.5
	Mode 5	294	26	24

Table B.2: Impedance data for the various trombone configurations, all with an unextended slide.

Mouthpiece	Frequency (Hz)	Impedance ($k\Omega$)	Quality Factor
Transparent	482	340	66
Transparent with Adapter	399	510	60
6BS	596	450	76
6BS with Adapter	502.5	610	82

Table B.3: Impedance data for the two mouthpieces used, both with and without the adapter piece.

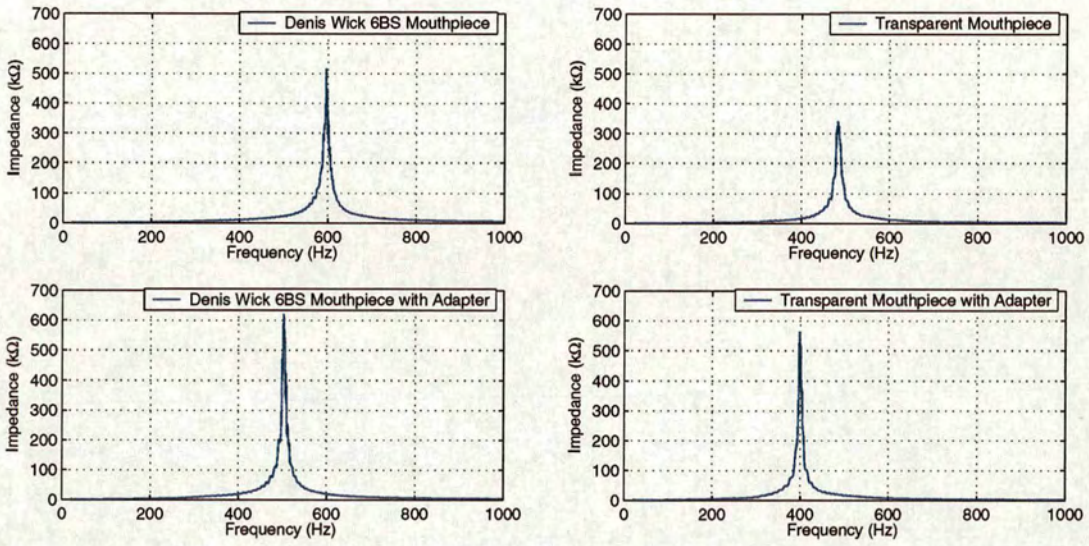

Figure B.2: Input impedance measurements for the mouthpieces used, with and without the adapter piece.

Appendix C

Lip Response Measurements

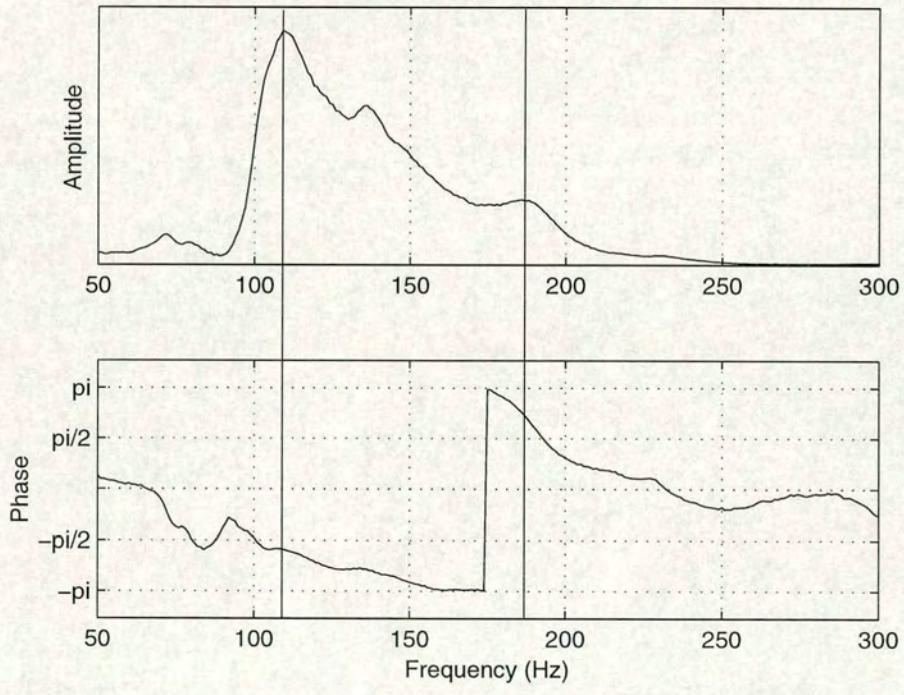

Figure C.1: Mechanical frequency response of the artificial lip reed.

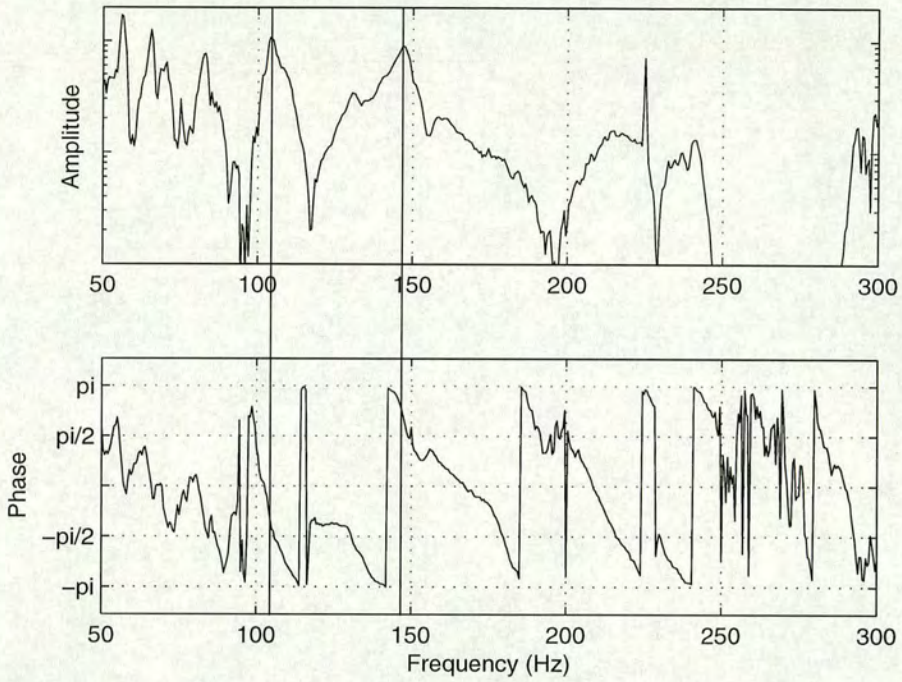

Figure C.2: Mechanical frequency response of the artificial lip reed.

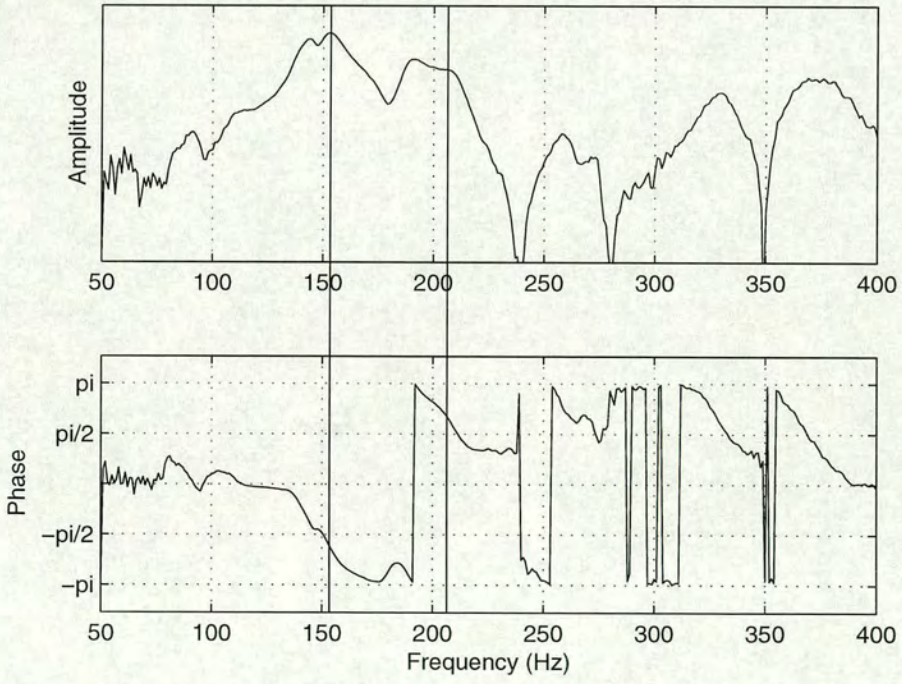

Figure C.3: Mechanical frequency response of the artificial lip reed.

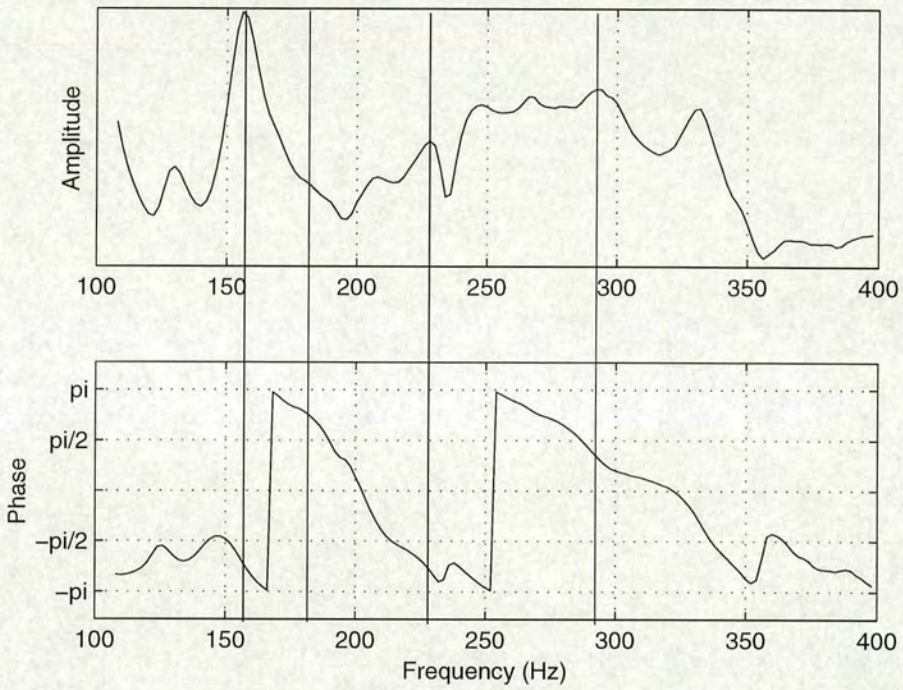

Figure C.4: Mechanical frequency response of the artificial lip reed.

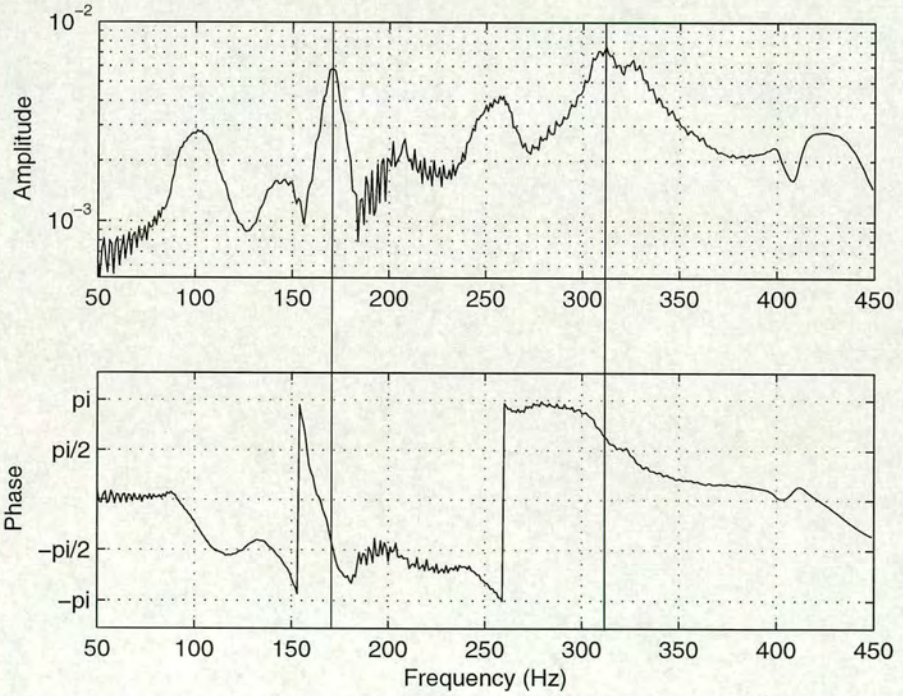

Figure C.5: Mechanical frequency response of the artificial lip reed.

Bibliography

[1] Acoustic Research Team. *BIAS 5.1 Manual*, 2001.

[2] S. Adachi and M. Sato. Time-domain simulation of sound production in the brass instrument. *J.Acoust.Soc.Am.*, 97:3850–3861, 1995.

[3] S. Adachi and M. Sato. Trumpet sound simulation using a two-dimensional lip vibration model. *J.Acoust.Soc.Am.*, 99:1200–1209, 1996.

[4] Y. Aurégan and C. Depollier. Snoring: linear stability analysis and *in–vitro* experiments. *Journal of Sound and Vibration*, 188(1):39–54, 1995.

[5] R.D. Ayers. New perspectives on brass instruments. In *Proc. ISMA 98*, 1998.

[6] J. Backus. Acoustic impedance of an annular capillary. *J.Acoust.Soc.Am.*, 58:1078–1081, 1975.

[7] J. Backus. Input impedance curves for the brass instruments. *J.Acoust.Soc.Am.*, 60:470–480, 1976.

[8] J. Backus. *The acoustical foundations of music.* W.W. Norton & Company, Inc., second edition, 1977.

[9] A.H. Benade. *Fundamentals of Musical Acoustics.* Oxford University Press, New York, 1976.

[10] M. Bertsch. Variabilities in trumpet sounds. In *Proc. ISMA 97*, 1997.

[11] D.M. Campbell. Nonlinear dynamics of musical reed and brass wind instruments. *Contermporary Physics*, 40:415–431, 1999.

[12] D.M. Campbell and C. Greated. *The musician's guide to acoustics.* Dent, 1987.

[13] Murray Campbell. Brass instruments as we know them today. In *Proc. SMAC 2003*, Stockholm, Sweden, August 2003.

[14] Y.M. Chang. Reed stability. *Journal of Fluids and Structures*, 8:771–783, 1994.

[15] F.C. Chen and G. Weinreich. Nature of the lip reed. *J.Acoust.Soc.Am.*, 99:1227–1223, 1996.

[16] D.C. Copley and W.J. Strong. A stroboscopic study of lip vibrations in a trombone. *J.Acoust.Soc.Am.*, 99:1219–1226, 1995.

[17] Cullen, Gilbert, and Campbell. Brass instruments: Linear stability analysis and experiments with an artificial mouth. *J.Acoust.Soc.Am.*, 86:704–724, 2000.

[18] J.S. Cullen. *A Study of Brass Instrument Acoustics using an Artificial Reed Mechanism, Laser Doppler Anemometry and Other Techniques.* PhD thesis, The University of Edinburgh, 2000.

[19] J.S. Cullen, J. Gilbert, D.M. Campbell, and C.A. Greated. Acoustical measurements in resonators driven by an artificial mouth, oscillation threshold behaviour. In *Proc. ISMA 1998*, pages 141–146, Leavenworth, WA, USA, June 1998.

[20] J.P. Dalmont, J. Gilbert, and J. Kergomard. Some aspects of tuning and clean intonation in woodwinds. *Applied Acoustics*, 46:19–60, 1995.

[21] P. Dietz and N. Amir. Synthesis of trumpet tones by physical modeling. In *Proc. ISMA 95*, Dourdan, France, 1995.

[22] S.J. Elliott and J.M. Bowsher. Regeneration in brass wind instruments. *Journal of Sound and Vibration*, 83:181–217, 1982.

[23] R. Di Federico and G Borin. Lip–excited wind instruments: a two dimensional model for the excitation mechanism. In *Proc. ICMC 97*, September 1997.

[24] R. Di Federico and G Borin. Synthesis of the trumpet tone based on physical models. In *Proc. ICMC 97*, pages 410–413, September 1997.

[25] N. H. Fletcher. Excitation mechanisms in woodwind and brass instruments. *Acustica*, 43:63–72, 1979.

[26] N. H. Fletcher. Autonomous vibration of simple pressure–controlled valves in gas flows. *J. Acoust. Soc. Am.*, 93(4):2172–2180, 1993.

[27] N.H. Fletcher, L. Hollenberg, J. Smith, and J. Wolve. The didjeridu and the vocal tract. In *Proc. ISMA 2001*, pages 87–90, September 2001.

[28] N.H. Fletcher and T.D. Rossing. *The physics of musical instruments.* Springer-Verlag, first edition, 1991.

[29] J. Gilbert. Physics of reed and brass instruments. In *Proc ISMA 02*, Mexico, 2002.

[30] J. Gilbert. Sound mechanisms of brass instruments, last twenty years results. In *Proc. Forum Acusticum*, Sevilla, Spain, 2002.

[31] J. Gilbert and J.F. Petiot. Brass instruments, some theoretical and experimental results. In *Proc. ISMA 1997 in Proc. Institute of Acoustics*, volume 19, pages 391–400, Edinburgh, UK, 1997.

[32] J. Gilbert, S. Ponthus, and J.F. Petiot. Artificial buzzing lips and brass instruments: Experimental results. *J. Acoust. Soc. Am.*, 104:1627–1632, 1998.

[33] N. Grand, J. Gilbert, and F. Laloe. Oscillation threshold of woodwind instruments. *Acustica / Acta Acustica*, 82, 1996.

[34] H.J.F. Helmholtz. *On the sensation of tone (1877).* Translated by A.J.Ellis, reprinted by Dover, 1954.

[35] A. Hirschberg, J. Gilbert, R. Msallam, and A.P.J Wijnands. Shock waves in trombones. *J. Acoust. Soc. Am.*, 99:1754–1758, 1996.

[36] P.J. Holmes. Bifurcations to divergence in flow induced oscillations: a finite dimensional analysis. *Journal of Sound and Vibration*, 53:471–503, 1977.

[37] K. Ishizaka and J. Flanagan. Synthesis of voiced sounds from a two-mass model of the vocal cords. *Bell Syst. Tech. J.*, 51:1233–1268, 1972.

[38] Wilfried Kausel. An attempt to use an electrical circuit simulator to better understand the relationship between a brass player's intonation and the instrument's input impedance. In *Forum Acusticum Sevilla 2002*, September 2002.

[39] Douglas H. Keefe. Physical modelling of musical wind instruments. *Computer Music Journal*, 16(4):57–73, 1992.

[40] Acoustic Research Team, Institut für Wiener Klangstil. http://iwk.mdw.ac.at/smart/english/art/artmain.htm.

[41] R. Laboissiere and X. Pelorson. Stability and bifurcation of the two–mass model oscillation: analysis of fluid mechanics effects and acoustical loading. In *Proc. ICPhS 95 (3)*, Stockholm, 1995.

[42] L. Le Marrec. Effet des conditions limites mécaniques de la glotte et des lèvres sur la production de sons voisés. Diplôme d'etudes approfondies d'acoustique, Universités d' Aix–Marseille II, 2001.

[43] N.J.C. Lous, G.C.J. Hofmans, R.N.J. Veldhuis, and A. Hirschberg. A symetrical two-mass vocal-fold model coupled to vocal tract and trachea, with application to prosthesis design. *Acustica*, 84:1135–1150, 1998.

[44] J. C. Lucero. Dynamics of the two–mass model of the vocal folds: Equilibria, bifurcations, and oscillation region. *J. Acoust. Soc. Am.*, 94(6):3104–3111, 1993.

[45] D.W. Martin. Lip vibrations in a cornet mouthpiece. *J. Acoust. Soc. Am.*, 13:305–308, 1942.

[46] R. Msallam, S. Dequidt, S. Tassart, and R. Caussé. Physical model of the trombone including non-linear propagation effects. In *Proc. ISMA 1997 in Proc. Institute of Acoustics*, volume 19, pages 419–424, Edinburgh, UK, 1997.

[47] R. Msallam, S. Dequidt, S. Tassart, and R. Caussé. Physical model of the trombone including non-linear propagation effects. application to the sound synthesis of loud tones. *Acustica*, 86:725–736, 2000.

[48] M.A. Neal. *A Study of the Brass Instrument Lip Reed Mechanism using Artificial Lips and Lattice Boltzmann Flow Simulations.* PhD thesis, The University of Edinburgh, 2002.

[49] M.A. Neal, O.F. Richards, D.M. Campbell, and J. Gilbert. Study of the reed mechanism of brass instruments using an artificial mouth. In *Proc. ISMA 2001*, pages 99–102, September 2001.

[50] M.A. Neal, O.F. Richards, D.M. Campbell, and J. Gilbert. Study of the lip reed destabilisation using an artificial mouth. In *Proc. IoA 2002*, March 2002.

[51] Polytec GmbH. http://www.polytec.de/polytec-com/l_vib/vib_uni.html.

[52] R.L. Pratt, S.J. Elliott, and J.M. Bowsher. The measurement of acoustic impedance of brass instruments. *Acustica*, 38:236–246, 1997.

[53] O. Richards, D. M. Campbell, J. Gilbert, and M. A. Neal. Use of experimental studies in determining a two–mass lip model. In *Forum Acusticum Sevilla 2002*, Sevilla, Spain, September 2002.

[54] O. Richards, D. M. Campbell, J. Gilbert, and M. A. Neal. Modelling the lip reed – computational and experimental investigations of the two–mode inward/outward striking behaviour. In *SMAC 2003*, Stockholm, Sweden, August 2003.

[55] X. Rodet and C Vergez. Physical models of trumpet–like instruments detailed behaviour and model improvements. In *Proc. ICMC 96*, Hong-Kong, 1996.

[56] D.B. Sharp. *Acoustic pulse reflectometry for the measurement of musical wind instruments.* PhD thesis, University of Edinburgh, 1996.

[57] W.J. Strong and J.D. Dudley. Simulation of a player–trumpet system. In *Proc. of SMAC 93*, pages 520–524, 1993.

[58] J.J. Thomsen. *Vibrations and stability, order and chaos.* McGraw-Hill, 1997.

[59] I.R. Titze. The physics of small–amplitude oscillation of the vocal folds. *J. Acoust. Soc. Am.*, 83(4):1536–1552, 1988.

[60] M.O. van Walstijn. *Discrete-Time Modelling of Brass and Reed Woodwind Instruments with Application to Musical Sound Synthesis.* PhD thesis, The University of Edinburgh, 2001.

[61] Ch. Vergez and X. Rodet. Model of the trumpet functionning: real time simulation and experiments with an artificial mouth. In *Proc. ISMA 97*, pages 425–432, 1997.

[62] Ch. Vergez and X. Rodet. Experiments with an artificial mouth for trumpet. In *Proc. ICMC 98*, pages 153–158, 1998.

[63] Ch. Vergez and X. Rodet. Air flow related improvements for basic physical models of brass instruments. In *Proc. ICMC 2000*, pages 62–65, 2000.

[64] Vision Research Inc. http://www.visiblesolutions.com.

[65] M.P. de Vries, H.K. Schutte, and G.J. Verkerke. Determination of parameters for lumped parameter models of the vocal folds using a finite–element method approach. *J. Acoust. Soc. Am.*, 106(6):3620–3628, 1999.

[66] S. Yoshikawa. On the modeling of self–oscillation in brass instruments. *J. Acoust. Soc. Am. Suppl.*, 84, S161, 1988.

[67] S. Yoshikawa. Acoustical behavior of brass player's lips. *J. Acoust. Soc. Am.*, 97:1929–1939, 1995.

[68] S. Yoshikawa and Y. Muto. Lip-wave generation in horn players and the estimation of lip-tissue elasticity. *Acustica/Acta Acustica*, 89:145–162, 2003.

Publications

M.A. Neal, O.F. Richards, D.M. Campbell and J. Gilbert. Study of the reed mechanism of brass instruments using an artificial mouth. In *Proc. ISMA 2001*, pages 99–102, Perugia, September 2001.

M.A. Neal, O.F. Richards, D.M. Campbell and J. Gilbert. Study of the lip reed destabilisation using an artificial mouth. In *Proc. IoA 2002*, March 2002.

O.F. Richards, D.M. Campbell, J. Gilbert and M.A. Neal. Use of experimental studies in determining a two–mass lip model. In *Proc. Forum Acusticum*, Sevilla, September 2002.

O.F. Richards, D.M. Campbell, J. Gilbert and M.A. Neal. Modelling the lip reed – computational and experimental investigations of the two–mode inward/outward striking behaviour. In *Proc. SMAC03*, Stockholm, August 2003.

S.R. Bromage, O.F. Richards, D.M. Campbell. Reproducibility and control of the embouchure of an artificial mouth for playing brass instruments. In *Proc. SMAC03*, Stockholm, August 2003

D.M. Campbell and O.F. Richards. Linear and nonlinear behaviour of human and artificial lip reeds. 146^{th} meeting: Acoustical Society of America. *J. Acoust. Soc. Am.*, 114(4, pt.2), 2003